(8C)

MEASUREMENT OF MIDDLE-EAR ACOUSTIC FUNCTION IN INTACT EARS: APPLICATION TO SIZE VARIATIONS IN THE CAT FAMILY

by

Gregory T. Huang

B.S., University of Illinois, Urbana-Champaign (1990)

S.M., Massachusetts Institute of Technology (1992)

Submitted to the Department of Electrical Engineering and Computer Science
in Partial Fulfillment of the Requirements for the Degree of
Doctor of Philosophy

at the

MASSACHUSETTS INSTITUTE OF TECHNOLOGY

February, 1999

Signature of Author ....
Department of Electrical Engineering and Computer Science
January 29, 1999

Certified by ....
William T. Peake
Professor of Electrical and Bio-engineering, M.I.T.
Thesis Supervisor

Certified by ....
John J. Rosowski
Associate Professor of Otology and Laryngology, Harvard Medical School
Thesis Supervisor

Accepted by ....
Arthur C. Smith
Chairman, Committee on Graduate Students
Department of Electrical Engineering and Computer Science

Measurement of Middle-Ear Acoustic Function in Intact Ears: Application to Size Variations in the Cat Family

by

Gregory T. Huang

Submitted to the Department of Electrical Engineering and Computer Science
on January 29, 1999 in Partial Fulfillment of the Requirements for the Degree of
Doctor of Philosophy

ABSTRACT

We seek a quantitative description of relationships between body size and the acoustic performance of the middle ear (ME). The cat family was chosen as the study group because of its qualitatively uniform (and distinctive) ME structure, large size range, and the extensive data available from domestic cats. This thesis consists of (1) the development of a method for estimating the acoustic admittance at the tympanic membrane (TM), Y_{TM}, in intact ears of different sizes, and (2) measurements of Y_{TM} in anesthetized exotic cats, which lead to correlations of ME sound-transmission properties with body size.

(1) The method involves (a) measuring admittance in the intact ear canal with an earphone-microphone system, and (b) transforming this admittance to the TM via a uniform-tube model of the canal determined in part by measurements with applied static pressures. Complications include nonuniform acoustic waves generated at the earphone's port, variations in canal diameter among subjects, and specification of the canal dimensions between the measurement point and the TM. Tests in domestic cats show that with attention to these issues the method is accurate for frequencies between 0.1-5 kHz.

(2) Y_{TM} is reported from 17 adult ears of 11 exotic-cat species ranging in size from sand cat (3 kg) to tiger (180 kg). Data from domestic cats support connections between Y_{TM} and specific ME structures via lumped-network models. For low frequencies, Y_{TM} is compliancelike for all species; total acoustic compliance increases with body size, but the compliance of the TM-ossicular system is *not* correlated with size. Structure-based rules describe dependences of ME sound transmission on size: (a) Low-frequency transmission increases with size; (b) the frequency of a transmission notch (which results from ME-cavity structures) decreases with size. These trends are consistent with the idea that in larger felids the ME frequency response is shifted to lower frequencies, with potential benefits for the detection of intraspecies vocalizations and sound-localization cues. These results suggest that body size provides a quantitative description of some features of auditory function in the cat family and possibly other groups.

Thesis Supervisor: William T. Peake
Title: Professor of Electrical and Bio-engineering, M.I.T.

Thesis Supervisor: John J. Rosowski
Title: Associate Professor of Otology and Laryngology, Harvard Medical School

ACKNOWLEDGMENTS

I found it difficult to judge the hearing ability of lions because mine was usually restricted by being in a car.

- George B. Schaller (1972, p. 84)

TABLE OF CONTENTS

CHAPTER 1
Introduction: On relating middle-ear structure to acoustic function in the cat family

CHAPTER 2
Estimating acoustic admittance at the tympanic membrane from measurements in intact ear canals

CHAPTER 3
Relating middle-ear acoustic function to body size in the cat family: Measurements and models

10

CHAPTER 1

Introduction: On relating middle-ear structure to acoustic function in the cat family

INTRODUCTION

The aims of this chapter are (1) to provide a broad introduction to the thesis and (2) to review a few results that motivate this project. The chapter begins by outlining a general approach to "comparative hearing" and introducing the basic structure and function of the auditory periphery (Section I). Next, the middle ears of the cat family are evaluated as a useful and interesting set of auditory structures to study (Section II). Complications in making acoustic measurements in these intact ears are discussed (Section III). Lastly, an overview of the goals and organization of the thesis is presented (Section IV).

I. GENERAL APPROACH

A. Basic ideas in comparative hearing

Studies in comparative hearing seek to relate the structure and function of the auditory system to the life history of the animal. Within this general approach, one might combine quantitative descriptions of the ear's anatomy and physiology with behavioral data, to construct hypotheses that include the significance of hearing in the animal's interactions with its environment. Tests of these hypotheses can provide insight into the selective pressures involved in the evolution of the auditory periphery, e.g., the disparate ear structures of birds (Manley, 1990; Manley and Gleich, 1992), reptiles (Manley, 1990; Miller, 1992), and mammals (Hopson, 1966; Crompton and Parker, 1978; Fleischer, 1978; Kermack and Musset, 1983; Echteler et al., 1994; Rosowski, 1992, 1994; Nummela, 1995).

Hearing in terrestrial mammals has been studied both as a model for human hearing and, more fundamentally, to determine the acoustic and auditory mechanisms that relate structural variations to functional variations (Fay, 1994). The latter approach makes use of the tremendous diversity in auditory function observed in terrestrial mammals. For instance, variations in the range of audible frequencies are much greater among mammals than among birds or reptiles (Fay, 1988; Dooling, 1992); the high-frequency hearing limit varies between 7 kHz in elephant (Heffner and Heffner, 1980), 15 kHz in human, 60 kHz in domestic cat, 70 kHz in mouse (Heffner and Masterton, 1980), and over 100 kHz in some species of bats (for review, see Grinnell, 1995).

Comparisons of auditory structure and function in extant mammals have led to hypotheses concerning the evolution of hearing and the adaptive benefits of structural variations. The following two examples show how these hypotheses can motivate (and suggest ways to investigate) basic questions regarding the *acoustic mechanisms* by which structural variations lead to functional variations. These examples are intended to give the reader a broad idea of the kinds of questions we are interested in pursuing, and to motivate the general study of the acoustic mechanisms of the ear, particularly the middle ear.

(1) It has been hypothesized that gerbils and kangaroo rats evolved specialized ear structures, e.g., large auditory bullae,[1] for increased low-frequency hearing sensitivity, in response to selective pressures to avoid predation by snakes and owls in their desert habitats (Lay, 1972; Webster and Webster, 1980; Webster and Plassmann, 1992). This hypothesis, which is based on structural, physiological, and behavioral measurements, motivates a basic physiological question: What are the acoustic mechanisms by which a large bulla (and/or other structural variations) might improve low-frequency sensitivity? This question can be approached from different points of view by (a) searching for correlations between low-frequency hearing and desert habitats, (b) testing whether *all* species with relatively large bullae (e.g., sand cat) have increased low-frequency sensitivity, (c) testing whether species with similar habitats and *small* bullae (e.g., desert ground squirrel) have decreased low-frequency sensitivity, and (d) measuring the sound-transmission properties of the ears of all the species above.

(2) A hypothesis of broader scope is that early mammals were driven to nocturnal activity to find food while avoiding predation, and that they evolved high-frequency hearing in response to selective pressures to localize sound sources in the dark (e.g., Masterton et al., 1969; Jerison, 1973; Heffner and Heffner, 1992). This hypothesis is based on the ability of most extant mammals to sense sounds of frequencies above 20 kHz (in contrast to extant reptiles), and evidence from the fossil record that the earliest mammals were small and coexisted with efficient, diurnal reptile predators. These ideas motivate a basic physiological question: What acoustic mechanisms might be responsible for the much greater high-frequency sensitivity of mammalian ears? It has been proposed that this sensitivity is related to the unique structure of the three-bone mammalian ossicular system. For example, Masterton et al. (1969, p. 973) state that, "Since the transmission of high-frequency vibrations from eardrum to cochlea is known to require this matching of impedances, there seems little reason to look beyond the evolution of the middle-ear

---

[1] "Bullae" refers to the bony prominences that enclose the middle-ear air spaces on the posteroventral aspect of the skull in some species (e.g., gerbils, cats).

ossicles for one explanation of the radical difference between mammals and nonmammals in the upper limit of hearing." However, a mechanistic relationship between ossicular structure and high-frequency sensitivity has not been demonstrated. To relate high-frequency hearing to acoustic mechanisms, one might (a) correlate variations in the structure of the ossicle(s), tympanic membrane (eardrum), and inner ear with variations in high-frequency audiometric limits among species (Rosowski, 1992; Hemilä et al., 1995), (b) develop and apply methods for measuring high-frequency (> 10 kHz) sound-transmission properties in ears of these species, and (c) develop and test theoretical models of high-frequency sound transmission through these ears.[2]

B. Acoustic function of the auditory periphery

This thesis focuses on the acoustic performance of the middle ear and the possible effects of this performance on overall auditory function in a mammalian taxon. The purposes of this section are to place the middle ear in a larger context and to motivate a measure of middle-ear acoustic function. We present a brief review of (1) the basic structures of the auditory periphery and (2) a theoretical framework for representing the acoustic signal-processing function of these structures (see Rosowski, 1991, 1994).

The auditory periphery -- which in terrestrial mammals includes the external ear, middle ear, and inner ear or cochlea -- serves to collect acoustic power from the environment and to transmit the resulting signals to the brain. The basic structures of the mammalian auditory periphery and 5 associated acoustic variables are depicted schematically in Fig. 1 (upper). Sound in surrounding space incident on the ear is represented by an acoustic plane wave of sound pressure P_{PW}. The incident wave interacts with the head and the structures of the external and middle ears, giving rise to the sound pressure P_{TM} just lateral to the tympanic membrane (TM), the

---

[2] It has been suggested that high-frequency transmission is limited by (a) the size and vibratory pattern of the TM (Khanna and Tonndorf, 1978) and (b) the mass of the ossicles (Hemilä et al., 1995). [Hemilä et al. (1995) describe a lumped-network model whose applicability to high frequencies ($f > 20$ kHz) is suspect. To represent acoustic behavior at these frequencies, finite-element models (or other distributed models) may be required (e.g., Funnell et al., 1992).]

interface between the external and middle ears. The resulting motions of the TM, represented by the volume velocity U_{TM}, are conducted through the ossicular chain such that the stapes footplate drives the cochlea with volume velocity U_{FP} (Guinan and Peake, 1967). The resulting sound pressure in the fluid just inside the cochlear entrance is represented by P_C.

Within this framework, some basic measures of acoustic function can be defined. In Fig. 1.1 (lower), the auditory periphery is represented as a combination of three electrical-analog networks: (1) The head-and-external-ear network is characterized by the pressure gain P_{TM} / P_{PW} and the radiation admittance (in the lateral direction) Y_E.[3] (2) The middle-ear network is characterized by the input admittance $Y_{TM} = U_{TM} / P_{TM}$, the transfer admittance U_{FP} / P_{TM}, and the pressure gain P_C / P_{TM}. (3) The cochlea network is characterized by the input admittance $Y_C = U_{FP} / P_C$, which represents the acoustic load on the middle-ear system.

This framework represents some features of the auditory periphery's acoustic performance (Siebert, 1970; Rosowski et al., 1986; Rosowski, 1991, 1994). For example, quantitative comparisons of Y_{TM} and Y_E can determine how well the external-ear admittance is "matched" to the middle-ear input admittance and hence how effectively sound power is delivered to the middle ear. Also, the efficiency of the middle ear in conducting sound power to the cochlea can be determined from the combination of Y_C, Y_{TM}, and U_{FP}. Calculations of these acoustic-performance features for a few species (human, domestic cat, and chinchilla) indicate that the external and middle ears exert a strong bandpass influence on the overall auditory function (Rosowski, 1991, Figures 6-10), which can explain much of the shape of behavioral thresholds or "audiograms" (Dallos, 1973; Rosowski, 1991, Fig. 12).[4]

---

[3] Acoustic admittance (reciprocal of acoustic impedance) is the ratio of volume velocity to sound pressure at a point. "Radiation admittance" generally refers to the admittance seen by a source transmitting into space. Here, Y_E is the admittance, just lateral to the TM, of the external-ear structures opening into surrounding space.

[4] The data contradict the idea that the middle ear acts as an ideal transformer to match the admittance of the external acoustic system to the admittance of the cochlea.

17

In this thesis, the middle-ear input admittance Y_{TM} is measured in intact ears of live subjects. The driving-point admittance Y_{TM} characterizes the auditory system medial to the TM in terms of some basic properties of the middle ear, e.g., total acoustic compliance and resistance (Onchi, 1961; Mundie, 1963; Møller, 1965; Zwislocki, 1970; Lynch, 1981; Rabinowitz, 1981); these properties can form the bases of comparisons of acoustic performance among species. In the future, measurements of other middle-ear transfer functions (which cannot be made non-invasively) in these species may provide more pieces of the puzzle.

II. USE OF THE CAT FAMILY

A. Overview

This section introduces the cat family (*Felidae*) as a valuable group of animals for auditory research. The motivation for selecting this group is presented in terms of a basic question in hearing mechanics and some attractive characteristics of the group (Section II B). Some details of the structure and function of middle ears of the cat family are then discussed to motivate the work in this thesis (Section II C).

B. General motivation

Extensive audiometric data show that the range of audible frequencies in mammals is generally shifted to lower frequencies in larger animals compared to smaller animals (Heffner and Masterton, 1980; Fay, 1988; Calder, 1996, p. 240). These data suggest a basic physiological question: What are the acoustic mechanisms responsible for this trend? Many functional variables of an animal's ecological life history -- e.g., territorial size, metabolism, and life span -- have been shown to be rather dependent on body size (McMahon and Bonner, 1983; Schmidt-Nielsen, 1984; Calder, 1996). Can hearing range and other performance features be related to middle-ear size and body size, and what are the underlying adaptive or ecological consequences (Masterton et al., 1969; Funnell and Laszlo, 1974; Rosowski, 1992; Hemilä et al., 1995; Nummela, 1995)?

To begin to answer these questions, we restrict our study to a manageable group of animals that are available for measurements. The cat family (*Felidae*) is an attractive study group for several reasons: (1) its large range of species size (more than a factor of 100 in body weight), (2) qualitatively similar middle-ear structure among species, (3) manageable number of well-defined species, 37 (Wozencraft, 1993), and (4) the extensive anatomical and physiological data available on the middle ear of one species, domestic cat (e.g., Møller, 1965; Guinan and Peake, 1967; Khanna and Tonndorf, 1972; Lynch, 1981; Decraemer et al., 1990; Peake et al., 1992). Furthermore, middle ears of the cat family have a distinctive middle-ear cavity structure and distinctive acoustic responses that may have adaptive significance. The following section reviews some of the available data on these middle ears.

C. Felid middle ears

1. Structure

Middle ears of the cat family have a distinctive cavity structure. In all felids, a bony septum divides the middle-ear air space into two distinct regions, the tympanic and bullar cavities, that are connected through a narrow opening that we call "the foramen" (Fig. 1.2). The bony septum is a defining feature of a taxonomic dichotomy in the mammalian order Carnivora: In the "catlike" families (*Feloidia* -- felids, hyenas, mongooses, and civets) this middle-ear feature is present, whereas in the "doglike" families (*Canoidia*, e.g., dogs and bears) it is not (Wozencraft, 1989, p. 508).[5] No adaptive benefits of the septum, to hearing or other functions, have been demonstrated, although its distinctive acoustic effects have been investigated in three felid species (Lynch, 1981; Puria, 1991; Peake et al., 1992; Huang et al., 1997a, b) (see below).

The configuration of the TM and ossicles in domestic cat has been classified as an "intermediate" type, between "microtype" (small size, with a firm attachment between malleus and tympanic bone, e.g. mice and bats) and "freely-mobile" (large size, with the malleus supported

---

[5] Bony middle-ear septa are also present in species of other mammalian orders, e.g., gerbil and chinchilla.

entirely by ligaments, e.g. humans and guinea pigs) (Fleischer, 1978). In this thesis, we focus mainly on the effects of the middle-ear cavities in the family, as structural data are available on this aspect; variations in the stiffness of the TM and ossicular chain among species are inferred (Chapter 3, Section III B 2).

2. Size variations

A broad aim of this thesis is to relate hearing performance to middle-ear size and body size in a group of structurally similar animals. The "scaling" (which implies a conservation of basic structure) of middle-ear size with body size is illustrated in Fig. 1.3, for three felid species that nearly span the family's size range. Among domestic cat, bobcat, and lion, body weight varies over roughly a factor of 50, while the middle-ear cavity structures appear to vary in linear dimensions by roughly a factor of 2 and are qualitatively similar (and distinctive) in shape (Huang et al., 1997a, b). Among domestic cat and lion, ossicle weights vary by a factor of 4-5 (Nummela, 1995), stapes-footplate area varies by a factor of 3-4, and tympanic-membrane area varies by a factor of 3 (Huang et al., 1997b). The next section reviews data on the acoustic consequences of these size variations.

3. Function

In this section, we review published data on how middle-ear acoustic function varies with size in the cat family. Figure 1.4 shows middle-ear input admittances (Y_{TM}) measured in the three felid species illustrated in Fig. 1.3. Two features of the acoustic responses are qualitatively similar among the species, as detailed below.[6]

(1) For low frequencies ($f < 1$ kHz), the admittances are compliancelike (magnitude slopes of 1 and angles near 0.25 periods) and span a factor of 3 in magnitude (Fig. 1.4). As size increases, the middle-ear response for low frequencies seems to increase. The quantitative

---

[6] In domestic cat, these two response features have also been observed in other middle-ear transfer functions, such as the transfer admittance U_{FP} / P_{TM} (Rosowski, 1994, Fig. 6.20).

20

differences in $|Y_{TM}|$ among the species suggest that middle-ear size variations affect the middle-ear response (and perhaps sound transmission) at low frequencies. Indeed, the compliance of the middle ear may be related to hearing sensitivity (Fleischer, 1978; Rosowski, 1992).

(2) Between 2-5 kHz, a sharp notch in $|Y_{TM}|$ and a positive angle transition occur, resulting from an antiresonance between the acoustic compliances of the middle-ear cavities and the acoustic mass of the narrow foramen (Peake et al., 1992; Huang et al., 1997b). As size increases in this sample, the center frequency of the admittance notch decreases. Although its presence indicates a decrease in middle-ear sensitivity over a narrow band of frequencies, the significance (if any) of the notch to hearing behavior is not known.[7] We seek insights into the possible adaptive significance of this feature.

In summary, measurements in a few species suggest the hypothesis that middle-ear function is qualitatively similar among all felids, with quantitative differences being related to body size. This thesis will test the hypothesis on a larger number of species and determine whether correlations of middle-ear performance with body size are significant (Chapter 3). Correlations with body size of low-frequency sensitivity and the notch frequency can suggest hypotheses regarding the adaptive significance of these features (Chapter 3, Section III C).

III. METHODOLOGICAL ISSUES

A. Experimental subjects

This thesis describes acoustic measurements made on *live*, anesthetized specimens of the cat family (Chapter 3). The experiments, performed in cooperation with curators of captive

---

[7] Behavioral audiograms of domestic cat (Fay, 1988, pp. 347-350) are inconclusive as to whether the threshold increases near 4 kHz, because of (1) averaging among subjects, (2) coarse sampling in frequency, (3) sound-test stimulus characteristics, and (4) failure to adjust thresholds for the transformation of sound pressure between the free field and the TM (Dallos, 1973, p. 117-126). However, measurements of cochlear potentials clearly show a similar sharp minimum at the same frequency as the admittance dip (Møller, 1965).

collections and veterinarians, were arranged to coincide with other procedures that required the animals to be anesthetized. Thus, we did not have much control over which species were available for measurements. Our strategy was to make measurements on enough specimens to span (roughly) the size range of the family. We achieved a moderate success rate; failures were caused by (1) difficulties in placing and sealing the acoustic-measurement system in the ear canal and (2) the apparently abnormal condition of some of the specimens' ears (Chapter 2, Section II B; Chapter 3, Sections I A, B).

B. Effects of the external ear

In live exotic-cat specimens, the procedure to measure the acoustic middle-ear input admittance (Y_{TM}) must be non-invasive. That is, the measurement method must work within the intact external ear. The concha and ear canal of domestic (and exotic) cats are rather long and narrow and are more complicated in shape than those of humans (Rosowski, 1994, Fig. 6.5); this geometry necessitated the development of special eartips for placement of an acoustic-measurement system in the canal. The measurement of admittance is made roughly 10 mm from the TM, for the relative comfort and safety of the subject and because of the length of the felid concha and canal.

Accounting for the acoustic effects of the canal space between the measurement point and the TM is a rather involved task, particularly for higher frequencies. It has been shown that a uniform cylindrical tube can approximate the main features of the domestic-cat canal's radiation admittance for frequencies below 10 kHz (Rosowski et al., 1988, Fig. 11). The simplicity of the approximation (and the associated mathematical description) has encouraged the use of a uniform-tube location transformation to estimate Y_{TM} in both cats and humans (Møller, 1965; Zwislocki, 1970; Lynch, 1981; Rabinowitz, 1981; Huang et al., 1997b). The accuracy of this method is tested in Chapter 2.

C. Use of static pressures in the canal

Measurements of acoustic admittance with varying static air pressures in the canal are used clinically (e.g., Margolis and Shanks, 1985) to assess the health of the middle ear and to allow removal of the acoustic effects of the canal at low frequencies ($f < 1$ kHz), for which the response of the middle ear is controlled by compliant (i.e., springlike) forces (for review, see Rosowski, 1994, Fig. 6.16). The basic idea is that static pressures stiffen the TM and middle-ear system such that the admittance measured at low frequencies is largely determined by the volume of air (canal space) between the measurement point and the TM. For low frequencies, the effect of this space can be represented by an acoustic compliance C_{EC} (proportional to the volume), so that the middle-ear compliance (C_{ME}) can be estimated from the measured compliance (C_{Meas}) by $C_{ME} = C_{Meas} - C_{EC}$.

To extend this approach to higher frequencies, estimates of the canal's volume and diameter can define the uniform-tube admittance-location transformation. In this way (and with some more complicated assumptions), Rabinowitz (1981) estimated Y_{TM} in humans for frequencies up to 4 kHz. In this thesis, a similar method for estimating Y_{TM} is tested in domestic cats (Chapter 2, Section II) and then applied to exotic cats (Chapter 3, Section I).

IV. OVERVIEW OF THESIS

This thesis presents the methods and results of a study of the acoustic effects of size variations on middle-ear function in a group of structurally-similar animals, the cat family. Within this context, the thesis has three main goals:

1. To develop and test a method for estimating, in intact ears, the middle-ear input admittance Y_{TM} (a useful measure of ear function).

2. To measure Y_{TM} in exotic-cat species, and thereby to determine correlations between middle-ear performance features and body size.

3. To develop and test structure-based models that represent the effects of body size on middle-ear performance, and to relate these trends to variations in hearing capabilities and possible adaptive benefits.

Chapter 2 describes the development and testing of a method to measure the middle-ear input admittance (Y_{TM}) in intact ears. The design issues and accuracy of the admittance-measurement system are investigated within the conceptual context of measurements in ear canals of different sizes. The errors in estimating Y_{TM} in domestic-cat ears are quantified. The method is presented within a context that is broader than the comparative study to which it is applied in this thesis (Chapter 3). The methodological issues are discussed with applicability to human clinical studies and the general use of acoustic systems designed for insertion into the ear canal.

Chapter 3 describes non-invasive experiments on anesthetized specimens from 11 exotic-cat species, ranging in size from sand cat (3.1 kg) to tiger (180 kg). The middle-ear input admittance (Y_{TM}) is compared among the species. Significant correlations of middle-ear acoustic properties with body size across the cat family are demonstrated. Relationships between body size and middle-ear sound transmission are inferred from a lumped-network model and connected to selective pressures that may affect hearing function in these animals. The results suggest that the comparative approach to relating structure, function, and ecology might be applied to other taxonomic groups in an effort to construct unifying hypotheses regarding the evolution of hearing in terrestrial mammals.

FIG. 1.1: Schematic diagram of the mammalian auditory periphery and theoretical framework for representing acoustic function. UPPER: The external ear consists of the pinna flange, concha, and ear canal. The middle ear consists of the tympanic membrane (TM), the 3 ossicles (malleus, incus, and stapes), the middle-ear air space, and the Eustachian tube (which is generally closed). The cochlea is a fluid-filled bony spiral which is partitioned by the basilar membrane; sensory cells and connected neurons in the cochlea transduce the motion of the cochlear structures into electrical impulses which propagate to the brain via the auditory nerve. For acoustic variables, see description below. LOWER: Electrical-analog network of the auditory periphery. The head and external ear are represented by a free-field-to-TM transformation. The middle ear is represented by a linear, time-invariant two-port. The cochlea is represented by a one-port load on the middle-ear system. Sound pressures are analogous to voltages, and volume velocities are analogous to currents. P_{PW} = sound pressure of an incident plane wave; P_{TM} = sound pressure just lateral to the TM; U_{TM} = volume velocity of the TM; P_C = sound pressure just inside the cochlea; U_{FP} = volume velocity of the stapes footplate. Y_E = acoustic admittance looking out (laterally) from the TM; Y_{TM} = middle-ear input admittance U_{TM}/P_{TM}; Y_C = cochlear input admittance U_{FP}/P_C. Each acoustic variable is a function of frequency; the sinusoidal steady state is assumed. (Adapted from Rosowski, 1991, Figures 2 and 3.)

FIG. 1.1

PINNA FLANGE

AUDITORY PERIPHERY
Lateral ←——→ Medial

MALLEUS, INCUS, & STAPES

BASILAR MEMBRANE

P_{PW}

EAR CANAL & CONCHA

U_{TM}
P_{TM}

U_{FP}
P_C

TM

COCHLEA

MIDDLE-EAR AIR SPACE

EUSTACHIAN TUBE

P_{PW} → HEAD & EXTERNAL EAR

U_{TM}
P_{TM} $^+_-$

MIDDLE EAR

U_{FP}
P_C $^+_-$

COCHLEA

Y_E Y_{TM}

Y_C
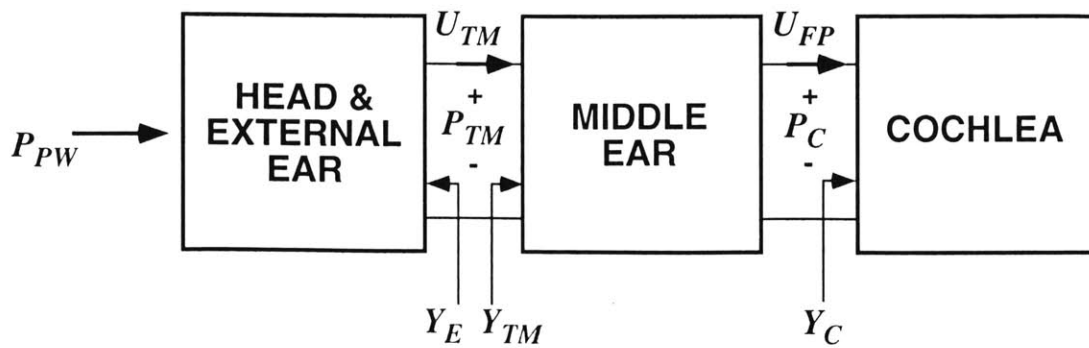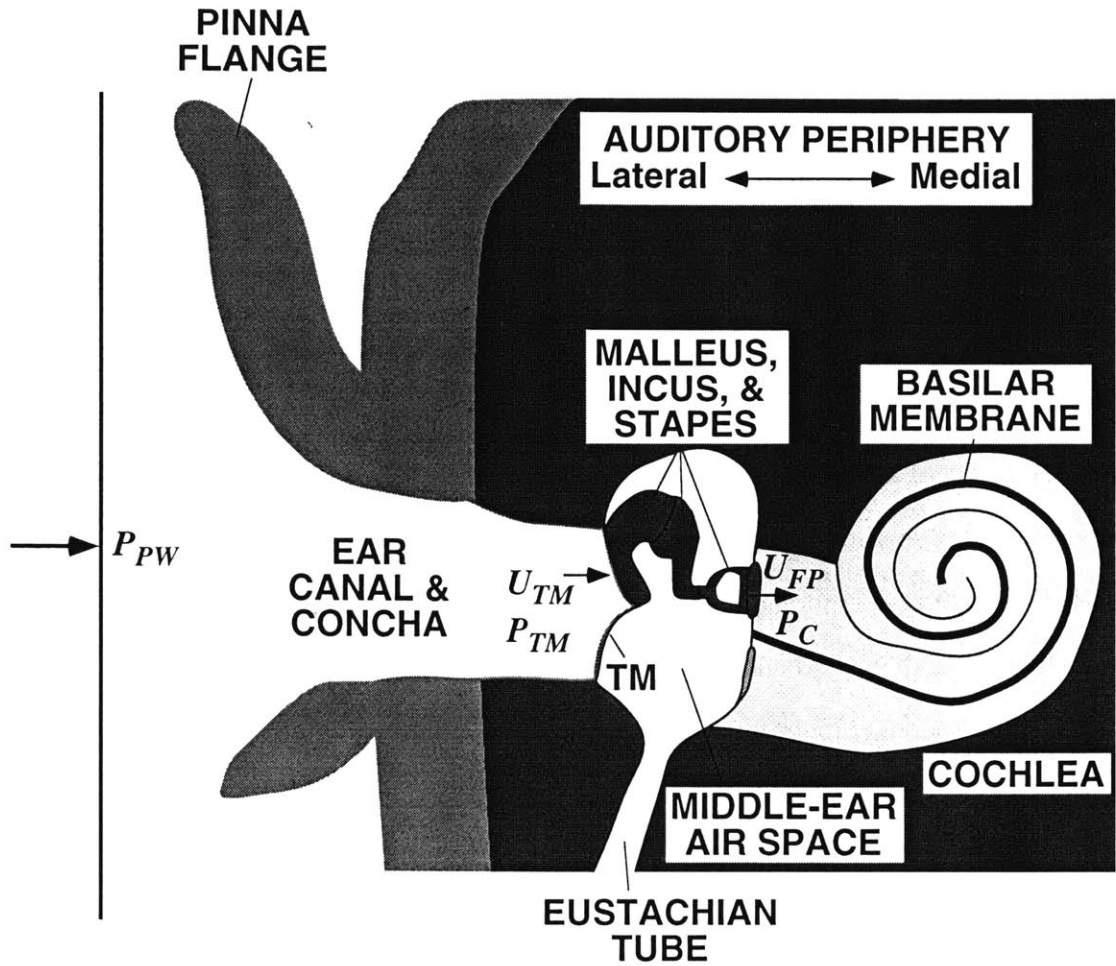
FIG. 1.2: Outline of a transverse (coronal) histological section through the middle ear of a domestic cat. Dark shading is bone, medium shading is fluid or soft tissue, and white is air-filled space. TM - tympanic membrane; I - incus; S - stapes; VII - 7th cranial nerve. This section was chosen to include both the TM and the foramen. The posterior regions of the TM and the bony ear canal are shown, such that their dorsoventral extent is smaller than it is at more anterior locations. (After Huang et al., 1997b, Fig. 1.)

FIG. 1.2

Domestic
Cat

5 mm

VII

BONE

I

INNER
EAR

S

TM

EAR CANAL

FORAMEN

TYMPANIC
CAVITY

BULLAR
CAVITY

BULLA

SEPTUM
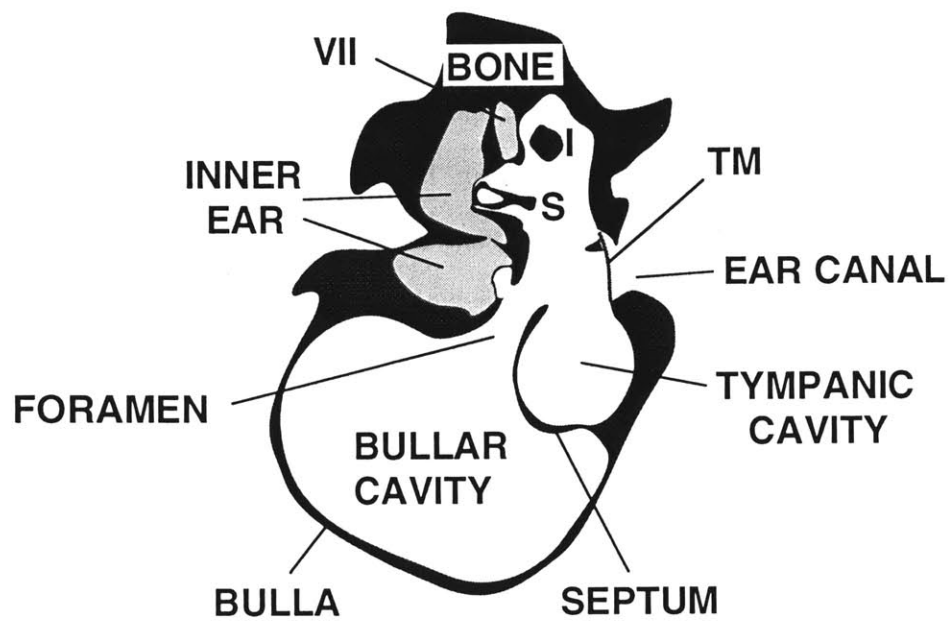
Dorsal

Lateral

FIG. 1.3: Scaling of middle-ear structural size with body size in the cat family. The transverse (coronal) middle-ear sections from bobcat and lion are from CT scans (Huang et al., 1997a, b). The domestic-cat section is the same as in Fig. 1.2. Sections were chosen to include both the TM and the foramen in the bony septum. The sections are all drawn on the same scale with shading convention as in Fig. 1.2. The body weights are species averages from Van Valkenburgh (1990, p. 184).

FIG. 1.3

DOMESTIC
CAT
3 kg

10 mm

BOBCAT
10 kg
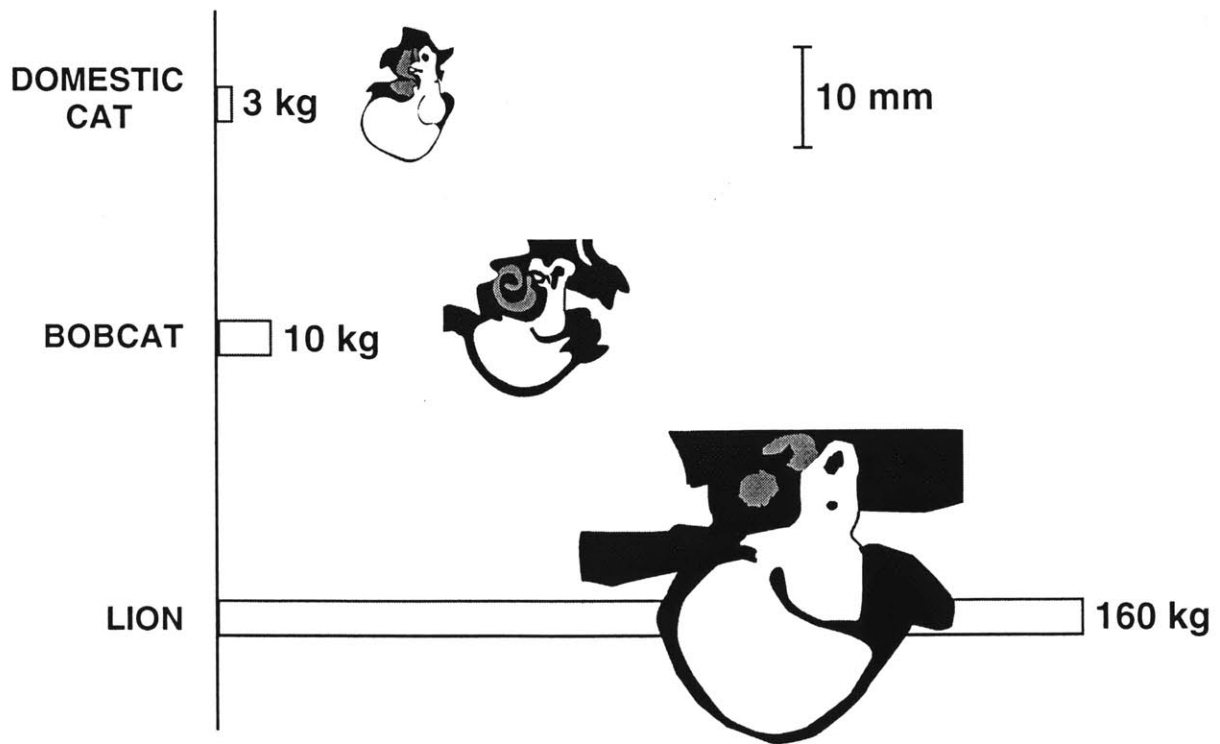
LION
160 kg

FIG. 1.4: Comparison of middle-ear input admittances (Y_{TM}) measured in three felid species: domestic cat, bobcat, and lion (one specimen of each). Admittance-notch frequencies: domestic cat - 4.4 kHz; bobcat - 3.5 kHz; lion - 2.8 kHz. Each measurement was made after resection of most of the external ear. The domestic-cat measurement is from Cat 53L of Lynch (1981) [also used in Huang et al. (1997a, b)]. The bobcat and lion measurements were made in one deceased specimen of each species (Huang et al., 1997a, b). Admittance-magnitude units: 1 μSiemen = 1/(mks MΩ) = 10^{-6} m³/(Pa s). Phase angles are plotted in periods (1 period = 2π radians).

FIG. 1.4
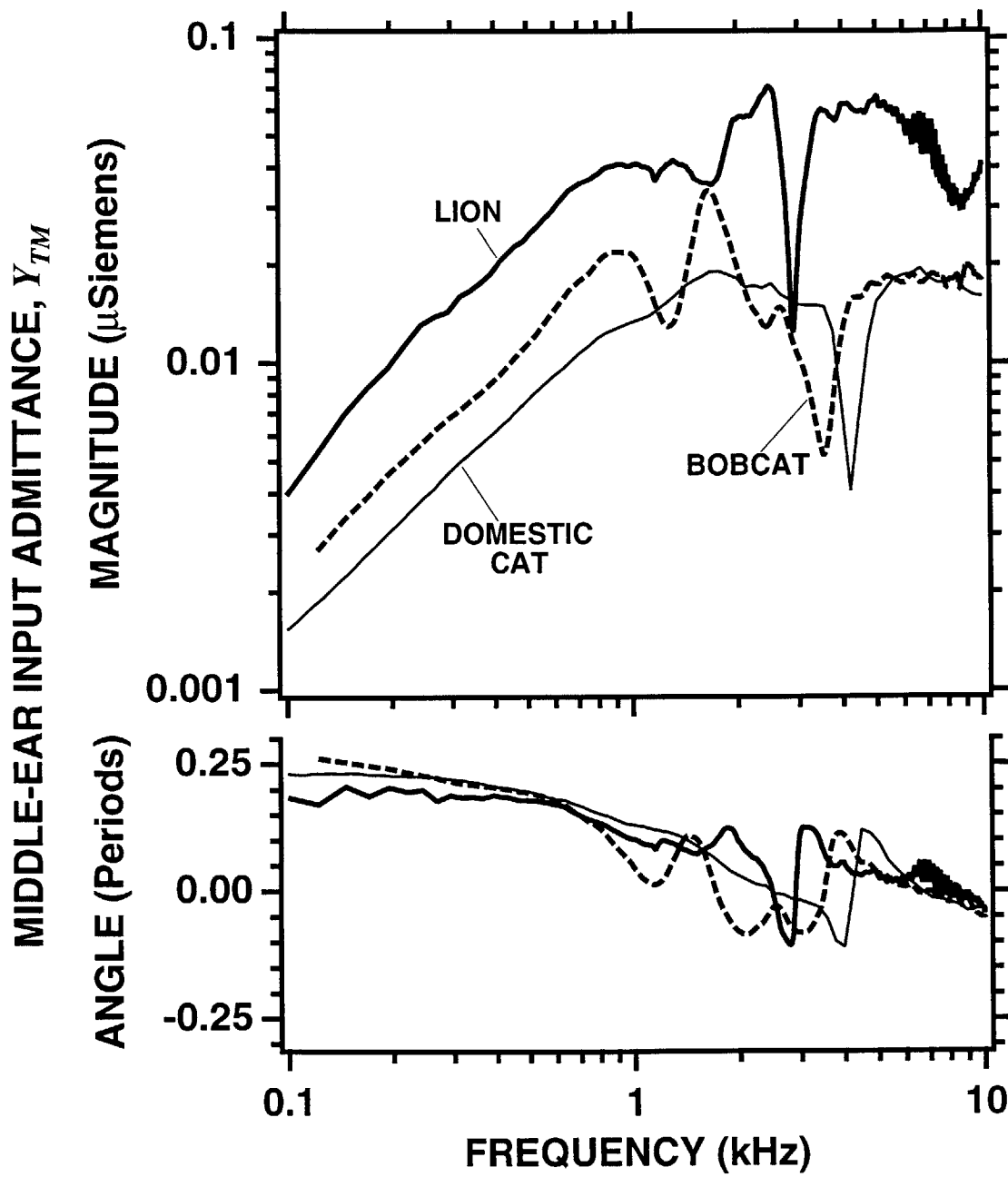
CHAPTER 2

Estimating acoustic admittance at the tympanic membrane from measurements in intact ear canals

ABSTRACT

As a step toward measuring the acoustic performance of live, intact middle ears, a method was developed for estimating the acoustic admittance at the tympanic membrane (TM), Y_{TM}. The method consists of (1) measuring the admittance in the external ear canal Y_{EC} with a commercially available sound source (earphone) and microphone system, and then (2) estimating the admittance at the TM via a uniform-tube approximation of the canal. With the goal of testing the accuracy of the method and determining the sources of error, admittance measurements were made in artificial loads and in domestic-cat ears.

The coupling of the acoustic system to the canal introduces complications associated with nonuniform waves generated at the earphone's narrow port, variations in canal diameter among subjects, and specification of the dimensions of the canal space between the measurement point and the TM. Tests in known acoustic loads show that (1) extension of the microphone tube medially beyond the earphone tube's narrow port increases accuracy for frequencies above 2 kHz, and (2) the system should be calibrated in loads having diameter within 10-15% of the ear-canal diameter, because the source's characteristics depend on the canal diameter.

In ear canals, the dimensions of the uniform-tube model are determined from admittances measured with static pressures in the canal and an area-estimation algorithm (Keefe et al., 1992). The overall method -- tested on domestic cat ears by comparing the estimated admittance to the admittance measured at the TM after removal of the external ear canal -- is accurate for frequencies up to 5 kHz. In domestic cats, the estimated Y_{TM} agrees with the measured Y_{TM} within 14% in the total compliance (averaged over 0.1-0.3 kHz) and 5% in the frequency of a middle-ear cavity antiresonance near 4 kHz. The data are used to test the idea that the acoustic-reflectance magnitude in the canal is independent of the measurement location. Sources of admittance errors include residual effects of nonuniform waves generated at the earphone's narrow port, estimation of the canal dimensions, nonuniform geometry of the canal, and earphone-microphone crosstalk. A continuing operational problem is the difficulty in placing and sealing the acoustic system in the cat's intact ear canal. These results suggest that the method (1) allows determination of some features of middle-ear acoustic function and (2) could be improved with changes in hardware design.

INTRODUCTION

A. Motivation

The acoustic admittance at the tympanic membrane (TM) Y_{TM} -- the ratio of the volume velocity of the TM to the sound pressure just lateral to the TM -- is a useful description of an ear's acoustic properties for scientific and clinical purposes.[8] Also known as the middle-ear input admittance, Y_{TM} characterizes the acoustic response of the middle ear (Onchi, 1961; Zwislocki, 1962; Mundie, 1963; Møller, 1965); it also affects the sound-pressure distribution along the ear canal and the flow of acoustic energy into the ear (Rosowski et al., 1986; Stinson and Khanna, 1994). Clinical hearing tests often include measurements of Y_{TM} to aid in the diagnosis of pathologies such as fluid in the middle ear and ossicular fixation (Jerger, 1975; Wilber and Feldman, 1976; Margolis and Shanks, 1985).

Accounting for the effects of the ear-canal space between the measurement point and the TM is a continuing issue. In the intact human ear, the acoustic probe is usually placed such that its tip is 8-15 mm lateral to the TM, for the comfort and safety of the subject (e.g., Keefe et al., 1993; Voss and Allen, 1994). In clinical admittance measurements, for frequencies below 1 kHz, the effect of the canal is represented by an air volume determined from the acoustic response with applied static pressure in the canal that stiffens the TM; the effects of the canal volume can be subtracted from the zero-static-pressure acoustic response to give the net middle-ear response (Margolis and Shanks, 1985). For higher frequencies, where acoustic behavior is complicated by spatial variations, one approach is to approximate the canal space by a rigid, cylindrical tube of uniform cross section; the measured admittance is then transformed via a uniform transmission-line model to give an estimate of Y_{TM}. With this method, Møller (1965) and Zwislocki (1970) were

---

[8] In fact, the phrase "at the TM" is ambiguous, because the TM terminates the ear canal obliquely (e.g., Stinson and Khanna, 1989). However, for frequencies below 6 kHz in human (10 kHz in cat), the sound pressure is essentially constant over the surface of the TM (Stinson, 1985; Chan and Geisler, 1990, p. 1237; Stinson and Khanna, 1994). For these frequencies, Y_{TM} represents a driving-point admittance at a point approximation of the TM.

able to estimate Y_{TM} in humans for frequencies up to 2 kHz. Rabinowitz (1981) estimated Y_{TM} for frequencies up to 4 kHz with a more elaborate scheme.[9] The errors involved in the transformation are thought to become significant for frequencies above 4 kHz (Rabinowitz, 1981, p. 1033; Huang et al., 1997, p. 1536) for distances of roughly 10 mm along a canal; however, the accuracy of the method has not been clearly tested in ears.

Because of these complications in measuring Y_{TM}, an alternative representation of the acoustics of the ear has been discussed in the literature. The acoustic reflectance in the canal R_{EC} -- the ratio of the reflected (laterally traveling) and incident (medially traveling) pressure waves -- is a measure of ear function that is closely related to admittance (Keefe et al., 1993; Voss and Allen, 1994; Keefe, 1997; Burns et al., 1998), with possible clinical uses (e.g., Levi et al., 1998).[10] The power reflectance $|R_{EC}|^2$ is thought to be insensitive to variations in measurement location (and in this way superior to admittance), because the energy lost in propagation through the canal is assumed to be small (Stinson et al., 1982, p. 766; Hudde, 1983, p. 246; Keefe et al., 1993, p. 2617; Voss and Allen, 1994, pp. 372-373). However, while $|R_{EC}|^2$ describes the flow of acoustic energy in the canal, this measure fails to describe some basic properties of the middle ear that are characterized by Y_{TM} (e.g., net compliance). In this work, relating the middle ear's acoustic properties to structure depends critically on being able to separate the acoustic effects of the canal space from the acoustic effects of the rest of the ear (Keefe et al., 1993, p. 2632; Voss and Allen, 1994, p. 379; Huang et al., 1997b, Fig. 4 and Table II).

---

[9] The volume of the residual canal was estimated by a different approach. Rabinowitz (1981) estimated a volume from admittance measurements made with static pressures in the canal, and then the volume was adjusted such that (1) the TM compliance was consistent with the subjects' perceived loudness changes with static pressures, and (2) Y_{TM} was consistent with a representative ear-canal sound pressure gain function. In contrast, Møller (1965) and Zwislocki (1970) estimated the volume by filling the canal with alcohol from a calibrated syringe. In all three studies, a value between 7.5-8.0 mm was assumed for the diameter of the human ear canal.

[10] In a uniform tube supporting uniform plane waves, the reflectance (or pressure reflection coefficient) is uniquely determined by the admittance normalized by the characteristic admittance of the tube. In this work, this simplified model will be assumed; reflectance is calculated from the measured admittance, with the characteristic admittance determined by the canal diameter at the probe's tip. (See Section III B.)

In this chapter, we develop and test a method [similar to that used by Rabinowitz (1981) in human ears] for estimating Y_{TM} from measurements made in the intact ear canal. Admittance measurements made at different positions in test loads and in ear canals are used to determine the size of errors involved in the method and the frequency range for which the method is accurate. Reflectances are also computed from the data to test the assumption of small energy loss in the canal. The issues addressed in this paper are relevant to the general study of the ear's mechanics via non-invasive measurements in the ear canal. Possible applications include (1) broadband clinical measurement techniques (e.g., tympanometry) that account for the ear-canal space (Stevens et al., 1987) or employ static pressures (Wada et al., 1989; Keefe and Levi, 1996; Margolis and Keefe, 1997), (2) the design of earphones and stimuli for virtual auditory-space systems (Blauert, 1983, pp. 358-367; Chan et al., 1993), and (3) studies of middle and external-ear function that require non-invasive measurements for (e.g.) interspecies (Chapter 3) or developmental (Keefe et al., 1993) comparisons.

B. Approach

This chapter has two main goals: (1) to develop a non-invasive method for estimating the admittance at the TM that is compatible with a range of external-ear geometries; and (2) to test the method both in known loads and in ears to determine the size of errors and the frequency range for which the method is accurate.

The basic method involves connecting an acoustic system, consisting of an earphone (sound source) and a microphone, to an ear canal (Fig. 2.1). The sound source produces a broadband "chirp" stimulus, and the microphone measures the resulting sound pressure in the canal. With the source's output characteristics determined from measurements made in known calibration loads, the acoustic admittance in the canal at the probe's tip, Y_{EC}, can be determined as a function of frequency from the sound pressure. The desired measurement is Y_{TM}, the admittance at the TM, which can differ significantly from Y_{EC} (e.g., Rabinowitz, 1981, Figures 5 and 7; Huang et al., 1997b, Fig. 4).

The configuration of the acoustic system in the ear canal can affect the accuracy of Y_{EC} measurements in two ways. (1) The position of the microphone-tube tip relative to the earphone-tube tip is important, because nonuniform waves are generated at the earphone-tube tip. Extending the microphone tube a short distance beyond the earphone-tube tip (as in Fig. 2.1) seems to reduce the contribution of nonuniform components in the measured pressure (Rabinowitz, 1981; Keefe et al., 1992; Brass and Locke, 1997). We will demonstrate the effects of the microphone-tube extension on admittance measurements. (2) The cross-sectional area of the canal at the measurement location can vary substantially between ears. We will show that variations in canal area can affect the source's characteristics and the measured admittance. The basic problem is that the process of sealing the acoustic probe into the canal (Fig. 2.1) affects the structure of the source.

The effect of the ear canal's geometry on our ability to estimate Y_{TM} is a second key issue. The shape of the canal is rather complex, with changes in both cross-sectional area and axial direction (Shaw, 1974; Stinson, 1985; Rosowski et al., 1988; Rosowski, 1994, pp. 183-185). The human ear canal has been approximated as a uniform tube (Stinson et al., 1982) and as a horn (Stinson, 1985; Rabbitt, 1988; Stinson, 1990), for measuring and modeling the power reflectance and pressure distribution along the canal. To estimate the acoustic compliance and resistance of the middle ear from measurements in the canal, Keefe et al. (1993, p. 2628) subtracted a conical approximation of the canal's volume. In domestic cat, Rosowski et al. (1988) used a uniform-tube model of the ear canal to represent its contribution to external-ear radiation-impedance measurements. In non-invasive procedures, we do not have access to structural measurements of the ear canal. Therefore in this work, for simplicity, we use a uniform-tube (transmission line) model, which requires the estimation of only the "effective" length and cross-sectional area of the canal.

C. Overview

This chapter is presented in two parts. In Section I, the admittance-measurement method is developed and tested in known acoustic loads, with special attention to two measurement issues:

(1) the position of the microphone-tube tip; and (2) variations in ear-canal (load) diameter between subjects. Next, the admittance-location transformation is defined and tested in known loads. In Section II, the overall method for estimating the admittance at the TM from measurements in the intact external ear is tested on anesthetized domestic cats. The estimated Y_{TM} is compared quantitatively to the admittance measured at the TM after removal of the external ear canal.

I. DEVELOPMENT OF METHOD: TESTS IN KNOWN LOADS

A. Admittance-measurement method

1. Hardware

We chose an acoustic-probe system (Etymotic Research ER-10C) that has three main advantages. (1) The earphone and microphone are encased in a compartment (referred to as the "acoustic assembly"); this arrangement reduces the likelihood that the source's characteristics may change as a result of movement of its components or entry of extraneous material. (2) The driver pre-amp and microphone amplifier are housed in a small battery-powered box, so that the system is quite portable. (3) Etymotic has (at our request) added a tube in the acoustic assembly through which a static-pressure source can be coupled to the ear canal (see Fig. 2.1). This design allows acoustic measurements to be made with static-pressure variations in the canal. In this report, acoustic measurements are made with this system, unless otherwise specified.

The acoustic system is used to stimulate the ear and to measure the acoustic admittance in the ear canal.[11] The basic arrangement is that the earphone and microphone are connected to tubes that are sealed into the canal. In Fig. 2.1, the acoustic assembly is shown coupled to an Etymotic "eartip" that contains both the earphone and microphone tubes. The system is acoustically sealed into the canal with a compressible foam or rubber plug that surrounds the eartip. The plugs are

---

[11] Stimuli are generated and electric responses measured with an Ariel DSP-16+ board and SYSID (Ariel) software (Puria and Allen, 1992), as in Huang et al. (1997).

available in different sizes to allow insertion into a wide range of human ear canals, from infant to adult. An Etymotic eartip with a foam-plug seal was used for all measurements in Section I. Other types of eartips and sealants, designed for use with cats, are described in Section II B.

2. Source calibration

The acoustic source is characterized by a Norton equivalent circuit consisting of a volume velocity source U_S in parallel with a source admittance Y_S (Flanders, 1932; Møller, 1960; Rabinowitz, 1981; Rosowski et al., 1984; Ravicz et al., 1992; Lynch et al., 1994). These source parameters are determined from sound-pressure measurements made in two types of cylindrical calibration loads of known admittance: (1) 15-m-long tubes (acoustic transmission lines) made of tygon (flexible plastic), and (2) short closed cavities 6-12 mm in length made of plexiglass. The length of a closed-cavity load, measured with calipers to within 0.5-mm accuracy, is defined as the distance between the microphone-tube tip and the load's termination. The calibration-load theoretical admittances are calculated with a lossy transmission-line model (Egolf, 1977; White et al., 1980; Keefe, 1984; Allen, 1986; Zuercher et al., 1988). For a given load diameter, Y_S and U_S are determined uniquely from measurements made in the two loads (see Lynch et al., 1994, p. 2186).[12]

For an unknown acoustic load, the sound pressure P_L produced by the source in the load is measured and the admittance Y_L calculated as

$$Y_L = (U_S / P_L) - Y_S. \tag{2.1}$$

The measurement system can be tested on other acoustic loads of theoretically known admittance. In the next section, we report the accuracy of the admittance-measurement system within the context of two issues that complicate the method.

---

[12] Some authors have used schemes in which measurements from four or more loads are used to create an overdetermined system of equations for the source parameters (Allen, 1986; Keefe et al., 1992). An advantage of this method is that the user does not need to determine the lengths of the calibration loads accurately.

B. Complications

1. Position of the microphone-tube tip

a. Background

In the standard Etymotic system, both the earphone and microphone tube openings are flush with the eartip termination and the surface of a foam or rubber seal. Trial admittance measurements with this configuration in test loads had significant errors above 1 kHz, particularly for loads having large diameters (10-12 mm). We found that accuracy was greatly improved by extending the microphone tube beyond the eartip termination (and earphone-tube tip) via a short section of steel tubing. The desirability of a microphone-tube extension has been reported for other acoustic-admittance probes (Rabinowitz, 1981; Keefe et al., 1992).

The common interpretation of this effect is that extending the microphone tube reduces the contribution of nonuniform waves in the vicinity of the microphone-tube tip. The small relative diameter of the earphone tube (0.5 mm) as compared to the load diameters (5-12 mm) leads to significant radial spreading of the driving acoustic wave into the load. This spreading requires nonuniform sound-pressure waves near the interface between the earphone tube and the load, where there is a large discontinuity in cross-sectional area (Miles, 1946; Ingard, 1948; Morse and Ingard, 1968; Karal, 1953). Brass and Locke (1997) performed a theoretical analysis in which they predicted the maximum contribution of nonuniform sound-pressure waves for different earphone and microphone tube configurations. Nonuniformities in the wave field can interfere with the uniform-plane wave assumption of the admittance-measurement scheme, leading to errors in calculated admittance. Since, for the frequencies of interest ($f < 10$ kHz), these nonuniform waves are "evanescent" or "cut off" (i.e., they decay exponentially with distance) in the canal, the extension of the microphone tube allows measurement of the sound pressure in a region of more nearly uniform plane waves. The spatial dependence of nonuniform waves is described in more detail in the following section.

b. Choice of microphone-tube extension length

An appropriate length for the microphone-tube extension can be estimated theoretically by considering how a sound-pressure wave's components vary along the axis (call it z) of a rigid cylindrical tube of radius a. In the sinusoidal steady state, solutions of the wave equation in cylindrical coordinates (r,φ,z) subject to the rigid-wall boundary condition have the form (adapted from Morse and Ingard, 1968)

$$P_{mn} = A \; \{\cos(m\varphi) \text{ or } \sin(m\varphi)\} \; J_m(\pi q_{mn} \, r/a) \, \exp(-j \, k_{mn} \, z) \, , \qquad (2.2)$$

where J_m is a Bessel function, πq_{mn} are the zeroes of $J_m{}'$ (the prime denotes a derivative with respect to the argument), A is a constant determined by the source, and m and n are integers. Eq. (2.2) represents one pressure component or "mode" whose spatial dependence is described by the mode number (m, n). The total pressure is the summation of these modes over (m, n), where $(0,0)$ is the uniform plane-wave component that we wish to measure. The dependence of each mode on axial distance z is controlled by the propagation wave number

$$k_{mn} = [(2\pi f/c)^2 - (\pi q_{mn}/a)^2]^{1/2} \, , \qquad (2.3)$$

where f is frequency and c is the speed of sound in air. For frequencies f below $f_{mn} = q_{mn} c/2a$ ("cutoff"), k_{mn} is imaginary and the (m, n) mode is evanescent (i.e., it decays exponentially with distance z).

In choosing an extension-tube length, a reasonable design criterion is that the nonuniform mode with the lowest cutoff frequency $[(1,0)]$ must decay by a factor of $1/e$ in this length, at the highest frequency of interest f_{max}. This length or "space constant" l_e is determined by setting the argument of the exponential in Eq. (2) equal to -1, with $m=1$, $n=0$. Substituting an expression for k_{10} from Eq. (2.3) gives

$$l_e = 1/(jk_{10}) = [(\pi q_{10}/a)^2 - (2\pi f_{max}/c)^2]^{-1/2} \, . \qquad (2.4)$$

We choose (1) f_{max}=10 kHz, because above this frequency, admittance-measurement accuracy is limited by other factors (see Section I B 3.), and (2) load diameter $2a = 12.5$ mm, the diameter of our largest test loads, which corresponds to a very large human ear canal. These values yield the greatest microphone-tube extension length needed: $l_e = 4.4$ mm. For an ear canal or test load having a smaller diameter, or for lower frequencies, the decay of the evanescent modes will be *more* rapid in z.

Although the above analysis assumes a circular ear-canal cross section, the results can be applied to more realistic (i.e., elliptical) canal geometries. For a given cross section, the cutoff frequency for nonuniform modes is largely determined by the greatest transverse dimension (Rabbitt and Friedrich, 1991). Thus, a microphone-tube extension of 4.4 mm should satisfy approximately the same criterion for an elliptical canal cross section with a major-axis length of 12.5 mm.

In our measurement systems, we created the extension in one of two ways: either (1) insertion of a section of steel tubing (inner diameter 1.9 mm) that fit snugly into the standard eartip's microphone tube; or (2) construction of special eartips consisting of separate earphone and microphone tubes made of tygon. The second configuration was used in cat ears for reasons developed in Section II B 3.

c. Effects of extension on measured admittance

Representative comparisons of admittance measurements and theory, and the resulting error ratios are shown in Fig. 2.2 for two test loads. Admittances were measured with and without a 4-mm microphone-tube extension, based on calibrations performed with and without the extension.[13] First, we focus on the left panels [Fig. 2.2(A)]. The test load is a rigidly-terminated tube with inner diameter 9.5 mm and length 30 mm (measured from the microphone-tube tip to the

---

[13] Repeated admittance measurements of these test loads (e.g., on different days) were quite repeatable with variations of less than 10% in magnitude and 0.03 periods in angle.

termination). This load provides a test of the system's ability to measure (1) the compliance of an earlike equivalent volume of air (roughly 2 cm^3) and (2) sharp midfrequency features such as the middle-ear cavity antiresonance present in cats near 4 kHz (Guinan and Peake, 1967; Lynch, 1981; Lynch et al., 1994; Huang et al., 1997). The theoretical admittance of the load was calculated with the lossy transmission-line model.

For frequencies below 1 kHz, the microphone-tube extension has little effect, as both source configurations do a good job of estimating the magnitude and angle of the load admittance [Fig. 2.2(A)]. Above 1 kHz, in constrast, the accuracy in admittance is generally greater with the extension than without the extension [Fig. 2.2(A), lower panel]. Without the extension, the errors are quite large above 2 kHz; the measurement underestimates the frequency of the admittance-magnitude maximum (a quarter-wave resonance) near 3 kHz by 20%, which is consistent with the addition of a series mass ("spreading inertance") associated with the nonuniform wave components (see Ingard, 1948; Karal, 1953). The measurement also fails grossly to approximate the shape of the admittance-magnitude minimum (a half-wave antiresonance) near 6 kHz, which we attribute to nonuniform waves at the microphone-tube tip that lead to errors both in the source parameters (Y_S and U_S) and in the measured pressure. Near 6 kHz, errors in the source admittance Y_S lead to particularly large errors in the measured admittance Y_L, because the load admittance is much smaller in magnitude than Y_S (Lynch et al., 1994).

With the microphone-tube extension, the measured and theoretical curves agree to within 15% (1.5 dB) in magnitude and 0.04 periods in angle up to 8 kHz, except near the frequencies of the extrema (3 and 6 kHz) where the errors are larger. Near these frequencies, small errors in the model load's length lead to large errors in the theoretical admittance. For frequencies above 8 kHz, the accuracy may be limited by (1) residual nonuniform-wave contributions to the pressures measured in the test load and in the calibration loads (see Section I B 1 d), and (2) crosstalk between the earphone and microphone (see Section II B 3 b.). The signal-to-noise ratio is not a

problem for this frequency range; in the 6-10 kHz region, the noise floor of our measurements is generally 20-30 dB below the signal.

For the right panels [Fig. 2.2(B)], the test load has the same inner diameter (9.5 mm) and is designed to respond more like a human ear for higher frequencies. The load consists of a section of tube (length 12 mm) terminated by an acoustic resistor leading to a section of closed tube (length 10 mm). The resistor is made from four Knowles BF-series acoustic dampers (each nominally 150 mks MΩ) inserted in parallel into a thin teflon disk that fits snugly in the tube. The total resistance is nominally 37.5 mks MΩ, and the volume of the closed-tube section, or backing cavity, is 0.7 cm^3. The resistance and cavity compliance values were chosen to approximate the resistance and compliance of the human middle ear (Zwislocki, 1970; Rabinowitz, 1981), while the tube section into which the probe is inserted approximates the ear canal.

For the theoretical admittance, the tube sections were modeled as lossy transmission lines, and a series resistance-mass lumped model was used for each of the four parallel Knowles dampers. The nominal resistance value (150 MΩ) was used. The mass value was obtained from the dimensions of the small tube that holds each damper (length 2.4 mm, inner diameter 2.0 mm). Accounting for the end corrections, the mass value used was 1606 kg/m^4 for each damper (Beranek, 1986, pp. 137-138). In this resistance-mass model, the discontinuity in area between the closed 9.5-mm-diameter tube and each small damper is accounted for in the end correction. This model differs from that used by Voss and Allen (1994) in that this model has no free parameters. The theoretical admittance is similar to admittances measured in human ear canals (Keefe et al., 1993; Voss and Allen, 1994) -- roughly compliancelike for a large frequency range, with a sharp negative phase transition above 7 kHz [see Fig. 2.2(B), upper panel].

Above 3 kHz, admittance measurements made in this load without a microphone-tube extension have larger errors than those made with an extension, particularly in phase [Fig. 2.2(B), lower panel]. Measurements made with the extension generally agree with the theoretical curves to within 25% (2.5 dB) in magnitude and 0.06 periods in angle up to 8 kHz (except for the magnitude

46

between 5-6 kHz). In contrast, measurements made without the extension differ from theory by 56% (7 dB) in magnitude and 0.27 periods in angle at 7 kHz. These results demonstrate that the microphone-tube extension is crucial for accurate admittance measurements above 3 kHz in an earlike load.

d. Effects of extension on inferred admittance at the termination

A goal of this paper is to test a method for inferring the admittance at the tympanic membrane from measurements made more laterally in the ear canal. The method uses a transmission-line transformation (Section I C). An important issue to address is the effect of the microphone-tube extension on this admittance-location transformation. That is, in a test load, we wish to compare the transformation of a measurement made with the extension to the same transformation of a measurement made without the extension. Here, we report the effects of the extension on an admittance transformation in the human-earlike load of Fig. 2.2(B).

In Fig. 2.3 we plot the inferred admittance at the "termination" -- the resistor and backing cavity, 12 mm from the measurement point -- based on the measurements in the upper panel of Fig. 2.2(B) made with and without an extension. The estimate with the extension is accurate to higher frequencies than the estimate without the extension. With the extension, the inferred admittance generally agrees with the theoretical within 25% (2.5 dB) in magnitude and 0.06 periods in angle for frequencies up to 6 kHz. With no extension, the inferred admittance has the same accuracy for frequencies up to only 3 kHz. The added frequency range could be essential for detecting middle-ear acoustic features in the 3-5 kHz range.

The frequencies at which the measurements diverge from theory are more clearly defined in Fig. 2.3 than in Fig. 2.2(B). Also, the errors are generally larger in these inferred admittances. We wish to understand the source of these errors and implications for measurements in an ear canal of roughly the same size (length 12 mm, diameter 9.5 mm). That is, are these errors the result of errors in the original measurements, or are they introduced by the location transformation?

Our hypothesis is that the main source of errors above 3 kHz (see solid curves in Fig. 2.3) is the presence of nonuniform waves associated with the narrow earphone tube, in the original measurements. To test this idea, we made similar measurements with a different acoustic system, referred to here as the "large source"; this custom-built system is capable of measuring admittance up to 15 kHz (Huang et al., 1997b). The volume velocity U_S and source admittance Y_S of the large source are similar in magnitude to those of the ER-10C between 3-10 kHz. The main differences between the large source and the ER-10C are (1) the earphone's output port is much larger, having a diameter of 4 mm versus 0.5 mm for the ER-10C, and (2) the microphone-tube tip is centered within the earphone port. Although the large, rigid tip of this source is not compatible with most external-ear geometries, it should generate smaller nonuniform-wave modes, because the area discontinuity between the source and the load is smaller (e.g., Karal, 1953).

In Fig. 2.3, the dotted curve is the admittance measured using the large source positioned 8 mm from the termination and transformed to the termination. The inferred admittance agrees well with the theoretical up to 10 kHz. The greater accuracy of this estimate for higher frequencies indicates that (1) the location transformation is not the main source of errors for this load; and (2) the configuration of the earphone and microphone ports in the large source greatly reduces the measurement error above 3 kHz. This result is consistent with the hypothesis that the narrow earphone tube of the ER-10C system limits the accuracy of admittance measurements above 3 kHz.

In summary, our interpretation of the data of this section is that the microphone-tube extension *reduces* the effects of nonuniform-wave modes generated at the tip of the narrow earphone tube, but *does not eliminate* them for frequencies above 6 kHz. The result that the larger source (with about the same signal-to-noise ratio) measures admittance more accurately than the ER-10C above 6 kHz is consistent with the idea that nonuniform waves are a continuing problem for our measurement system (ER-10C) at higher frequencies.

2. Intersubject variations in ear-canal diameter

a. General configuration

Human ear canals can vary in diameter from 5-11 mm in infants and adults (Keefe et al., 1993). Figure 2.4 shows the Etymotic ER-10C system inserted into loads having diameters similar to that of an infant's ear canal [Fig. 2.4(A)] and an adult's ear canal [Fig. 2.4(B)]. The sound source undergoes two main changes from load (A) to load (B): (1) the volume of air space around the microphone-tube extension becomes greater; and (2) the seal fills a larger diameter and, as the material is a standard foam plug, the material is less compressed. These two factors can affect the characteristics of the effective source, as all components to the left of the vertical dashed lines are part of the source. Thus, the source parameters Y_S and U_S for load (A) are, in general, different from Y_S' and U_S' for load (B). In this section, we explore how diameter variations of the load affect the calibration of the source (i.e., Y_S and U_S) and the measurement of admittance.

b. Effects of diameter variations on source characteristics

For a given load diameter, the source parameters -- admittance Y_S and volume velocity U_S -- are determined from measurements in two calibration loads of known admittance. Figure 2.5 shows (A) Y_S and (B) U_S determined from measurements in calibration loads of three different diameters spanning the size range of interest. The source admittances are all roughly compliancelike up to 1 kHz, but they vary in frequency dependence for higher frequencies. The source-admittance magnitude increases monotonically with increasing diameter of the load (except for the largest diameter at the highest frequencies). The Y_S curves span a factor of about 3 in low-frequency magnitude associated with a factor of 4 change in cross-sectional area of the load. This result suggests that increasing the air volume around the microphone-tube extension and/or expanding the foam plug may result in larger contributions of these structures to $|Y_S|$. The U_S curves, in contrast, are fairly independent of the load diameter. An interpretation is that the volume-velocity source is determined mainly by the characteristics of the earphone and the dimensions of the narrow earphone tube.

49

Additional acoustic measurements were made to determine which structures contribute significantly to the source admittance Y_S. The basic approach consists of three steps: (1) approximating the air space around the microphone-tube extension by a lumped admittance, Y_{AIR}; (2) measuring the admittance of the foam-plug surface (looking back into the source), Y_{FOAM}; and (3) comparing Y_{AIR} and Y_{FOAM} to Y_S for different load diameters. For each diameter, Y_{AIR} was approximated as a lumped acoustic compliance determined by the volume of a cylinder of air having the length of the extension (4 mm). Also, for each diameter, Y_{FOAM} was measured by using a foam plug and eartip as a passive "load" on the measurement system. That is, the acoustic system was inserted into a tube that was terminated by a standard Etymotic foam plug and eartip (not coupled to an acoustic assembly) whose microphone and earphone tubes were blocked with acoustic putty at the foam surface. The admittance at the terminating foam surface (Y_{FOAM}) was inferred via a uniform-tube location transformation (Section I C). Admittances based on measurements at different distances from the foam surface differed in magnitude by as much as 40% above 2 kHz; hence, we took Y_{FOAM} to be the mean of estimates from three different locations along the tube.

Figure 2.6(A) shows a comparison of measured admittance contributions of the foam-plug surface (Y_{FOAM}) and the air space around the microphone-tube extension (Y_{AIR}), for two load diameters. For the smaller-diameter load (6.2 mm), $|Y_{FOAM}| < 0.5\ |Y_{AIR}|$ and therefore the foam contributes little to the source admittance, whereas for the larger-diameter load (9.5 mm) $|Y_{FOAM}|$ and $|Y_{AIR}|$ are approximately equal for some frequencies and thus the foam surface contributes significantly to the source admittance. Apparently, with the eartip compressed for insertion into the smaller-diameter loads, the foam-plug surface is effectively rigid.

A network model for the source admittance (Fig. 2.6, lower) consists of three components: Y_{FOAM} (dependent on diameter), Y_{AIR} (dependent on diameter), and Y_{EARTIP} (not dependent on diameter), such that

$$Y_S = Y_{FOAM} + Y_{AIR} + Y_{EARTIP}, \qquad (2.5a)$$

50

where Y_{EARTIP} represents the admittance looking back through the eartip and includes the contributions of the earphone tube, the microphone tube, and the microphone diaphragm. To test for the independence of Y_{EARTIP} on diameter, in Fig. 2.6(B) we compare Y_{EARTIP} for the two diameters, computed as

$$Y_{EARTIP} = Y_S - Y_{FOAM} - Y_{AIR}. \tag{2.5b}$$

The two curves are in good agreement to nearly 3 kHz; that is, in this frequency region, Y_{EARTIP} does not seem to depend on load diameter. For higher frequencies, there are large differences between the Y_{EARTIP} curves. A possible explanation is that the right side of Eq. (2.5b) is sensitive to small errors in Y_S, Y_{FOAM}, and Y_{AIR} if these quantities are nearly equal to one another. Above 3 kHz, Y_S [Fig. 2.5(A)] and Y_{AIR} are similar for the smaller diameter, and Y_S and $(Y_{FOAM}+Y_{AIR})$ are similar, particularly in their imaginary parts, for the larger diameter; thus, for this frequency range, the subtractions in Eq. (2.5b) can lead to large errors in Y_{EARTIP} . In summary, the three-component source-admittance model is consistent with the data for frequencies up to 3 kHz, with effects of load-diameter variations represented by changes in the admittances of (1) the air volume around the microphone-tube extension and (2) the foam-plug surface.

c. Effects of diameter variations on measured admittance

To characterize the acoustic system for measuring admittance in ears, the "calibration diameter" -- the diameter of the known calibration loads -- should be chosen equal to the ear canal's diameter at the measurement point. In practice, however, the canal diameter is neither known accurately nor constant. The dependence of the source characteristics on the load diameter suggests that uncertainty in the canal diameter can introduce errors in the measured admittance. The goal of this section is to quantify errors in the measured admittance that result from differences between calibration diameters and test-load diameters. The general size and frequency dependence of the resulting errors are applicable to ears.

Our basic approach is to compare measured admittances that are computed with source parameters based on different calibration diameters. Admittance measurements are shown in Fig. 2.7 for a closed cylindrical test cavity having inner diameter 6.2 mm and length 31.3 mm. The measurement with the "equal-diameter" calibration agrees well with the theoretical curve up to 9 kHz, whereas with the "larger-diameter" calibration the admittance magnitude is low by 15-20% below 0.6 kHz, and large errors occur in both magnitude and angle above 4 kHz. The low-frequency error results from attributing too great a fraction of the total acoustically "sensed" volume to the source and hence attributing too little volume (and compliance) to the load. The large higher-frequency errors are due in large part to the presence of the deep, sharp minimum in admittance magnitude near 5.5 kHz. In this frequency region, where $|Y_L| < |Y_S(d=9.5 \text{ mm})|$, the computed admittance is very sensitive to small errors in Y_S [see Eq. (1)], and the measurement has large errors and fails to capture the shape of the minimum. These results demonstrate that use of a calibration diameter of human-adult size for measuring admittance in an infant-sized canal can produce two types of errors: (1) a low-frequency compliance (or equivalent volume of air) error of 15-20%; and (2) a gross failure to capture the shape of minima in admittance magnitude in the midfrequency range. The latter error may apply to domestic cats (and other felid species), which have a sharp notch in middle-ear input admittance between 3-5 kHz.

Next, admittance errors introduced by variations in calibration diameter are examined for a test load with a smoother, more human-earlike frequency dependence in the midfrequency range. Figure 2.8 shows admittances measured in an artificial ear simulator (Zwislocki-type DB-100 coupler, Knowles Electronics, formerly Industrial Research Products). This load consists of a tube (inner diameter 7.5 mm) terminated by a microphone diaphragm, with four lossy, side-branch resonators within 5 mm of the termination.[14] We observe that differences in calibration diameter

---

[14] Measurements made in this particular simulator differ from the original specifications (Zwislocki, 1970) and from measurements made by Voss and Allen (1994). It seems likely that this simulator was defective, e.g., through dust buildup or damage. This defect is not crucial here, as the load needs only to have a more earlike admittance than a closed tube of the same equivalent volume (see Fig. 2.7), a criterion which it does satisfy.

of 25% lead to errors of approximately 15% in admittance magnitude below 2 kHz for the "larger-diameter" calibration, which is similar to the result in the compliancelike region in Fig. 2.7. For higher frequencies, the admittance errors are larger, on the order of 40% in magnitude and 0.2 periods in angle for the "smaller-diameter" calibration. These results demonstrate that differences of 25% in calibration diameter can lead to sizeable errors in both magnitude and angle -- particularly above 2 kHz -- in an adult-sized simulated ear canal.

To avoid admittance errors of this size in ears, the difference between the calibration diameter and the ear-canal diameter at the measurement point must be less than 25%. For test loads, we have found that the calibration diameter should be within 15% of the load diameter to measure the low-frequency magnitude within 10% and to capture the shape of sharp midfrequency features (such as in Fig. 2.7). For an ear canal, we apply the same rule and use a calibration diameter within 15% of the canal diameter estimated acoustically (Keefe et al., 1992); this procedure is described in greater detail below (Section II D 2).

C. Admittance-location transformation

1. Context

Having addressed above the issues in measuring Y_{EC}, we turn our attention to estimating Y_{TM} via an admittance-location transformation. The goals of this section are (1) to define the uniform-tube transformation and (2) to test its accuracy with a relatively simple acoustic load. (In fact, the results in Fig. 2.3 were obtained with this transformation, but the focus was the effect of the microphone-tube extension.) Here, we wish to demonstrate the "baseline" accuracy of the transformation, with a load in which the parameters of the transformation can be directly measured. The application to ears is described and tested later, in Section II.

2. Uniform-tube model

The transformation is defined in terms of locations along the ear canal. The acoustic system, with the eartip inserted into the external ear canal, measures the admittance Y_{EC} roughly

10 mm from the TM (Fig. 2.1). The desired quantity is the admittance Y_{TM} in the canal just lateral to the TM. To correct for the difference in location, a lossless cylindrical-tube model of the ear-canal space has been employed (Møller, 1965; Zwislocki, 1970; Rabinowitz, 1981; Lynch et al., 1994),

$$Y_{TM} = Y_0 \frac{Y_{EC} - jY_0 \tan(kl)}{Y_0 - jY_{EC} \tan(kl)},$$ (2.6)

where Y_{EC} is the admittance measured at the microphone-tube tip; $Y_0 = \pi a^2/(\rho_0 c)$ is the characteristic admittance of the tube, l is the length of the tube, a is the radius of the tube, $k = 2\pi f/c$ is the wave number, ρ_0 is the density of air, c is the propagation velocity of sound in air, f is the frequency, and $j = \sqrt{-1}$. [15] This transmission-line model has two parameters, the length l and radius a of the tube, corresponding to the effective dimensions of the ear-canal space. Discussion of the method for determining these parameter values in ears is deferred until Section II D.

3. Test of transformation in simulated ear canal

To test the accuracy of the admittance-location transformation with our modified ER-10C system, we used a stable acoustic configuration that *is* a uniform tube, the Zwislocki-type DB-100 ear coupler (see Fig. 2.8) and made admittance measurements at several positions along the length of the tube. The eartip's position was controlled by a micromanipulator and checked with calipers when possible. In Fig. 2.9, we report measurements made in the coupler at two positions 10 mm apart, and compare the more "medial" measurement (Y_{MEDIAL}) with an estimate obtained by applying the transformation (Eq. 2.6) to the more "lateral" measurement (Y_{EC}). The measured and estimated Y_{MEDIAL} curves agree within 20% in magnitude and 0.04 periods in angle up to 6 kHz. Above 6 kHz, the magnitudes start to separate, differing by 35% at 8 kHz.

---

[15] For the frequency range (0.1-10 kHz) and ear-canal diameters of interest (5-12 mm), the inclusion of viscous and thermal losses in the transmission-line model yields no significant differences from the lossless model.

The size of the higher-frequency differences between the measured and estimated Y_{MEDIAL} curves is similar to the size of errors in direct admittance measurements made in other test loads [e.g., the thick curves in Fig. 2.2(B)]. These errors are probably an effect of nonuniform waves generated at the earphone-tube tip in the test load and the calibration loads. The "large source" result in Fig. 2.3 shows that the location transformation does not necessarily introduce additional errors. Taken together, the results of Fig. 2.3 and Fig. 2.9 demonstrate that the "baseline" accuracy of the transformation is limited by the accuracy of our admittance-measurement system. That is, with an accurate description of a uniform-canal space, the transformation does not introduce additional errors.

II. TESTS OF THE METHOD IN EARS

A. Scheme of experiments

The main purpose of these experiments was to determine difficulties in applying the method to ears and to test the accuracy in estimating Y_{TM} with measurements in the external ear canal and at the TM. Admittance measurements were made in anesthetized domestic cats with two configurations of each ear (when possible): (1) in the intact external ear canal with varying static pressure in the canal; and (2) near the TM with varying static pressure, after surgical removal of most of the external ear canal. Measurements in configuration (1) were used to determine both Y_{EC} and the parameters of the ear-canal transformation [Eq. (2.6)] and thereby estimate Y_{TM}. The measurements in configuration (2) yielded a measured Y_{TM} and allowed quantitative comparisons to be made between the estimated Y_{TM} ["Y_{TM}(est.)"] from configuration (1) and the measured Y_{TM} ["Y_{TM}(meas.)"] from configuration (2). In this way, the overall accuracy of the method was assessed.

B. Methods and materials

1. Subjects

Treatment of experimental animals conformed to the guidelines of the National Institutes of Health, and experimental protocols were approved by the Animal Care committees at the Massachusetts Institute of Technology and at the Massachusetts Eye and Ear Infirmary.

Measurements were made on 8 adult domestic cats weighing between 2.4 and 3.3 kg (Table 2.1). In this report, individual subjects are referred to by the chronological order of experiments (1-8); the experiments were performed over the course of one year. Except where noted, the acoustic measurements reported were made on ears with clean ear canals, healthy-appearing, translucent TMs, no signs of middle-ear infection (as examined through an otoscope), and no indication of middle-ear static pressure buildup (based on repeated measurements over 5-10 minutes).

The kind of results obtained for each ear are summarized in Table 2.1. Although measurements were made on 12 ears (Cats 3-8) after development of the basic methods, experimental complications required the exclusion of 6 ears from tests of the admittance-location transformation: 3L, 4L, 5R, 6R, 6L, and 7R. The most common problems were (1) failure to obtain a stable seal of the eartip in the intact canal (Cats 1-4) and (2) damage to the TM (Cats 5-7).

2. Animal preparation

Cats 3-8 were anesthetized with intraperitoneal injections of Dial (75 mg/kg), with booster doses given as indicated by a withdrawal response to a toe pinch. Minimal exposures of both auditory bullae were made, to allow middle-ear cavity venting without disturbing the muscles of the pinnae. A scalpel was used to drill a small hole (diameter 1-2 mm) in the posterior part of each bulla, through which a plastic vent tube (inner diameter 0.3 mm, length 90-100 mm) was inserted and cemented to the bulla. Cats 5 and 6 exhibited some bleeding from the mucosal lining of the bulla; fluid and blood were periodically removed from the cavity by fine absorbent paper points.

For Cats 7 and 8, the bulla hole was made slightly larger to allow a cleaner incision in the mucosal layer, and the vent was inserted through a small metal nut cemented to the bone. There was no problem with bleeding in these two subjects. During the course of measurements, the vents were periodically removed to check for fluid in either the bullar cavity or the vent and then replaced. After measurements were completed in the intact external ear, the pinna flange, concha, and most of the cartilaginous ear canal were surgically removed to allow placement of the acoustic system in the short remaining portion of the ear canal, near the TM. This latter configuration is referred to as the "resected external ear".

Cats 1 and 2 were treated somewhat differently from the others, as they were also subjects for other experiments. In an initial session, acoustic measurements were made in the intact ear under Nembutal anesthesia, with no surgery performed. After the animal was recovered 10-14 days later, the external ear was resected on one side under Dial anesthesia. For Cat 1, measurements near the TM were made only with the middle-ear cavities opened (not reported here). For Cat 2, measurements near the TM were made with the bullar cavity vented but the middle-ear cavities otherwise intact.

3. Motivation for developing a custom eartip

a. Geometry of the cat's external ear

Initial attempts to insert and seal the acoustic system into intact ear canals were unsuccessful because of the geometry of the cat's external ear. The shape of the concha is quite complex; it narrows toward the entrance of the ear canal, and a sharp bend in the cartilaginous tube exists at the canal-concha border (Rosowski et al., 1988, p. 1699). This geometry makes it very difficult to visualize the eartip and the canal entrance as the eartip is inserted. As a result, in initial attempts the microphone-tube tip was often in the concha and/or a poor acoustic seal occurred.

We found that the standard Etymotic eartip (length 20 mm), when coupled to the acoustic assembly, was not long enough to reach through the concha and into the cat's ear canal. Also,

foam and rubber seals (Etymotic) were too large and/or too inflexible to navigate the sharp bend at the canal entrance. Consequently, we investigated the use of a longer eartip and a different type of seal for use with cats.

b. Earphone-microphone crosstalk

In developing an eartip for use with cats, we found that the length of the eartip affected the accuracy of admittance measurements. Measurements made with longer Etymotic eartips (30-35 mm) had large errors near the frequency of the admittance-magnitude maximum associated with the quarter-wave resonance of test loads. It was hypothesized that the errors were the result of low sound-pressure levels, which made crosstalk between the microphone tube and earphone tube significant. To test this idea, acoustic measurements were made to determine the level of the crosstalk.

Figure 2.10 shows microphone output voltages measured in a test load with the microphone tube open (normal) and plugged at its distal tip, for three different types of eartips. The microphone voltage response with the microphone tube plugged is an estimate of the "artifact" level, where artifact refers to the portion of the microphone output resulting from signals other than the sound pressure at the tip of the microphone tube. Possible sources of artifact include mechanical vibration, acoustic coupling through the wall of the earphone tube and the microphone tube, and electric coupling between the input to the earphone and output of the microphone. Artifact measurements were made with the eartip inserted into different loads (including free space) and were found to be essentially independent of the load. The dependence of artifact level on the type of eartip (demonstrated in Fig. 2.10) was repeatable and stable over time.

With the standard Etymotic eartip [Fig. 2.10(A)], the signal-to-artifact ratio is at least 30 dB except near the signal's sharp minimum near 3 kHz (quarter-wave resonance of the load), and above 7 kHz. For measurements in intact cat ears, an eartip with longer sound tubes is necessary to reach the ear canal. With a longer eartip of the same configuration (specially ordered from Etymotic), however, the artifact level increases in the midfrequencies, from 0.8-4 kHz [Fig.

2.10(B)]. In fact, a clear progression of increasing midfrequency artifact level occurs with eartips of increasing intermediate lengths (not shown). The measured signal at the location of the minimum near 3 kHz is primarily artifact, which would result in large errors in the measured admittance. Thus, in this case, it might be difficult to capture the shape of a sharp midfrequency feature such as the cat's middle-ear-cavity admittance minimum, whose effect in the ear canal can be a pressure *minimum* (Huang et al., 1997). Artifact levels were found to increase with increasing load diameter, because the sound-pressure level in a larger load is reduced whereas the artifact level is unchanged.

In response to this demonstration of significant artifact, we constructed custom eartips from separate earphone and microphone tubes made of tygon [Fig. 2.10(C)]. This eartip has a greater wall thickness between the microphone and earphone tubes than the Etymotic eartip and still couples easily to the ER-10C acoustic assembly. With this eartip, the measured artifact level is reduced in the range 0.5-4 kHz (to the noise level for 1-2 kHz), and is generally somewhat smaller than that of the standard Etymotic eartip for those frequencies. Our interpretation is that for the midfrequencies (1-6 kHz), the artifact observed with the longer eartip is the result of acoustic crosstalk between the microphone and earphone tubes. The custom eartip reduces the acoustic crosstalk and allows the pressure minimum to be resolved.

For frequencies above 7 kHz, all three artifact estimates increase sharply and are quantitatively similar (Fig. 2.10). This response is observed even when the microphone amplifier is switched off but is not seen when the stimulus is disconnected. These observations are consistent with the idea that in this frequency region, electric crosstalk in the acoustic assembly or the amplifier box dominates. This electric crosstalk, which could limit the accuracy of admittance measurements above 9-10 kHz, is not a serious constraint on our results because other problems make the acoustic measurements inaccurate in this high-frequency range.

4. Acoustic measurement procedures

a. Intact external ear

Insertion and sealing of the acoustic system into a cat's intact ear canal was a continual problem. The method is illustrated schematically in Fig. 2.11. The custom eartip consists of separate earphone and microphone tubes (length 30-35 mm), both of which pass through a flexible, conical "guide" made from Permatex Blue RTV silicone sealant. The guide keeps the tubes together and aids in sealing the eartip into the canal. Eartips with guides that narrow medially are easiest to insert into cat ear canals. A typical guide has length 10 mm, lateral diameter 7 mm, and medial diameter 5 mm.[16] An orthodontic rubber band (diameter 4.8 mm, force value 3.5 ounces) doubled around the tubes just lateral to the guide provides extra cohesion and support. The microphone tube protrudes 3-4 mm past the earphone-tube tip on the medial end.

Our measurement procedure for ears of domestic (as well as exotic) cats was as follows. First, the concha, ear canal, and TM were examined with an otoscope for wax or other irregularities (e.g., blood or mites). A mold was then made of the concha and the lateral portion of the ear canal in two steps. First a cotton dam was inserted into the canal with curved forceps to stop the flow of earmold material lateral to the TM. Second, hearing-aid earmold impression material (Westone) was injected into the concha via a large syringe. The earmold, which hardened in 3-4 minutes, provided a record of the size and shape of the concha and of the canal near the desired position of the acoustic probe. After examination of the earmold, the acoustic system was placed (by hand) such that the microphone-tube tip was just medial to the bend at the canal-concha border. Pulling the pinna flange in a posterodorsal direction tended to straighten the bend and facilitate the insertion of the eartip. Responses to a few acoustic stimulus presentations were

---

[16] To construct each guide, a thick coating of RTV silicone sealant is applied around the eartip near its distal end and shaped either (1) with a fine hand tool or (2) by inserting the eartip into an otoscope speculum for a smooth taper. The guide material cures in about a day.

viewed on an oscilloscope and the computer as quick indicators of the eartip's position and the patency of the sound tubes.

To form a static-pressure and acoustic seal, earmold impression material ("sealant") was injected into the concha behind the eartip guide (Fig. 2.11). As detailed in Section II E, it was crucial for the sealant to reach the guide and to fill the space directly lateral to the guide. After the sealant hardened, static pressure was introduced into the ear canal manually via another syringe and measured with a water manometer. If the static pressure was not stable, the acoustic system and sealant were removed from the ear and the insertion procedure repeated. With a functioning seal, admittances were measured with static pressures in the ear canal for two purposes: (1) to sense any buildup of static pressure in the middle ear; and (2) to determine the dimensions of the ear-canal space between the measurement point and the TM (see Section II D). Generally, the static-pressure level (in mm H_2O) was varied in steps from 0 to -300, 0 to +200 (+300 was not maintained in most ears), and back to 0. A few (2-4) admittance measurements were taken at each zero-static-pressure setting. Returning the static pressure to zero did not seem to restore the initial condition immediately; rather the admittance tended to "drift" back to within 20% of the initial measurement after 30-40 seconds. After completion of the measurement series, the acoustic system and seal were removed, examined, and compared with the initial earmold to give an indication of the eartip's position in the canal during the measurement.

With the custom eartip, the calibration of the acoustic system was slightly different from that reported in Section I (with standard Etymotic eartips), in both procedure and source characteristics. Measurements were made in two calibration loads and at least one test load with earmold sealant injected behind the eartip guide to approximate the configuration in the ear. A calibration was performed for each eartip, because of variability in the shape of the guides and the extent of the sealant in the ear.[17] The source admittance Y_S and volume velocity U_S associated

---

[17] In some ears, the sealant went past the lateral end of the guide, between the guide and the ear-canal wall. In some other ears, the sealant did not reach the guide.

61

with the custom eartips have some quantitative differences from those reported in Fig. 2.5: (1) Y_S has a different structure of local extrema from 1-4 kHz; and (2) $|U_S|$ is lower by 5-10 dB above 4 kHz. These differences are probably due to the greater length of the custom eartip. However, the trend with load diameter is the same, and the accuracy of admittance measurements in closed test loads is similar to that shown in Fig. 2.2(A) and Fig. 2.7 (see Chapter 3, Fig. 3.1).

b. Resected external ear

After completion of the intact-ear measurements, the external ear was resected 5-8 mm lateral to the bony ear canal and the acoustic admittance was measured within a few millimeters of the TM. For this location, a standard Etymotic eartip with a rubber seal was convenient to couple the acoustic assembly to the residual cartilaginous canal and to hold static pressures. A piece of steel tubing inserted into the distal end of the microphone tube served as a microphone-tube extension of 3-4 mm beyond the earphone-tube tip. Measurements were made with static pressures in the residual ear canal, as above, for the same purposes.

5. Operational difficulties

The overall success rate in intact cat ears was roughly 50%, where success is defined as a stable and complete acoustic and static-pressure seal of the eartip in the ear canal during admittance measurements. That is, in about half of the attempts, the acoustic system and sealant had to be removed, cleaned, and reinserted into the ear. The main reason for this fairly low success rate is the restrictive geometry of the cat's concha and canal (not accurately portrayed in Fig. 2.11). This geometry makes insertion of the eartip into the canal a time-consuming task on its own, even with the custom eartip and guide, because movement of the guide is impeded by complexities in the shape of the cartilaginous walls and the earphone and microphone tubes must be pushed and curved in the proper direction.

The narrow shape of the concha also impedes the placement of the syringe for injection of the sealant. For a complete seal, the sealant material needs to surround the earphone and

microphone tubes in the concha all the way to the lateral edge of the guide. Achievement of such a

seal often required several attempts and is a continuing problem. (The consequences of an

incomplete ear-canal seal -- i.e., one in which static pressure holds in the canal but the sealant does

not reach the guide -- are discussed in Section II E 2.) These operational difficulties were

overcome by repeated trials, in general.

C. Admittance measurements in ears

1. Intact external ear: Y_{EC}

Admittance measurements were made in each ear with the external ear intact. The

measurement location (distance to the TM) could vary substantially among ears. To indicate the

intersubject similarities and differences, admittances Y_{EC} (with zero static pressure) measured in 7

ears are plotted in Fig. 2.12. All of the admittances are roughly compliancelike for frequencies

below 1 kHz, except for Cat 4 whose angle deviates substantially from 0.25 periods above 0.3

kHz. The equivalent volumes derived from these compliances range over approximately a factor of

2, from 0.77-1.6 cm^3, but 5 of the 7 ears are within 0.9-1.1 cm^3. [In this report, acoustic-

compliance values C are computed from admittances Y by averaging $\mathrm{Im}\{Y\}/(2\pi f)$ over 10

frequency points f between 0.1-0.3 kHz, where $\mathrm{Im}\{\}$ denotes the imaginary part. The

compliances are expressed as equivalent volumes of air computed as $C(\rho_0 c^2)$, where ρ_0 is the

density of air and c is the speed of sound in air.] The midfrequency (1-4 kHz) admittance

magnitudes are qualitatively similar -- a broad peak around 1.5 kHz, a broad dip from 2-3 kHz,

and then increasing with frequency. Above 5 kHz, the curves diverge in both magnitude and

angle. These Y_{EC} measurements are the data which are transformed via Eq. (2.6) to estimate

admittances at the TM.

2. Resected external ear: Y_{TM}

Measurements of admittance at the TM with the external ear resected were made to test the

accuracy of the ear-canal transformation. Admittances Y_{TM} (measured at the TM with zero static

pressure) in 5 of the 7 cats (of Fig. 2.12) are plotted in Fig. 2.13. The admittances were measured within 5 mm of the TM and corrected for the short distance to the TM with the uniform-tube model, where the parameters were determined from measurements with static pressure (Section II D). The measurements are quantitatively similar to those reported by Lynch et al. (1994, Fig. 12), for frequencies below 6 kHz. The admittances are compliancelike below 1 kHz and range in equivalent volume from 0.35-0.6 cm^3. For 1-3 kHz, there is a broad local maximum in magnitude and a negative-going angle. A prominent notch occurs between 3.7-4.1 kHz at the frequency of the middle-ear cavity antiresonance. The depth of this notch is quite variable among ears. We also observe that the notch is not present in the admittances measured more laterally in the intact ears (Fig. 2.12); thus, accounting for the intact ear-canal space is crucial for resolution of this feature. The spread of the data is generally less than that of Fig. 2.12, particularly in the angles, which is consistent with smaller variability in the measurement location. However, between 6-9 kHz, variations among different ears are greater than those in Lynch et al. (1994). Possible reasons for this discrepancy include (1) normal intersubject variability and (2) greater errors in our admittance data due to the configuration of the acoustic source (see Sections I B 1 c-d, Figures 2.2 and 2.3).

D. Transformation from Y_{EC} to estimated Y_{TM}

1. Approach and preview

In this section, we discuss the procedure for selecting the parameter values [see Eq. (2.6)] used to transform Y_{EC} (Fig. 2.12) into Y_{TM}(est.), the estimated admittance at the TM. The procedure includes the measurement of admittances with varying static pressures, to estimate the volume of the canal space (Section II D 2 b). We then demonstrate the effects of small variations in the parameter values on the transformed admittance Y_{TM}(est.) (Section II D 3). Lastly, we demonstrate the repeatability of the transformation as applied to multiple insertions of the acoustic system into the same ear (Section II D 4).

64

2. Choice of uniform-tube parameters

a. Radius

The uniform-tube transformation [Eq. (2.6)] has two parameters, radius and length. For each ear, the parameter values were determined from acoustic measurements in the ear. First, the radius of the ear canal at the location of the microphone-tube tip was estimated from an algorithm described and tested (in artificial loads) by Keefe et al. (1992). Described briefly, the time-domain formulation assumes that the load is of sufficient length that the initial pressure recording (at "time zero", or the first sample in time) contains only a forward-going wave. This initial pressure is assumed to be determined entirely by the characteristic admittance of the load, which gives an approximate expression for the radius of the load

$$a = \sqrt{\frac{\rho_0 c}{\frac{\pi}{N} \sum_{i=1}^{N} \mathrm{Re}\{1/Y_L(i)\}}} \tag{2.7}$$

where Y_L is the measured load admittance, Re{ } denotes the real part, i is the frequency index, N is the number of frequency samples, and the summation arises from the inverse discrete Fourier transform evaluated at time zero.

For cat ear canals, we found that the algorithm gave radius estimates that were within 10% of estimates based on earmold impressions, provided the summation range was chosen so as to reject admittance points with negative real parts (which often occurred at the lowest and highest frequencies). Typically we used N=300 frequency samples, corresponding to a bandwidth of 0.1-7.4 kHz, because over this frequency range admittances measured in a test load were generally as accurate as the thick curves in Fig. 2.2(A). The final estimate of radius was taken as the mean of the estimates from all admittance measurements made with zero static pressure in the canal.

For a few ears (3), a calibration-iteration procedure was performed. If the acoustically estimated ear-canal diameter differed from the calibration-load diameter by more than 10%, a new acoustic calibration was performed (with calibration diameter equal to the estimate). The ear-canal

admittances were then recalculated with the new source parameters. From the new admittances, a new diameter was estimated from Eq. (2.7). In every case, the new diameter estimate "converged" to within 10% of the new calibration diameter. Our interpretation is that the new calibration gave a better approximation of the source parameters in these ear canals.

b. Length

Admittances measured with static pressures in the ear canal were used to estimate the volume of the canal space (and hence its length, given the radius above). Figure 2.14 shows admittances Y_{EC} from one domestic cat as a function of static-pressure level applied in the ear canal. For low frequencies, the admittance magnitude decreases monotonically with increasing levels of static pressure (of either sign) in the canal; thus, below 1 kHz the static pressure apparently stiffens the TM. For higher frequencies, the behavior of Y_{EC} with static pressure is more complicated -- strong asymmetries occur with respect to positive or negative pressures, including several sharp features in the positive-pressure admittances. Near 2 kHz, the admittance measured with static pressures is *greater* in magnitude than with zero pressure. These changes with static pressure are repeatable and representative of our data.

In the compliancelike region below 1 kHz, the changes in admittance magnitude with static pressure (Fig. 2.14) are generally smaller than those previously reported in cats (Møller, 1965, Fig. 11; Margolis et al., 1978, Fig. 4; Lynch, 1981, p. 250). An explanation is that in the previous studies, measurements were made within a few millimeters of the TM, whereas in Fig. 2.14 measurements were made in the intact ear canal at a more lateral position. As the total measured compliance is the sum of the canal compliance and the middle-ear compliance, we would expect the more lateral measurement to be less sensitive to changes in the TM stiffness. Thus, the direction of the discrepancy is consistent with the measurement location in the ear canal (see below).

In clinical admittance measurements, the volume of the canal space is approximated by the compliance or equivalent volume measured with large static pressures in the canal (Jerger, 1975;

Wilber and Feldman, 1976; Margolis and Shanks, 1985). The assumption (not adopted by Rabinowitz, 1981) is that the TM is made effectively rigid by large static pressures, at least for low frequencies. Data from our cats can be used to determine the accuracy of this approximation. In Fig. 2.15, compliances from the Y_{EC} curves of Fig. 2.14 are compared to compliances measured in the same ear *near the TM* (with most of the canal resected). Over the range of negative static pressures, the compliance in the intact canal ranges from 0.37-1.1 cm^3 (9.5 dB), while the compliance near the TM ranges from 0.05-0.73 cm^3 (23 dB). The difference between compliances measured at the two locations is equivalent to a "correction" volume that seems roughly independent of static-pressure level.

For both curves (Fig. 2.15), the compliances are lower for large negative pressures than for positive pressures of the same magnitude. This result suggests that negative pressures stiffen the middle ear more than positive pressures. For this reason, the compliance measured in the intact canal at the most negative static pressure would seem to give a better estimate of the canal volume than the compliance measured at the most positive pressure. Compliances in 7 ears measured near the TM at -300 mm H$_2$O are all less than 0.1 cm^3 (e.g., Fig. 2.15), which is consistent with the results of Lynch (1981, p. 249). As these values include a residual canal volume that is typically at least 0.05 cm^3 (Lynch et al., 1994, p. 2193), the compliance of the stiffened middle ear must be less than 0.1-0.05 = 0.05 cm^3, which is much smaller than the compliance measured in the intact canal for the same condition (e.g., 0.37 cm^3 in Fig. 2.15, which would lead to a maximum error of 14%). Thus, for large negative static pressures in the canal, assumption of a rigid TM at low frequencies seems to be reasonable for calculation of the canal volume.

In conclusion, the volume of the intact ear-canal space V_{EC} is estimated from the admittance Y_{EC} at low frequencies measured at the most negative static pressure (-300 or -400 mm H$_2$O) [consistent with the results of Shanks and Lilly (1981)]. The calculated compliance is converted into an equivalent volume of air. This volume (V_{EC}) and the radius estimate from above

(*a*) determine the length l of the model tube, $l = V_{EC}/(\pi a^2)$. The values of l and a then define the ear-canal transformation, from Eq. (2.6).

3. Effects of variations in parameter values

The sensitivity of the ear-canal transformation to variations in its parameters determines the effects of errors in the parameters. The effects of small changes in the length l and radius a were computed for three cats. Representative results are reported for one cat (Fig. 2.16). The result of the transformation [Y_{TM}(est.)] and the changes in Y_{TM}(est.) resulting from changes of $\pm 10\%$ in the parameter values are shown. In general, the admittance is more sensitive to the parameter variations for high frequencies than for low frequencies, and sharp spectral features are affected more than smooth spectral features. The depth of the admittance-magnitude notch near 4 kHz is strongly affected (by nearly a factor of 4), as is the size of the sharp phase transition at the notch frequency. The frequency of the notch, however, is only changed by $\pm 5\%$, and the low-frequency compliance or equivalent volume changes predictably. The general shapes of the magnitude and angle of Y_{TM}(est.) remain the same.

4. Effects of variations in eartip placement

If the admittance-location transformation is accurate, then the inferred admittance at the TM [Y_{TM}(est.)] should be independent of the location at which Y_{EC} is measured. Here, we report measurements that test this expected invariance as well as the repeatability of the canal measurement (Fig. 2.17). Two measurements made in each of two intact ears are plotted in the upper panels. For each ear, two "insertions" were made, where each insertion consisted of (1) coupling the acoustic system to the ear canal, (2) injecting the earmold material to form a static seal, and (3) measuring admittances with static pressures in the canal. The admittances Y_{EC} in the upper panels were measured with zero static pressure. The lower panels show the results of transforming the Y_{EC} curves in the upper panels to the location of the TM, Y_{TM}(est.).

The admittances Y_{EC} from different insertions in Cat 3 are similar in shape [Fig. 2.17(A), upper]; the two curves agree to within 40% in magnitude and 0.08 periods in angle. For Cat 8, however, the admittances Y_{EC} from different insertions are quite different quantitatively and in their shape [Fig. 2.17(B), upper]. One might conclude that the change in the position of the eartip in the ear canal was greater between insertions in Cat 8 than in Cat 3.

The ear-canal parameter values (dimensions) are larger for Cat 3 than for Cat 8, implying that Y_{EC} was measured farther from the TM in Cat 3 than in Cat 8. A domestic cat's mean ear-canal length (minimum distance between the medial and lateral ends) is 9.5 mm (Rosowski et al., 1988, p. 1699); with a circular cross-section approximation, the mean radius is 3.4 mm at the canal-concha boundary and 2.5 mm at the narrowest part. The parameter values used in Fig. 2.17 are consistent with these anatomical measurements. The inferred difference in eartip position between insertions is 3.8 mm for Cat 3 and 3 mm for Cat 8, yet the two Y_{EC} curves differ more in Cat 8. Our interpretation is that the Y_{EC} measurement in Cat 8 is more sensitive to the location difference because the eartip is closed to the TM.

The indication from the bottom panels (Fig. 2.17) is that the overall method gives repeatable results for frequencies up to roughly 5 kHz. For both ears, the two Y_{TM}(est.) curves are similar in shape and agree quantitatively -- generally within 20% in magnitude and 0.05 periods in angle -- in this frequency range. Thus, the main message is that variations in measurement location between source insertions are accounted for by the transformation procedure. Near the midfrequency notch in admittance magnitude and for higher frequencies, the differences between the estimates are larger, which suggests that the error in the method is greater.

E. Comparisons of estimated Y_{TM} to measured Y_{TM}

1. Illustrative cases

In this section, we test the overall accuracy of the method for estimating the admittance at the TM (Y_{TM}) in intact external ears. We report results from four cat ears. The results from these

ears were selected based on three criteria: (1) The state of the middle-ear cavities and TM was carefully monitored throughout the experiment; (2) the acoustic response to variations in static pressure was consistent and repeatable with both configurations of the external ear; and (3) the seal (earmold material) completely filled in the canal-concha space behind the eartip guide. Measurements were made in 7 ears that failed to meet one or more of these criteria (see Table 2.1). Of these, 4 ears suffered from unstable preparations (damaged TM or blood in the middle-ear cavities), 2 ears showed unstable (not repeatable) changes with static pressure, and in 3 ears the seal did not completely fill in the space behind the eartip (discussed in Section II E 2).

Figure 2.18 shows comparisons of Y_{TM} (est.) to the measured admittance at the TM (with resected external ear, as in Fig. 2.13), Y_{TM}(meas.). The parameters for the ear-canal transformation are given in each plot. The parameters imply that the Y_{EC} measurements were made 7-10 mm lateral to the TM, which is roughly consistent with independent estimates based on earmolds and otoscope examinations. The Y_{TM}(meas.) curves were corrected for the residual canal space, typically 3-4 mm in length and 2.5-3 mm in radius. These admittances are regarded as the "true" Y_{TM}. In Fig. 2.19, the error ratios of Y_{TM}(est.) to Y_{TM}(meas.) are plotted for the same ears.

In general, the estimated and measured admittances are similar in shape below 5 kHz, with some quantitative differences (Fig. 2.18). In all 4 ears, Y_{TM}(est.) is compliancelike for frequencies below 1 kHz and exhibits a notch in magnitude and a positive angle transition between 3-4 kHz. The Y_{TM}(meas.) curves share these features, although there are differences of at least a factor of 2 (6 dB) in the notch-frequency region for 3 ears, and |Y_{TM}(est.)| is overestimated by 25-35% (2-2.5 dB) below 0.5 kHz for 2 ears. Except for Cat 7 (see below), the errors below 2 kHz are all less than 5 dB in magnitude and 0.08 periods in angle, and are in fact generally less than 3 dB and 0.05 periods (Fig. 2.19).

Above 5 kHz, the estimated and measured curves diverge quantitatively and exhibit large variations with frequency (Fig. 2.18). At 8 kHz, all 4 ears have errors of at least 8 dB in

magnitude and 0.15 periods in angle, with some ears having much greater errors. For these

frequencies, our measurements suggest two contributors to these errors: (1) the measurements of

Y_{EC} that the estimates are based on have increased errors; and (2) Y_{TM}(est.) is sensitive to small

errors in the ear-canal transformation parameters (see Fig. 2.16).

The Y_{TM}(meas.) curve from Cat 7 [Fig. 2.18(B)] has some sharp features between 0.7-2

kHz that could be the result of a physical change in the TM. At the end of the external-ear

measurement series, sharp features were observed in the sound-pressure response below 1 kHz.

The TM was examined with an otoscope, and a small spot of blood was observed on the

anterodorsal quadrant of the TM. The blood was not present in earlier observations of the TM.

After resection of the external ear, measurements made near the TM consistently showed the sharp

features in Fig. 2.18(B). Hence, our interpretation is that a small change in the TM between the

measurement of Y_{EC} and Y_{TM} was the source of this difference. Still, Y_{TM}(meas.) for this ear

has features that are within the "normal" range, as compared with Fig. 2.13 as well as Lynch et al.

(1994): (1) an equivalent volume of 0.45 cm^3, and (2) a prominent notch and sharp angle transition

near 4 kHz. In addition, variations in measured compliance with static pressure in this ear were

similar to those shown in Fig. 2.15.

2. Effects of an incomplete ear-canal seal

The consequences of an incomplete earmold-sealant injection are shown in Fig. 2.20. For

frequencies between 2-4 kHz, the error in admittance magnitude is greater than 5 dB. The notch in

magnitude near 4 kHz [in Y_{TM}(meas.)] is not captured in Y_{TM}(est.), and the error approaches 20

dB (factor of 10) at this frequency. A clear difference in the coupling of the acoustic system in this

ear (compared to the ears in Fig. 2.18) is that the earmold material did not completely fill the space

lateral to the eartip guide. Thus, although static pressure was stable, it is likely that extra volume

lateral to the eartip was acoustically coupled to the ear canal and therefore affected the admittance

measurements. This explanation is consistent with the estimated ear-canal length (chosen to match

the canal-volume estimate, given a radius estimate) being unrealistically large, 25 mm; in our experience, a domestic cat's ear canal never exceeds 20 mm in length.

This result is instructive because it indicates a way to assess the quality of the ear-canal seal, independent of the acoustic response. Results from two other ears (not reported here) had errors similar to those in Fig. 2.20 and shared the common feature that the seal did not completely fill in the space behind the eartip guide. We conclude that it is crucial for the earmold material to fill the space in the canal behind the guide and around the sound tubes. Care must be taken to place the tip of the earmold syringe deeply into the concha -- as close as possible to the eartip guide -- before injecting around the sound tubes. Upon removal of the acoustic system, the configuration of the seal around the eartip can be examined. If the seal does not fill the space behind the eartip, the data from that measurement series should, in general, be rejected.

III. DISCUSSION AND CONCLUSIONS

A. Conclusions on methodological issues

1. Admittance-measurement system

(1) If the earphone port is much smaller in diameter than the ear canal (as in the ER-10C system), then extending the microphone tube 3-4 mm past the earphone port is crucial for accurate admittance measurements above 2 kHz (Fig. 2.2).

(2) The main source of errors above 2 kHz is the large discontinuity in cross-sectional area between the earphone tube and the load, which generates nonuniform waves. The microphone-tube extension improves admittance accuracy for higher frequencies, but it does not eliminate the problem above 6 kHz. The evidence for this conclusion includes (a) increased accuracy of an acoustic source whose earphone port is much larger than that of the ER-10C (Fig. 2.3), (b) slightly larger errors in admittance for larger load diameters (compare Fig. 2.2(A) and Fig. 2.7), and (c)

the rejection of other possible error sources in this frequency range such as low signal-to-noise ratio and crosstalk between the earphone and microphone (Fig. 2.10).

(3) The source admittance depends greatly on the diameter of the ear canal or load; its magnitude increases with increasing diameter [Fig. 2.5(A)]. Thus, knowledge of the ear-canal diameter is essential in the acoustic-calibration procedure for a source of this configuration (extended microphone tube and flexible seal).

(4) To avoid large errors in admittance, particularly above 3 kHz (Fig. 2.8), the calibration measurements should be made in loads having diameter within 10-15% of the canal diameter.

2. Admittance-location transformation in ears

(1) Tests in domestic cats show that the method is generally accurate for frequencies up to 5 kHz, with larger errors occurring for higher frequencies. The estimated canal dimensions (in Fig. 2.18) are roughly consistent with structural measurements in domestic-cat ears (Rosowski et al., 1988).[18]

(2) Above 5 kHz, there are three main sources of error. First, our admittance measurements in test loads have increasing errors above 6 kHz that are probably due to nonuniform waves. Second, the ear-canal transformation becomes more sensitive to small errors in its parameters above 2 kHz (Fig. 2.16), although the frequency of the notch is relatively unaffected. Third, the irregular geometry of the canal might introduce greater errors for higher frequencies, for two reasons. (a) Consider the shape of the canal space at the location of the microphone-tube tip. This geometry (and its effect on the eartip guide -- see Fig. 2.11) is part of the source, but the source is calibrated in smooth cylindrical loads. This structural discrepancy

---

[18] Ear-canal molds reported by Rosowski et al. (1988, Table I, p. 1699) had minimum cross-sectional area at a point about midway between the canal-concha boundary and the TM. A tube model of the canal with this small radius (2.5 mm) represented radiation-impedance measurements of the external ear fairly well. Here, in contrast, a larger radius tends to be used in the admittance-location transformation [e.g., 3.5 mm in Fig. 2.17(A)], which is consistent with reported dimensions of the canal-concha interface.

might be significant at higher frequencies. (b) The comparison of a tube model to a canal impedance measurement in Rosowski et al. (1988, Fig. 11) suggests that errors resulting from the approximation of the canal as a uniform tube increase above 6 kHz.

3. Design improvements and further work

(1) The magnitude of nonuniform modes generated by the narrow earphone tube can be reduced with a high-impedance acoustic system with a larger earphone port. The earphone and microphone tubes should be housed in an eartip that remains flexible and can be sealed in intact external ear canals of different sizes.

(2) A smaller acoustic assembly (or considerably longer eartips) would facilitate the placement and sealing of the acoustic system in the intact ear canals of cats (and possibly other species). The assembly's present size limits its mobility in the concha and makes the insertion of both the eartip and the syringe for injection of sealant difficult.

(3) Obtaining a stable and complete (i.e., space-filling) seal in the intact canal of cats is a continuing problem. The main reason is the deep, narrow concha and sharp bend at the canal-concha border. In this work, we have endured a fairly low success rate per eartip insertion (roughly 50%) by repeated trials. It might be possible to design a different method for sealing the acoustic system in the canal, e.g., through use of an inflatable cuff around the eartip that can be controlled from outside the canal and concha (Rabinowitz, 1981). Failing that approach, different sealant materials could be tested for their facility in reaching the eartip guide. For example, a more fluid material might flow more easily past the canal bend and fill in the space behind the guide more completely.

(4) Further measurements could be made to test the strength of nonuniform wave components, e.g., by varying the length of the microphone-tube extension. It is also possible that the use of a calibration load of greater length (> 8-10 mm) would reduce the effects of nonuniform waves on the source calibration. Keefe et al. (1992) described (but did not demonstrate)

"evanescent mode interactions between the ends of the tubes," that degraded accuracy when the diameter-to-length ratio of the load was greater than 0.3. However, a longer calibration load would introduce sharp resonances in the frequency range of interest.

(5) Further measurements could be made to quantify the effects of the nonuniform ear canal: e.g., admittance measurements in a rigid-walled negative mold of the canal, or admittance measurements with the TM braced by fluid in the tympanic cavity to see how well the data can be represented by a closed uniform-tube model.

B. Reflectance in the ear canal

At any position along the ear-canal axis, the pressure reflectance (or reflection coefficient) R in the ear canal is related to the admittance measured at that position Y_L by the expression

$$R = \frac{Y_0 - Y_L}{Y_0 + Y_L} , \tag{2.8}$$

where Y_0 is the characteristic admittance of the canal. For a given position in the canal, the quantity $|R|^2$ -- the squared magnitude of the pressure reflectance, or "power reflectance" -- is the fraction of the incident acoustic power that is reflected. Interpretation of reflectance data in the literature often assumes that $|R|^2$ is approximately independent of position in the canal, i.e., that energy dissipation in the canal is small (e.g., Keefe et al., 1993; Voss and Allen, 1994). In fact, little direct evidence exists to support this assumption.

Our admittance measurements in the external ear canal and at the TM (in the same ear) can be used to test the idea that $|R|^2$ is independent of the measurement position in the ear canal. Figure 2.21 shows the power reflectances computed for the 4 ears of Fig. 2.18 at the TM and in the intact ear canal. For convenience of notation, let $|R_{TM}|^2$ be the power reflectance at the TM, calculated from Eq. (2.8) with $Y_L = Y_{TM}$ and the estimated canal diameter at the TM; let $|R_{EC}|^2$ be the power reflectance at the more lateral position in the ear canal, calculated from Eq. (2.8) with $Y_L = Y_{EC}$ and the estimated external ear-canal diameter. In each case, the canal diameter estimate is from Eq. (2.7).

For each ear (with the same caveat for Cat 7 as in Section II E 1), $|R_{TM}|^2$ and $|R_{EC}|^2$ are quantitatively similar below 5 kHz (Fig. 2.21). All of the reflectances show a broad minimum near 2 kHz and a sharper peak between 3-4 kHz. At the minimum, the middle-ear input admittance is most closely matched to the characteristic admittance of the canal, and power transfer from the canal to the middle ear is maximized at 70-80%. The sharper peak results from the middle-ear cavity antiresonance and corresponds in frequency to the sharp admittance notch in the data of Fig. 2.18 (see also Lynch et al., 1994, Figs. 22 and 23). The similarity of these spectral features in each pair of reflectance curves is consistent with the assumption of spatial independence.

Is there any evidence here that disagrees with a lossless-canal assumption? The differences between $|R_{TM}|^2$ and $|R_{EC}|^2$ for frequencies between 1-6 kHz can be accounted for by variations of $\pm 10\%$ in ear-canal diameter, which is within our tolerance. However, for $f=0.5$ kHz, all 4 ears show $|R_{TM}|^2 > |R_{EC}|^2$, and this result is *not* affected by small variations (10%) in diameter, except for Cat 8 (left ear). For this frequency, the values of $|R_{TM}|^2 - |R_{EC}|^2$ for Fig. 2.21(A-D) are 0.13, 0.16, 0.05, and 0.11 respectively, for a mean value of 0.11. For comparison, we computed reflectances from the admittances measured at different locations in the Zwislocki ear simulator [Fig. 2.21(A)]. The difference between power reflectances measured 10 mm apart in the simulated canal is less than 0.02 for frequencies up to 1 kHz.

Our interpretation is that at 0.5 kHz, approximately 11% of the incident power is dissipated in the cat's ear canal. At this frequency, the dissipation from viscous and thermal losses is not nearly enough to account for this result based on use of the estimated canal lengths, radii, and the properties of air as input to a lossy transmission-line model. Therefore, although the data do not provide a clear test of ear-canal losses over most of the frequency range, they point to another loss mechanism (e.g., non-rigid behavior of the canal walls, or complexities in the canal's shape) as significant near 0.5 kHz.

C. Measuring features of the middle-ear input admittance

In this section, we evaluate the accuracy of the measurement method for specific features of Y_{TM}. Table 2.2 summarizes the size of errors, for the ears in Fig. 2.18, in measuring 6 middle-ear admittance features of interest. The mean error in total middle-ear acoustic compliance is 14%. The mean low-frequency (0.22 kHz) magnitude error is 21%, and the error in the frequency of the admittance notch is 5%. In the frequency region of the notch (3-5 kHz), errors in admittance magnitude are very large because of the sharp changes in magnitude with frequency. (For discussion of the possible functional significance of these features, see Chapter 3, Section III.) For a given net compliance, the lowest frequency for which the angle is 1/8 of a period or 45 degrees ($f_{45^{\circ}}$) is a measure of the resistance of the middle ear and cochlea and is estimated with an error of 30%; the frequency tends to be underestimated, i.e., the resistance tends to be overestimated, which is consistent with the idea that ear-canal losses seem to be significant for low frequencies (see Section III B).

The low-frequency values of $|Y_{TM}|$ (and derived net compliances) tend to be overestimated. A possible reason for the error is that the volume estimate from the measurement in the external ear with -300 mm H_2O (Fig. 2.14) is low, because of either (1) displacement of the TM in a lateral direction or (2) constriction or stiffening of the ear-canal walls. Explanation (1) can be rejected from a fairly simple argument: With a one-dimensional piston-in-a-cylinder approximation, the TM displacement is the product of the TM's mechanical compliance, the static pressure acting on the TM, and the TM area. With the values 4.45 mm/N for the TM compliance (mechanical analog of 1 cm^3 acoustic equivalent volume of air -- see domestic-cat data in Chapter 3, Fig. 3.9), 2940 Pa for the pressure acting on the TM (-300 mm H_2O), and 40 mm^2 for the TM area (Rosowski et al., 1988; Huang et al., 1997b, Table I), the TM displacement would be 0.5 mm. Assuming a canal radius of 2.5 mm, the resulting volume change would be less than 0.01 cm^3, which is very small compared to the estimated canal volumes (0.2-0.4 cm^3).

However, explanation (2) cannot be rejected from the available data. Fig. 2.15 shows a decrease of 14% with negative static pressure in the equivalent volume enclosed between the intact-ear measurement point and a point near the TM. Of the three other ears in which this comparison can be made, two ears show decreases of 5-10% and one ear shows an increase of 6%. It seems possible that the mechanics of the cartilaginous-canal walls might affect our estimates of acoustic compliance (Keefe et al., 1993). Still, on the average, our error in estimating the net middle-ear compliance for low frequencies is ±14%, which is generally acceptable.

D. Application to comparative studies in live subjects

In this chapter, we have developed and tested a non-invasive method for measuring the input admittance of the middle ear, which characterizes the middle ear's acoustic performance. The basic method is designed for measurements in the intact ears of live subjects (humans or animals). We plan to apply the method to a comparative study of middle-ear acoustic performance in live, anesthetized species of the cat family. Measurements in these ears allow us to track features of middle-ear admittance and sound transmission across the family, so that we may begin to describe how auditory function is related to systematic variations in body size (Chapter 3). Ultimately, such a description may lead to tests of hypotheses that unify the structural, functional, and ecological variables that determine the role of hearing in the survival and evolution of these animals.

TABLE 2.1: Summary of measurements made and experimental problems encountered in 8 domestic cats (14 ears). Cats 1-2 were primarily used for development of methods; Cats 3-8 were used in experiments designed primarily to test the admittance-location transformation in the ear canal. Column 5 (rightmost) lists the admittances measured in each ear canal at 2 different locations: Y_{EC}, in the intact external canal, and Y_{TM}, near the TM after removal of most of the cartilaginous canal. Problems encountered are shown in parentheses following the affected measurements.

Cat	Sex	Weight (kg)	Ear	Measurements (experimental or methodological problems)
1	M	2.7	R	Method development: Y_{EC} (problems placing and sealing eartips of Etymotic configuration *), Y_{TM} (middle-ear cavities opened)
2	M	2.9	R	Method development: Y_{EC} (longer eartip of Etymotic configuration *), Y_{TM} (no microphone-tube extension)
3	F	3.2	R	Y_{EC}, Y_{TM}
			L	Y_{EC} (problems placing and sealing custom eartip *)
4	M	2.4	R	Y_{EC} (extra space included in seal **), Y_{TM}
			L	Y_{EC} (static-pressure leak), Y_{TM} (unstable changes with static pressure)
5	M	3.0	R	Y_{EC} (unstable changes with static pressure), Y_{TM} (TM slightly damaged)
			L	Y_{EC} (extra space included in seal **), Y_{TM} (slight bleeding in middle-ear cavities)
6	F	2.8	R	Y_{EC} (TM perforated, bleeding in middle-ear cavities)
			L	Y_{EC} (TM perforated, problems placing and sealing eartip)
7	M	3.1	R	Y_{EC} (TM damaged), Y_{TM} (TM damaged)
			L	Y_{EC}, Y_{TM} (change in TM suspected ***)
8	F	3.3	R	Y_{EC}, Y_{TM}
			L	Y_{EC}, Y_{TM}

* See Section II B 3 and Fig. 2.10 for descriptions of different eartips.
** See Section II E 2.
*** See last paragraph of Section II E 1.

TABLE 2.2: Percent differences between the estimated Y_{TM} and the measured Y_{TM} curves for 4 ears (see Figs. 17 and 18): % Difference = (Estimated - Measured) / (Measured) X 100 %. Ears: "L" and "R" denote left and right ears; "(a)" and "(b)" denote different insertions of the probe in an ear. "Abs. mean" is the mean of the absolute values of the 6 errors in each row. The quantity C_{ME} is the total middle-ear acoustic compliance, computed as the average of $\mathrm{Im}\{Y_{TM}\}/(2\pi f)$ over 10 frequency points f between 0.1-0.3 kHz, where $\mathrm{Im}\{\}$ denotes the imaginary part. The quantity f_{Ynotch} is the frequency of the local minimum in admittance magnitude near 4 kHz. The "measured f_{Ynotch}" refers to comparing the admittances at the same frequency, f_{Ynotch} of the measured curve. The "respective f_{Ynotch}" refers to comparing the estimated Y_{TM} at the estimated curve's f_{Ynotch} to the measured Y_{TM} at the measured curve's f_{Ynotch}. The quantity $f_{45°}$ is the lowest frequency for which the angle of Y_{TM} is less than 1/8 of a period (45 degrees), except for Cat 7 for which the sharp dip in angle near 0.8 kHz was discounted.

% DIFFERENCES	Cat 3(a)	Cat 3(b)	Cat 7	Cat 8L	Cat 8R(a)	Cat 8R(b)	Abs. Mean
C_{ME}	16 %	19%	27 %	-5 %	9 %	10 %	14 %
$|Y_{TM}|$ (0.22 kHz)|	27 %	34 %	34 %	-8 %	10 %	12 %	21 %
$|Y_{TM}|$ (measured f_{Ynotch})|	63 %	400 %	160 %	160 %	250 %	800 %	306 %
$|Y_{TM}|$ (respective f_{Ynotch})|	58 %	144 %	140 %	-2 %	49 %	302%	116 %
f_{Ynotch}	1 %	5 %	6 %	5 %	4 %	9 %	5 %
$f_{45°}$	-25 %	-59 %	-26 %	6 %	-28 %	-36 %	30 %

81

FIG. 2.1: Schematic diagram of the acoustic probe coupled to an external ear canal. The black area represents the pinna, concha, and cartilaginous ear canal. The unshaded (white) areas represent air filled spaces -- ear canal, middle-ear cavity, Eustachian tube, and the microphone and earphone tubes of the acoustic probe. Y_{EC} is the acoustic admittance measured at the microphone-tube tip's location in the ear canal. Y_{TM} is the acoustic admittance at the tympanic membrane (TM), i.e., the middle-ear input admittance. The acoustic assembly (Etymotic Research ER-10C) is coupled to the ear canal through a flexible plastic "eartip" that houses both the microphone and earphone tubes. An acoustic and static-pressure seal surrounds the eartip in the canal. The outer diameter of the eartip is 3.3 mm. Inner diameters: microphone tube 1.9 mm, earphone tube 0.5 mm. The static-pressure tube and the extension of the microphone tube (3-4 mm beyond the earphone-tube tip) are customized additions.

FIG. 2.1

ACOUSTIC ASSEMBLY

MICROPHONE

STATIC PRESSURE TUBE

EARPHONE

MICROPHONE TUBE

EARPHONE TUBE

"EARTIP"

PINNA AND CONCHA

MIDDLE EAR

SEAL

EAR CANAL

Y_{EC}

Y_{TM}

TM

COCHLEA

MICROPHONE-TUBE EXTENSION

EUSTACHIAN TUBE

83
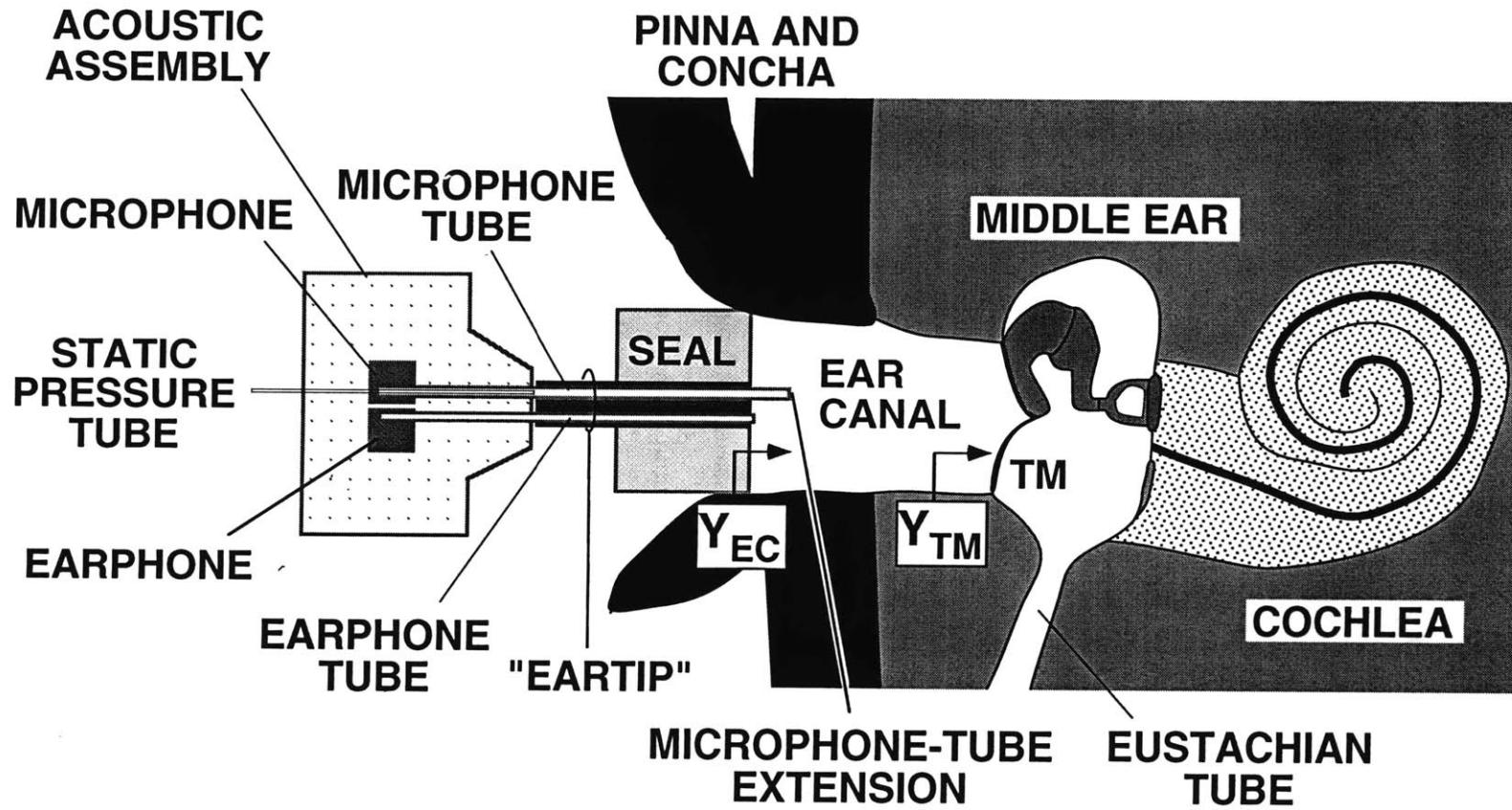
FIG. 2.2: Effects of the microphone-tube extension on admittance measurements. Results are shown for two test loads: (A) a cylindrical plexiglass tube having inner diameter 9.5 mm and length 30 mm with a rigid termination; (B) a similar cylindrical tube having inner diameter 9.5 mm and length 12 mm with a resistive-compliant termination -- an acoustic resistor (nominally 37.5 mks $M\Omega$) that connects to a closed cavity having the same inner diameter and length 10 mm. Admittances, in the upper panels, were measured with and without the microphone-tube extension; each configuration was calibrated in two reference loads. In the upper left panel, the dashed curves are difficult to see because they nearly overlay the thick curves, below 8 kHz. Theoretical admittances were computed from a lossy transmission-line model for the tubes and a lumped resistance-mass model for the acoustic resistor. Errors, in the lower panels, are the ratios of measured admittances to theoretical admittances. The frequency scale is the same in the upper and lower plots. Admittance magnitude units: 1 μSiemen = 1/(mks $M\Omega$) = 10^{-6} m^3/(Pa s). Phase angles are plotted in periods (1 period = 2π radians).

FIG. 2.2

TEST LOADS

(A) TUBE WITH RIGID TERMINATION

(B) TUBE TERMINATED BY RESISTOR AND CAVITY
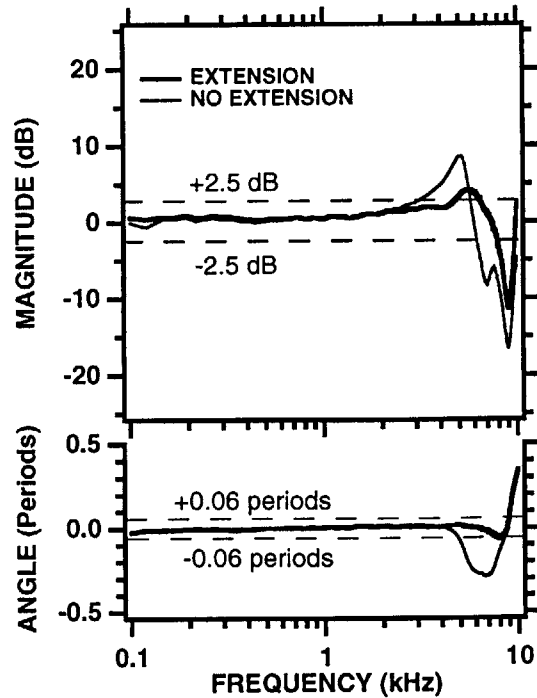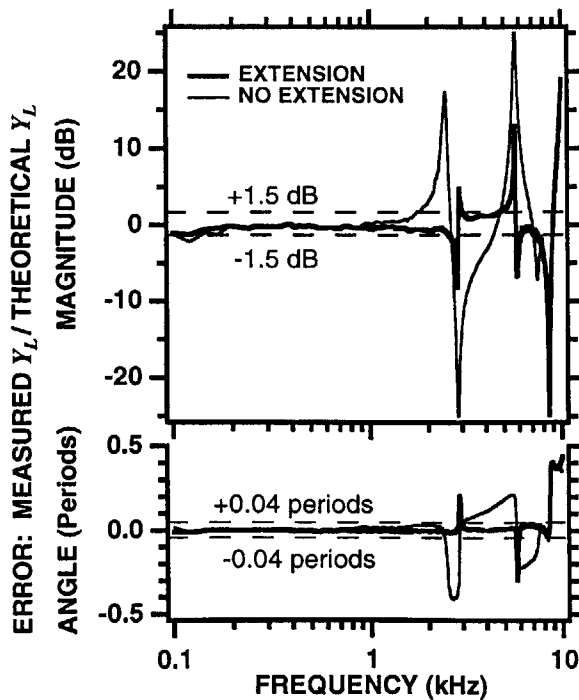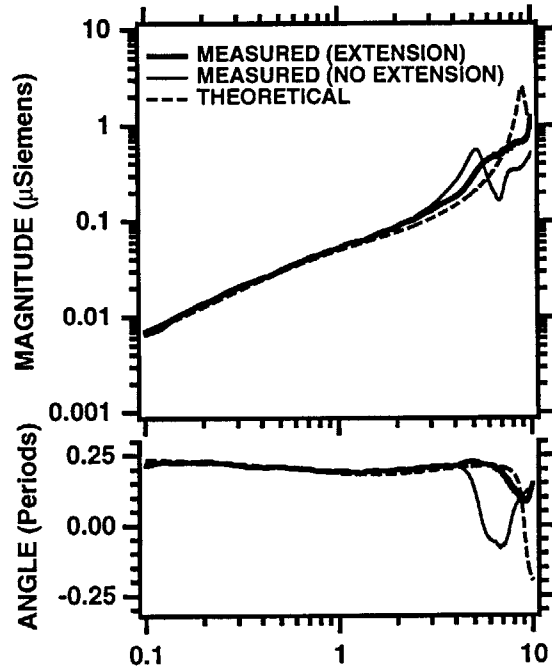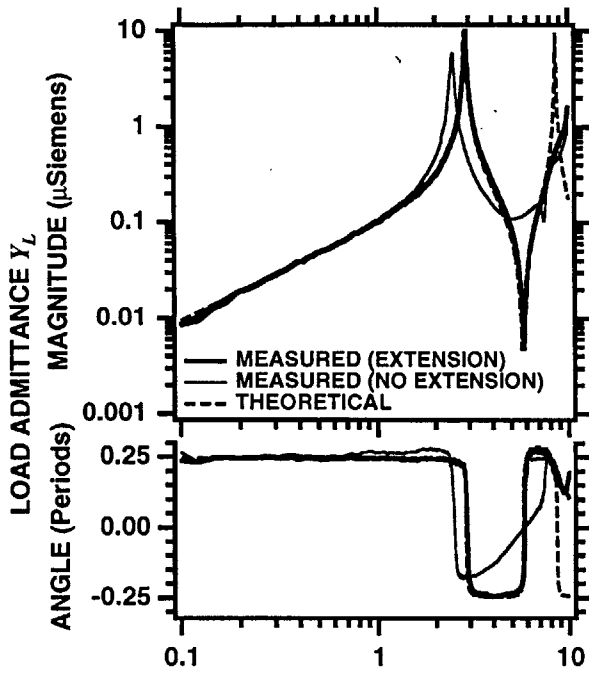
FIG. 2.3: Effects of variations in measurement method on the inferred admittance of the earlike

termination of the test load of Fig. 2.2(B). The admittance measurements reported in Fig. 2.2(B)

were transformed to the location of the acoustic resistor via a uniform-tube (length 12 mm) plane-

wave model. The "large source" measurement was made 8 mm from the resistor, using an

acoustic source with a large earphone port (e.g., Huang et al., 1997b), and transformed to the

same location. The theoretical admittance (upper panel) and error ratios (lower panel) were

computed as in Fig. 2.2.

FIG. 2.3

RESISTOR-CAVITY TERMINATION (12-mm TUBE)
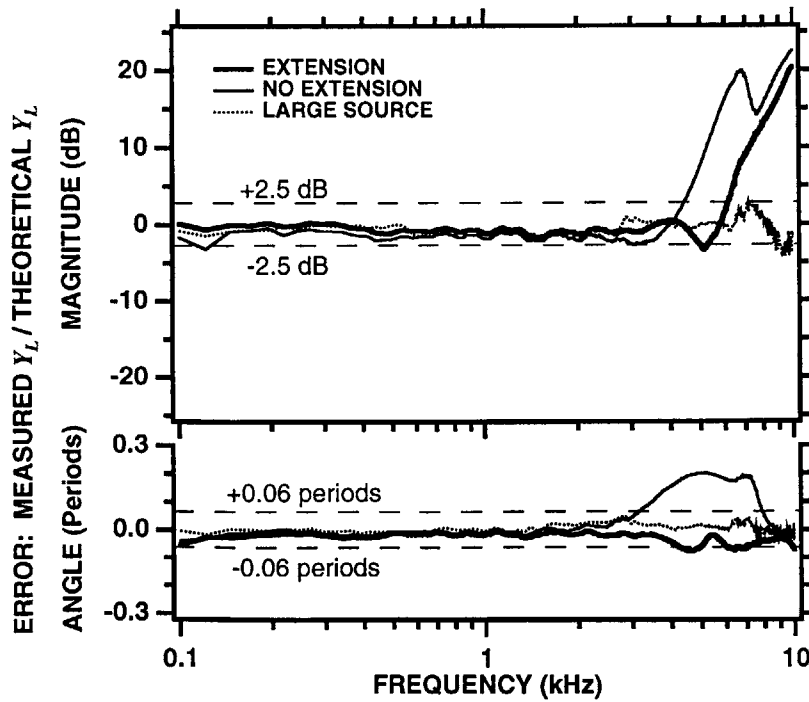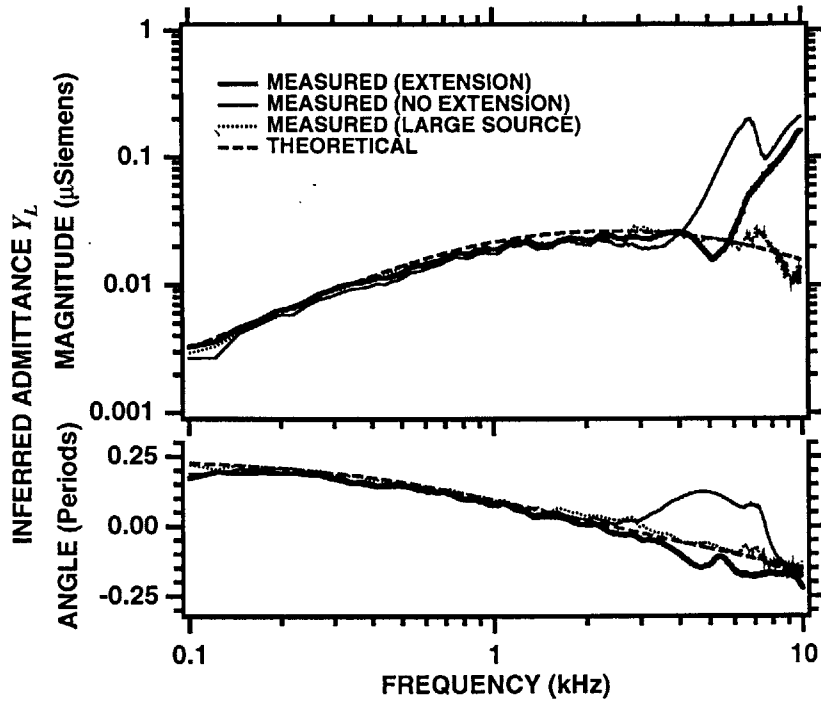
FIG. 2.4: Diagrams illustrating differences in the "source" with the acoustic system (ER-10C) coupled to ear canals of different diameters: (A) human infant or small cat species; (B) human adult or large cat species. To simplify the figure, the microphone and earphone tubes are shown without the eartip's outer material (Fig. 2.1). The dashed vertical lines at the locations of the microphone-tube tips are the interfaces between the sources and loads. In the circuit analogs (lower portion), the source is represented by an ideal volume-velocity source (U_S or U_S') in parallel with a source admittance (Y_S or Y_S'). The ear (or test load) is represented by a load admittance (Y_L or Y_L'). Differences in configuration of both the seal and the air space around the microphone-tube extension can affect the source parameters U_S and Y_S.

FIG. 2.4

EFFECTS OF VARIATIONS IN EAR-CANAL DIAMETER

(A) HUMAN INFANT OR SMALL CAT SPECIES

(B) HUMAN ADULT OR LARGE CAT SPECIES
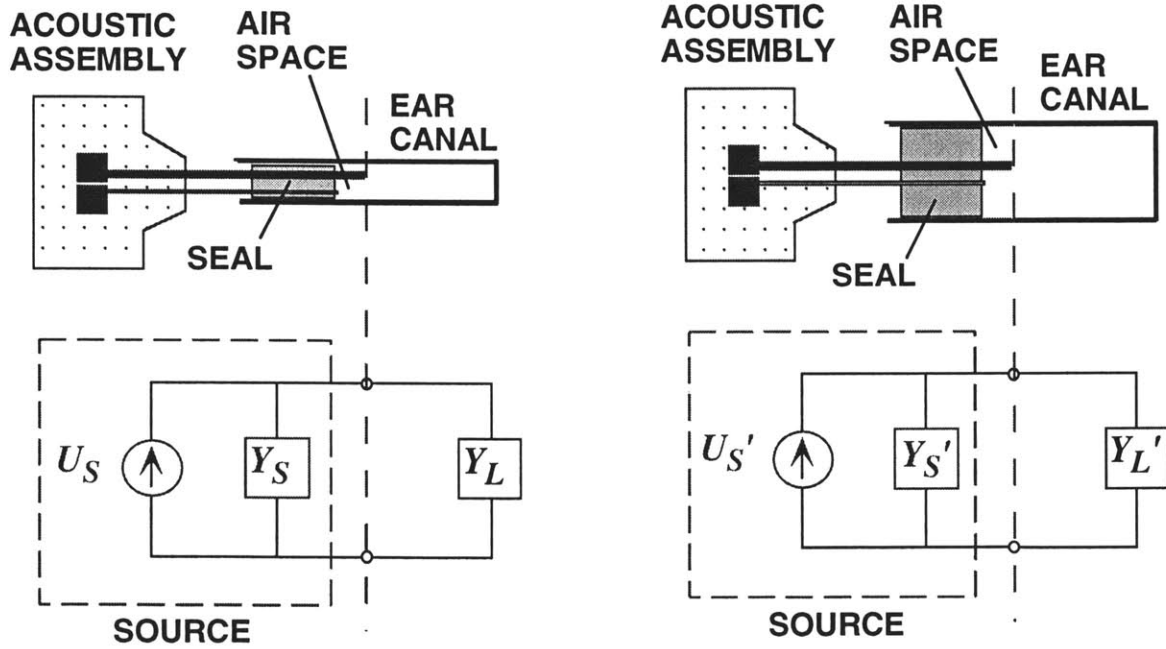
FIG. 2.5: Effects of load-diameter variations on the source parameters. Norton equivalent source parameters (computed from measurements) are shown for three diameters (6.2 mm, 9.5 mm, and 12.5 mm): (A) source admittance Y_S; (B) ideal-source volume velocity U_S, for 1-volt-peak stimulus level. For each diameter, Y_S and U_S were determined from measurements in two "reference" loads: (1) a closed tube of length 6-12 mm, and (2) a tube of length 15 m terminated by an acoustic resistor. To compute U_S, the microphone was calibrated to determine absolute sound-pressure levels.

FIG. 2.5

NORTON EQUIVALENT SOURCE PARAMETERS

(A) SOURCE ADMITTANCE Y_S

(B) IDEAL VOLUME-VELOCITY SOURCE U_S
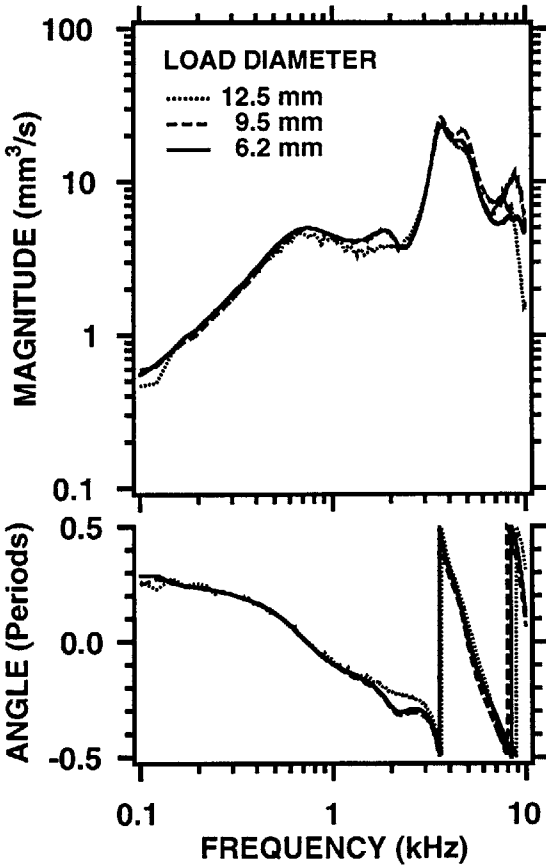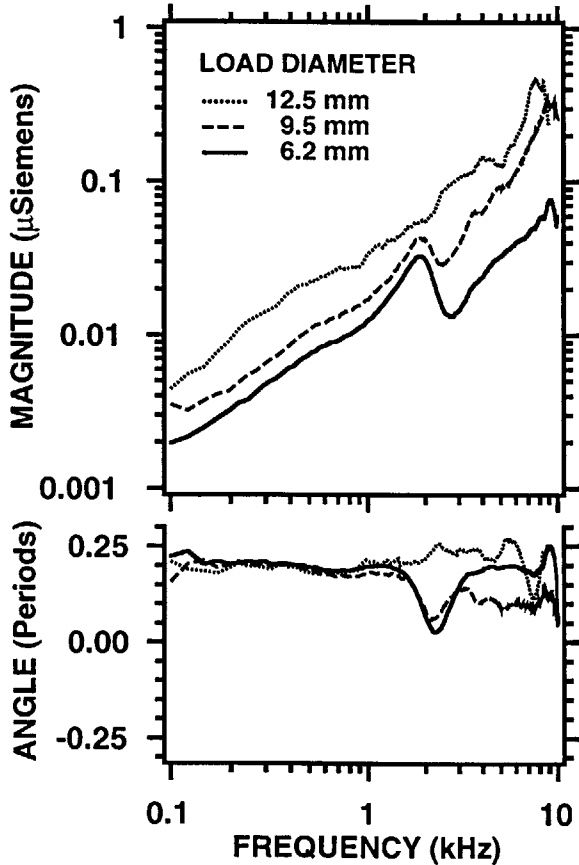
FIG. 2.6: Effects of load-diameter variations on the admittance of structural components of the acoustic measurement system. (A) Admittance contributions of a foam-plug seal (measured Y_{FOAM}) and the air volume around the microphone-tube extension (compliancelike Y_{AIR}), for two different diameters. Each Y_{FOAM} curve is the mean of three estimates from measurements made in a tube terminated by the foam. The angles of the Y_{AIR} overlay each other on 0.25 periods. (B) Admittance contribution of Y_{EARTIP} (microphone, earphone, and sound tubes) for the two diameters, computed by subtracting the foam and air-volume admittances in (A) from the total source admittance Y_S [Fig. 2.5(A)]. This computation tests the idea that Y_S can be represented by the parallel combination of Y_{FOAM}, Y_{AIR}, and Y_{EARTIP} (lower portion) as in Eq. (2.5).

FIG. 2.6

SOURCE-ADMITTANCE COMPONENTS

(A) Y_{FOAM}, Y_{AIR}

(B) $Y_{EARTIP} = Y_S - Y_{FOAM} - Y_{AIR}$
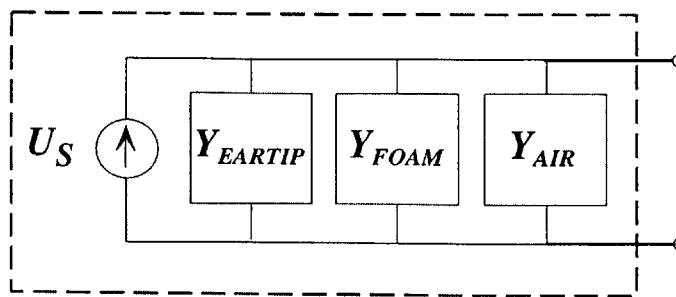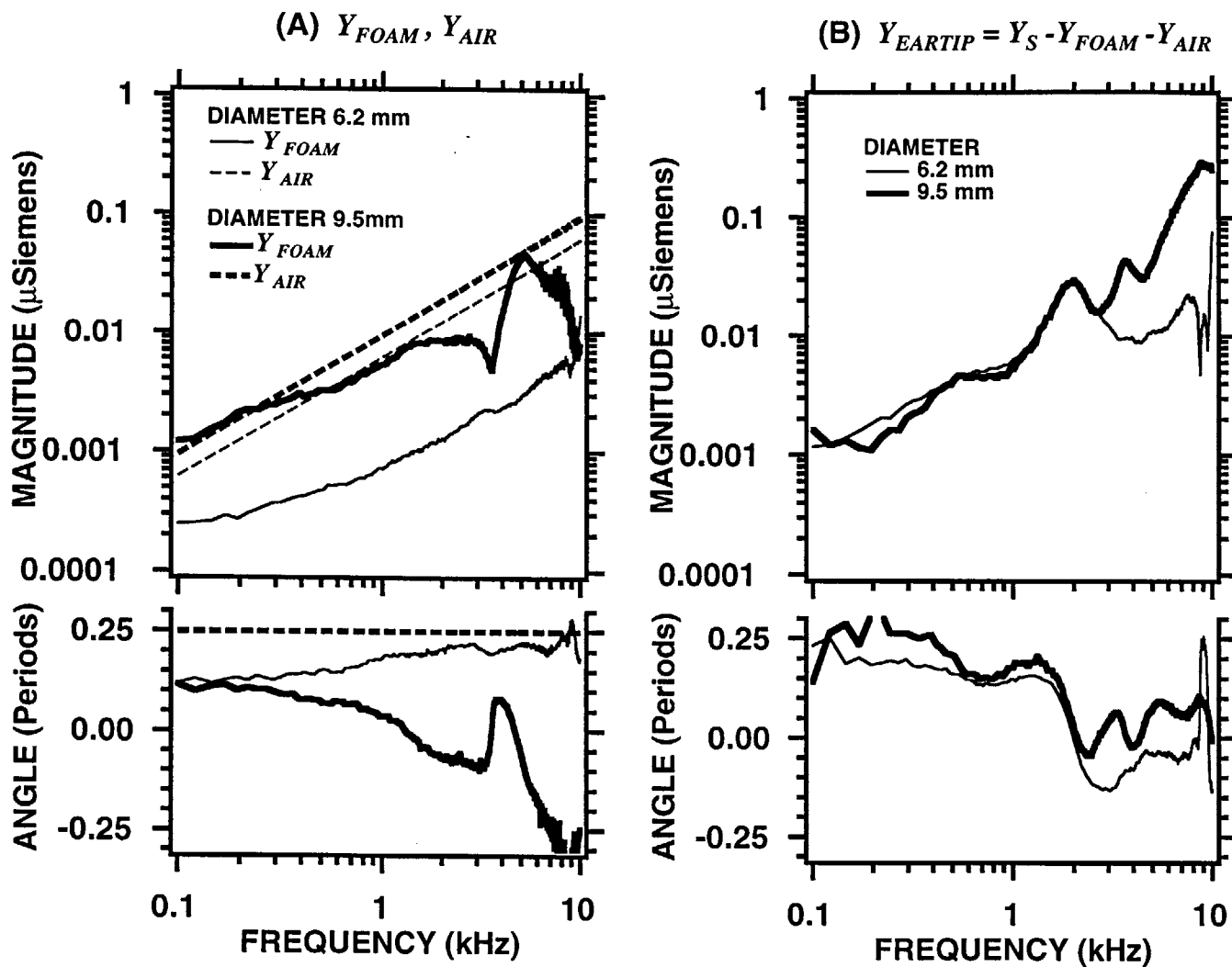
FIG. 2.7: Demonstration of errors in admittance measurements resulting from unequal test-load

and calibration-load diameters. The test load is a closed cylindrical tube of inner diameter 6.2 mm

and length 31.3 mm. The "equal diam." curves were computed with source parameters based on

calibration measurements in known loads having the same diameter (6.2 mm). The "larger diam."

curves were computed with source parameters based on calibration measurements made in known

loads 9.5 mm in diameter. The data are cut off at 9 kHz because for higher frequencies, admittance

measurements in test loads of this diameter (6.2 mm) have large errors.

FIG. 2.7

MEASURED WITH
CALIBRATION DIAMETER d
— EQUAL DIAM.(d=6.2 mm)
— LARGER DIAM.(d=9.5 mm)

---- THEORETICAL
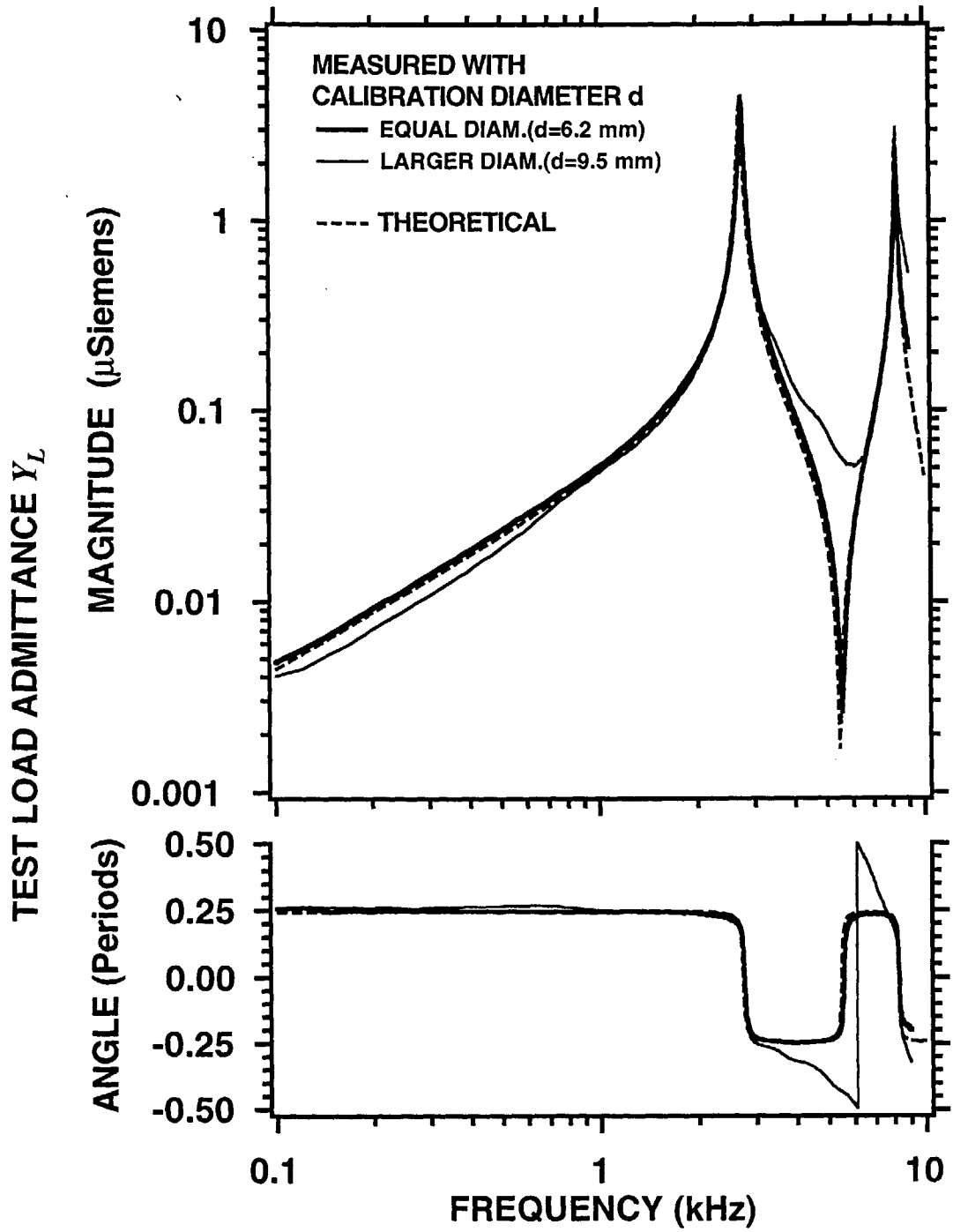
FIG. 2.8: Effects of different calibration-load diameters on the admittance measured in a

commercial ear simulator. The ear simulator is a Zwislocki-type DB-100 coupler (Knowles)

having inner diameter 7.5 mm. The measurement was made 15 mm from the inner termination.

The three calibration diameters are the inner diameters of the reference loads used to compute three

pairs of source parameters (and hence three admittances). The data are cut off at 8 kHz because for

higher frequencies, admittance measurements in test loads of this diameter (7.5 mm) have large

errors.

FIG. 2.8

MEASURED WITH
CALIBRATION DIAMETER d
—— EQUAL DIAM. (d=7.5 mm)
▬▬▬ LARGER DIAM. (d=9.5 mm)
------ SMALLER DIAM. (d=6.2 mm)

FIG. 2.9: Test of the admittance-location transformation in an ear simulator (see Fig. 2.8 caption). Y_{EC} was measured 15 mm from the inner termination. Y_{MEDIAL} was measured 10 mm "medial" to Y_{EC}, i.e., 5 mm from the inner termination. "Y_{MEDIAL} estimated" was computed by transforming Y_{EC} through a uniform tube having diameter 7.5 mm and length 10 mm, via Eq. (2.6).

FIG. 2.9

TEST OF ADMITTANCE-LOCATION TRANSFORMATION
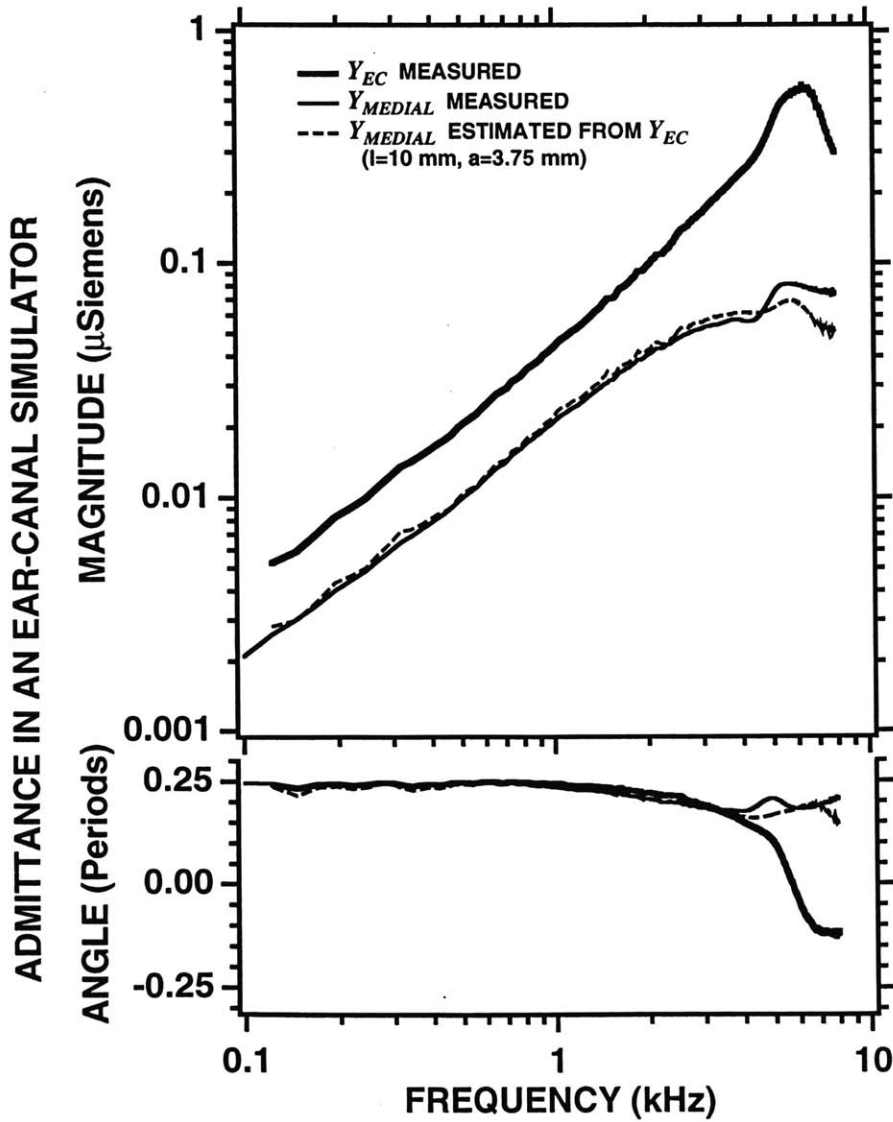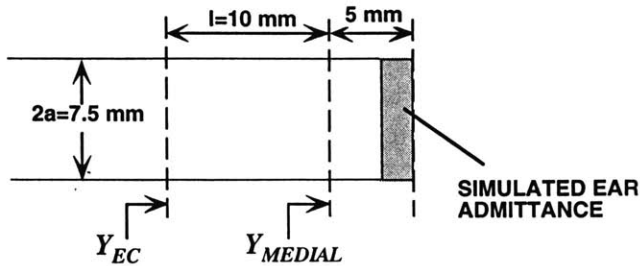
FIG. 2.10: Comparison of microphone output levels for different types of eartips: (A) standard Etymotic eartip (length 20 mm), (B) longer Etymotic eartip (length 35 mm), (C) custom eartip constructed from two separate plastic tubes (length 35 mm): microphone tube's inner diameter 1.6 mm, outer diameter 2.9 mm; earphone tube's inner diameter 0.5 mm, outer diameter 1.5 mm. The test load is the rigid cavity of Fig. 2.7. To estimate the level of "artifact" for each eartip, the voltage response of the microphone was measured before ("normal") and after plugging the distal end of the microphone tube with a piece of steel wire coated with petroleum jelly. To the extent that the "microphone tube plugged" magnitudes are substantially below the "normal" measurements, the artifact is not significant.

FIG. 2.10

ARTIFACT LEVELS FOR DIFFERENT EARTIPS

(A) STANDARD ETYMOTIC EARTIP   (B) LONGER EARTIP   (C) CUSTOM EARTIP

20 mm   35 mm   35 mm
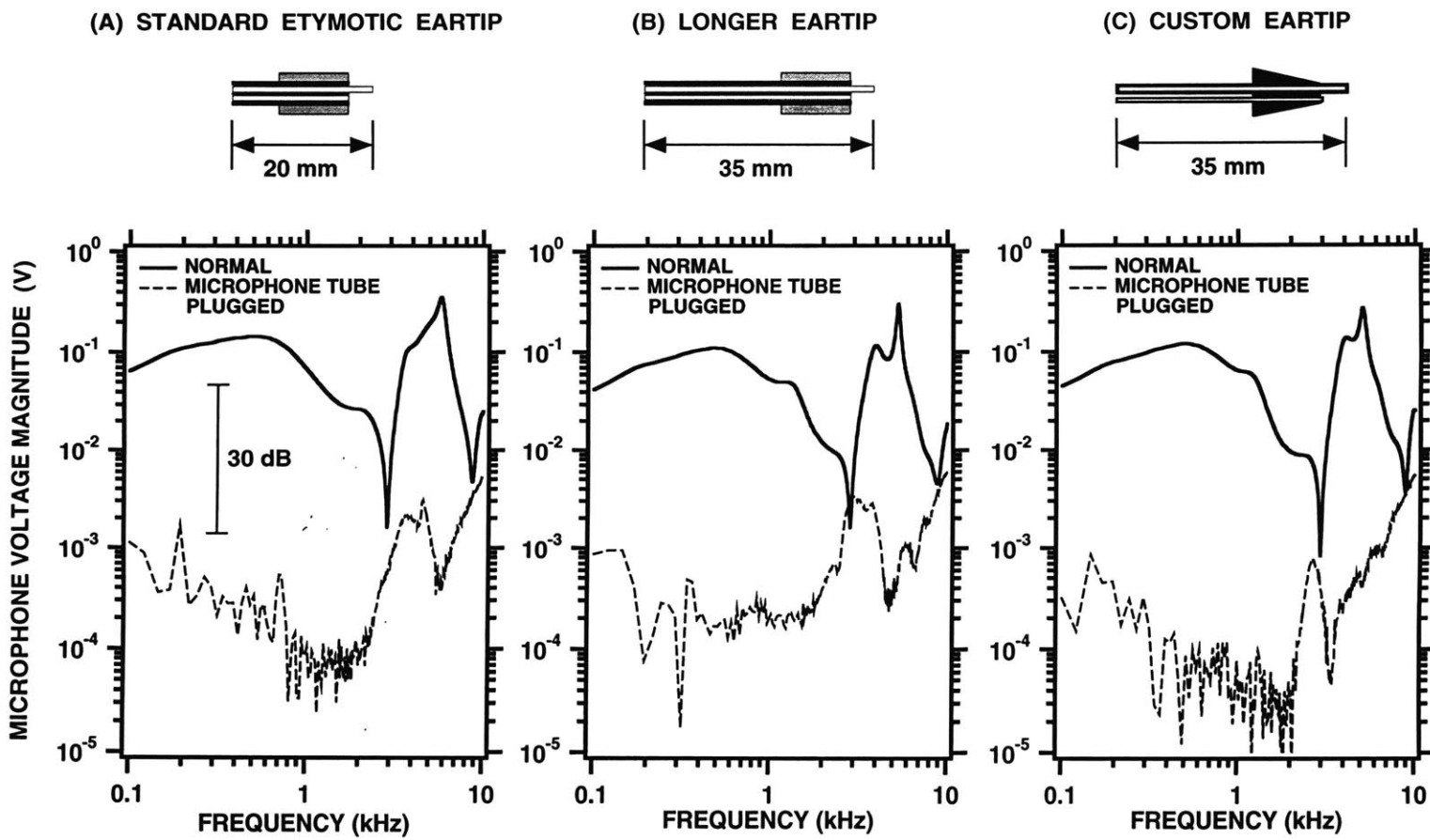
FIG. 2.11: Method of acoustic measurement in an intact cat ear. The schematic does not attempt to portray the external ear's anterior-posterior configuration. The custom-made eartip -- two plastic tubes with a silicone "eartip guide" -- is inserted just medial to the sharp bend at the canal-concha border (shown schematically). Hearing-aid earmold-impression material is injected behind the eartip guide via syringe to form a static-pressure seal in the ear canal and to hold the eartip in place. The tube in the back of the acoustic assembly couples a static pressure source to the ear canal through the microphone tube. A cable from the acoustic assembly carries the electric stimulus and response signals to and from the computer.

FIG. 2.11

SYRINGE FOR INJECTION
OF EARMOLD MATERIAL

PINNA
FLANGE

TUBE TO STATIC-
PRESSURE SOURCE

ELECTRICAL CONNECTIONS
FROM COMPUTER
TO EARPHONE

TO COMPUTER
FROM MICROPHONE

EARPHONE TUBE

SUPERIOR

EAR CANAL

TM

MEDIAL

ACOUSTIC
ASSEMBLY

CONCHA

EARTIP
GUIDE

SEALANT
(EARMOLD
MATERIAL)

MICROPHONE
TUBE

MICROPHONE-TUBE
EXTENSION
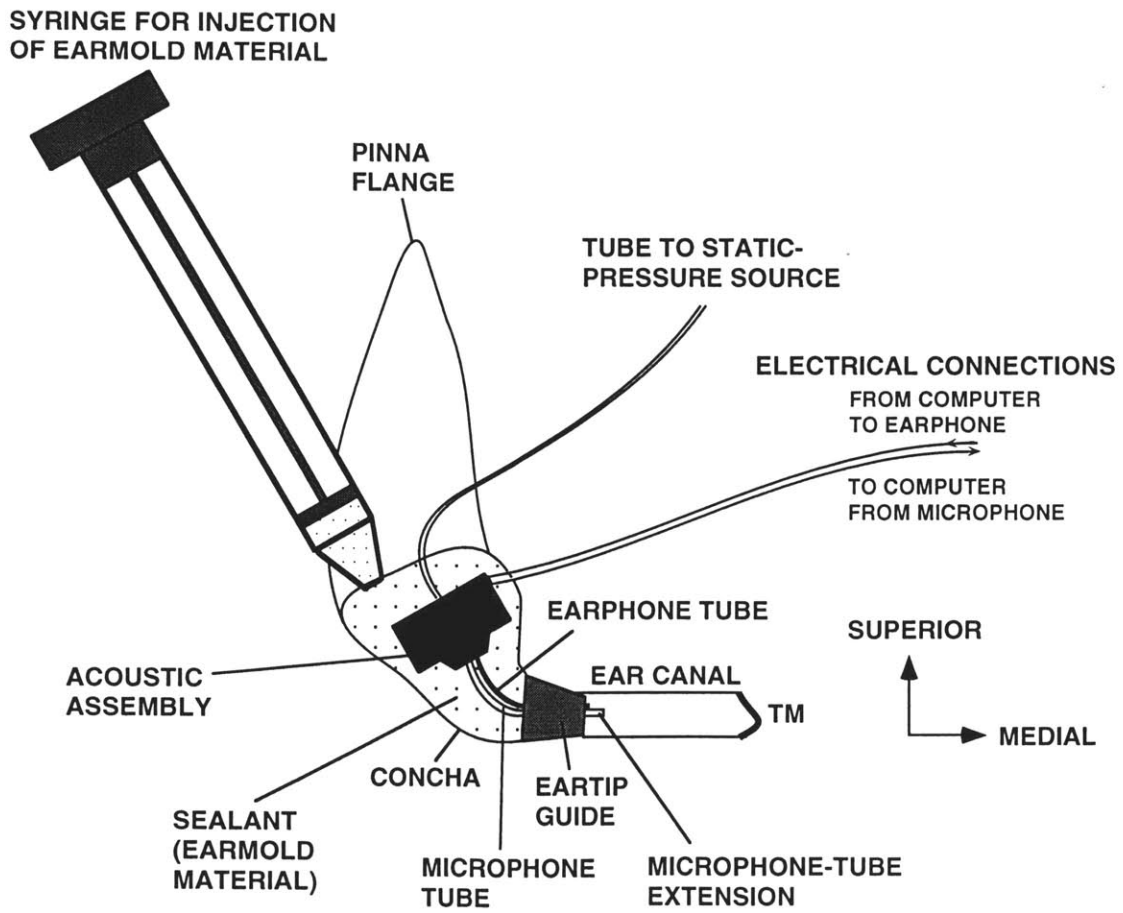
FIG. 2.12: Admittances Y_{EC} measured in the intact ear canal of 7 domestic cats. Cats 1 and 2 were measured with long Etymotic eartips [30-35 mm, see Fig. 2.10(B)] sealed in the canal with earmold-impression material. All other measurements were made with the custom eartip and seal depicted in Fig. 2.10(C) and Fig. 2.11. In all cases, a static-pressure seal was maintained in the ear canal. The data are cut off at 9 kHz because for higher frequencies, admittance measurements in test loads of these diameters (5-7 mm) have large errors.
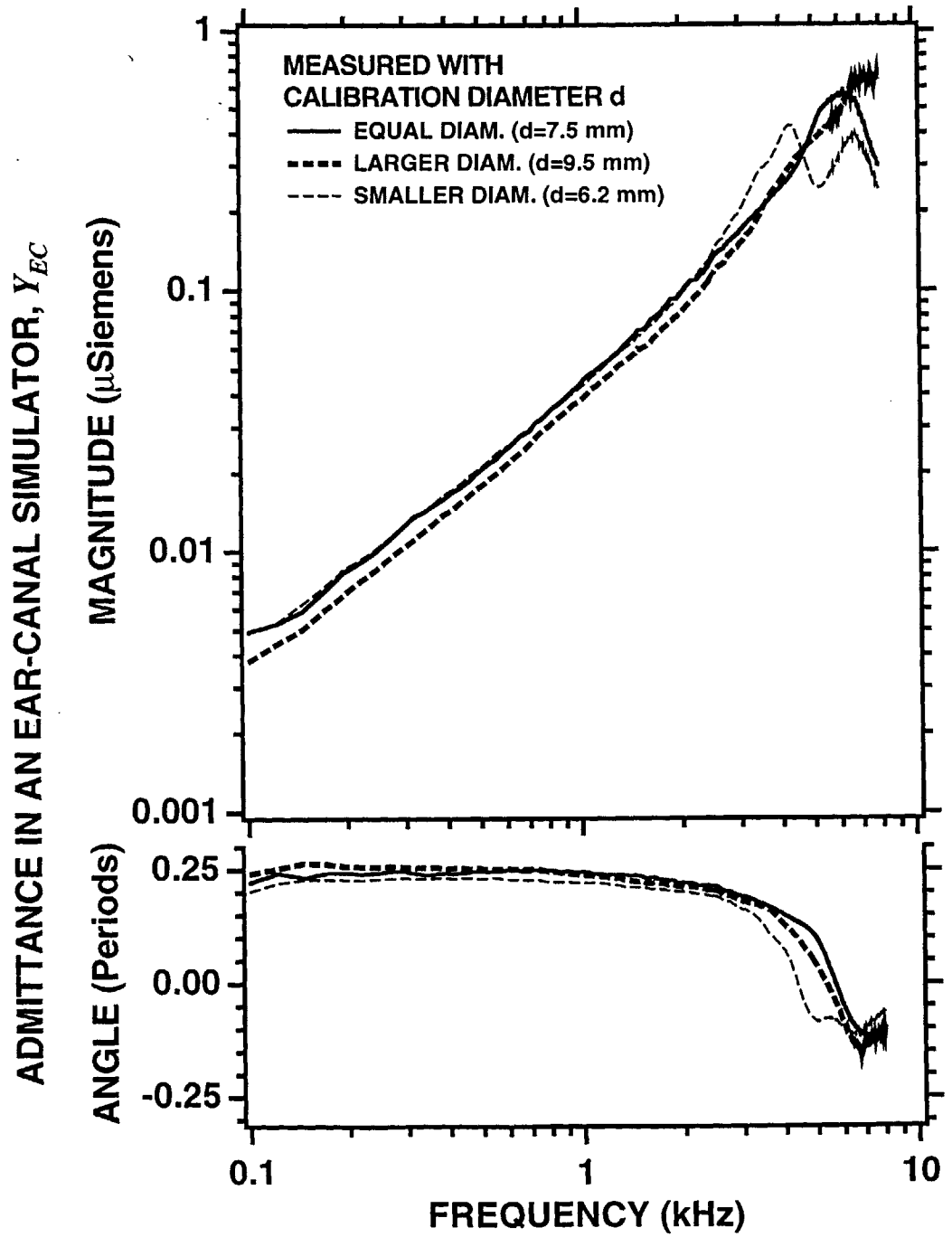
FIG. 2.12
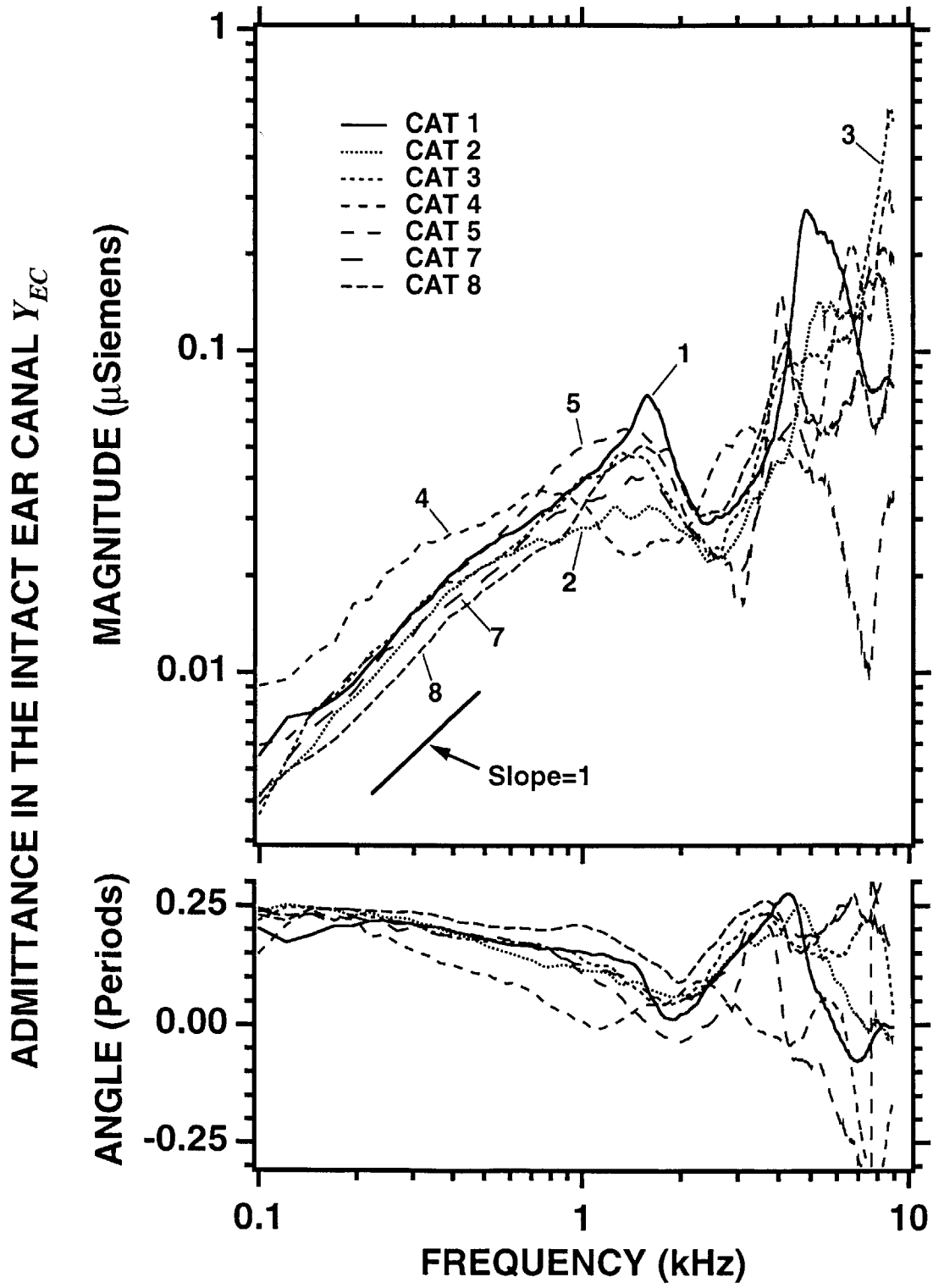
FIG. 2.13: Admittances Y_{TM} measured at the TM after resection of the external ear in 5

domestic cats. The admittances were measured with a standard Etymotic eartip, rubber seal, and a

microphone-tube extension, except for Cat 2 which was measured without an extension. The tip

of the microphone tube was roughly 5 mm from the umbo (tip of the manubrium of the malleus).

In each case, the residual ear-canal space (less than 0.1 cm^3) was accounted for by a uniform-tube

transformation with parameters (length and radius) determined from measurements with static

pressure (see Fig. 16 caption). Range of parameters: length 3-5 mm, radius 2-3 mm. The effects

of the transformation are significant for frequencies above 4 kHz.

FIG. 2.13

107
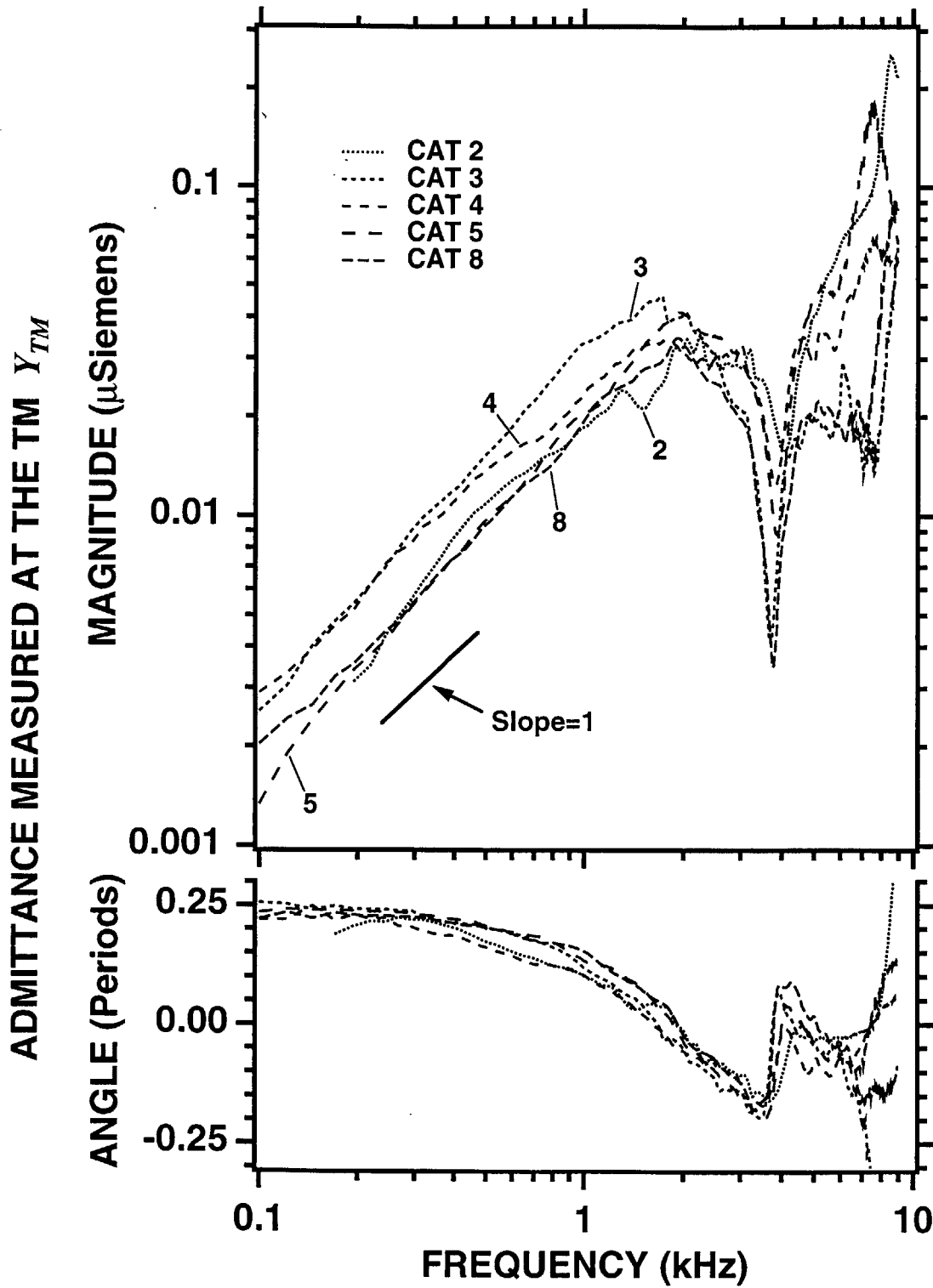
FIG. 2.14: Effects of static-pressure variations in the ear canal on admittances Y_{EC} measured in an intact ear (Cat 3): (A) negative-static-pressure series; (B) positive-static-pressure series. Static pressures in the canal, given in mm H_2O (1 mm H_2O = 0.98 Dekapascals = 9.8 Pa), were produced with a syringe and measured with a water manometer. Admittance measurements with zero static pressure were made before and after each pressure series. The duration between the "Before" and "After" measurements was approximately 5 minutes. The low-frequency acoustic compliance with -300 mm H_2O was used as an estimate of the volume of the ear-canal coupling space (0.37 cm^3 for this ear).

FIG. 2.14

ADMITTANCE IN THE INTACT EAR CANAL, Y_{EC} (Cat 3)

(A) Negative Static Pressures in Ear Canal
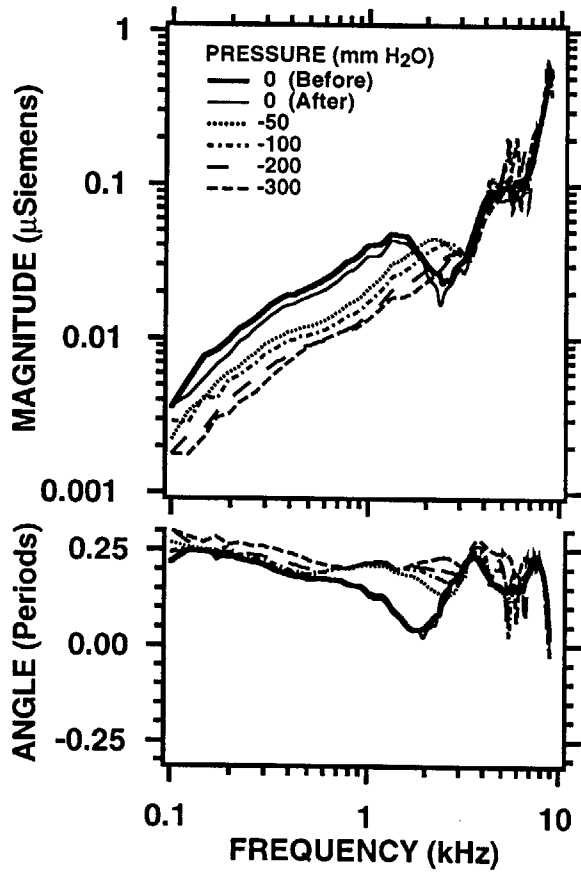
(B) Positive Static Pressures in Ear Canal
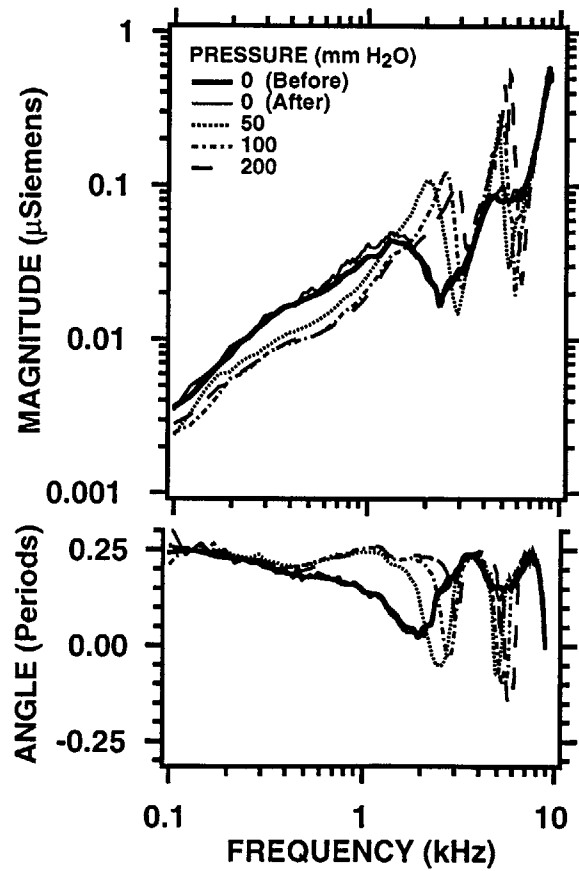
FIG. 2.15: Comparison of acoustic compliances measured in the intact ear canal and near the TM, with varying static pressures (Cat 3). The data test the idea that the intact-canal volume can be estimated from the compliance measured with large static pressures. "Intact ear canal" (solid circles) data are from the Y_{EC} curves of Fig. 2.14. "Near TM" (ex'es) data are from admittances measured near the TM with the external ear canal resected. Compliance values and differences between the two canal locations are labeled for static-pressure levels of -300, -150, 0, 100, and 200 mm H_2O. Acoustic compliances were computed from admittances Y by averaging $Im\{Y\}/(2\pi f)$ over 10 frequency points between 0.1-0.3 kHz; compliance values are expressed as equivalent volumes of air. The data points, taken at discrete static-pressure levels, are connected by straight line segments.

FIG. 2.15
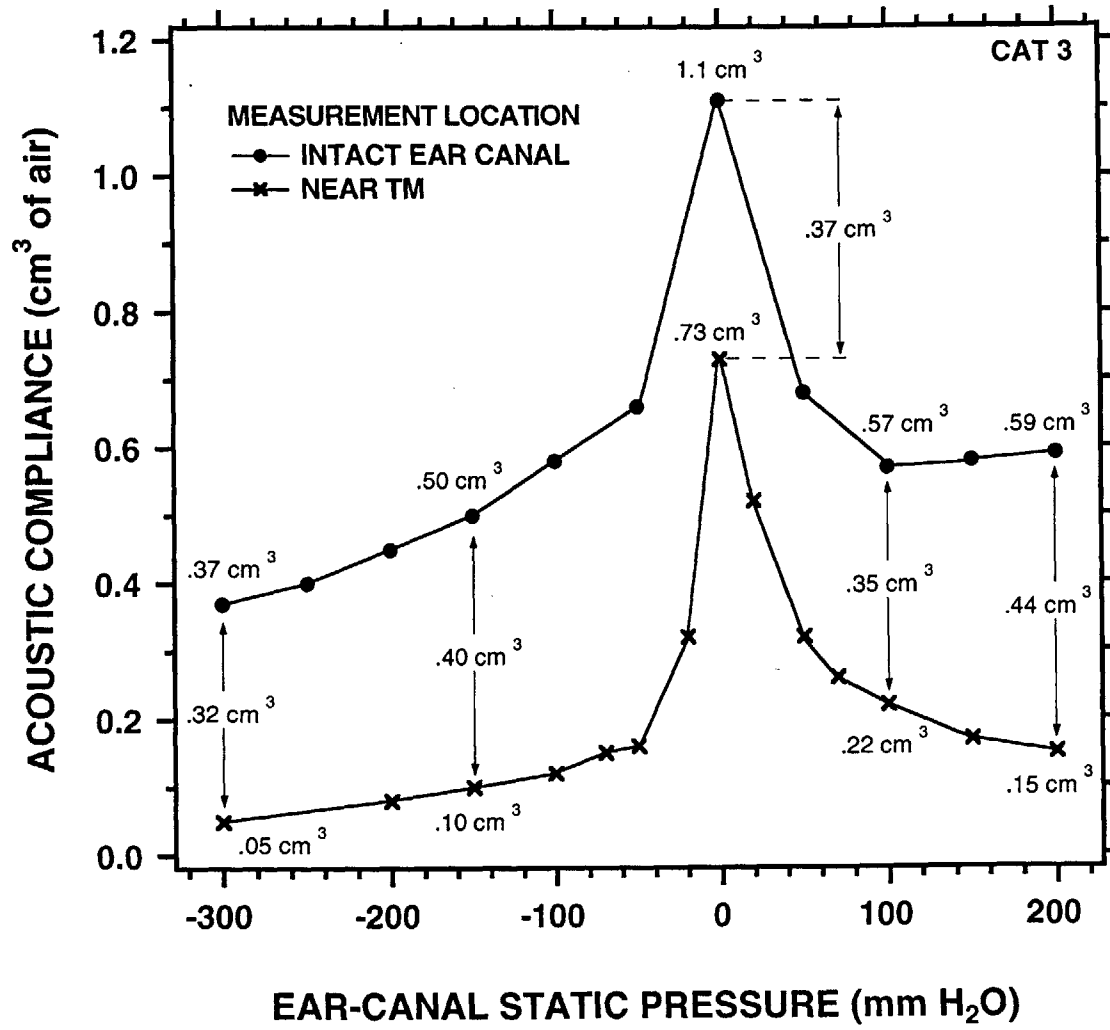
FIG. 2.16: Effect of ear-canal parameter variations on estimated Y_{TM}. Estimated admittances are shown for one intact ear (Cat 3). The thick curve is the estimate from Eq. (2.6), with ear-canal parameters (length l and radius a) determined from (1) a volume estimate from low-frequency tympanometry and (2) a radius estimate based on Y_{EC} and Eq. (2.7), after Keefe et al. (1992). The other curves show the estimated admittances calculated with ear-canal parameters altered by $\pm 10\%$.

FIG. 2.16
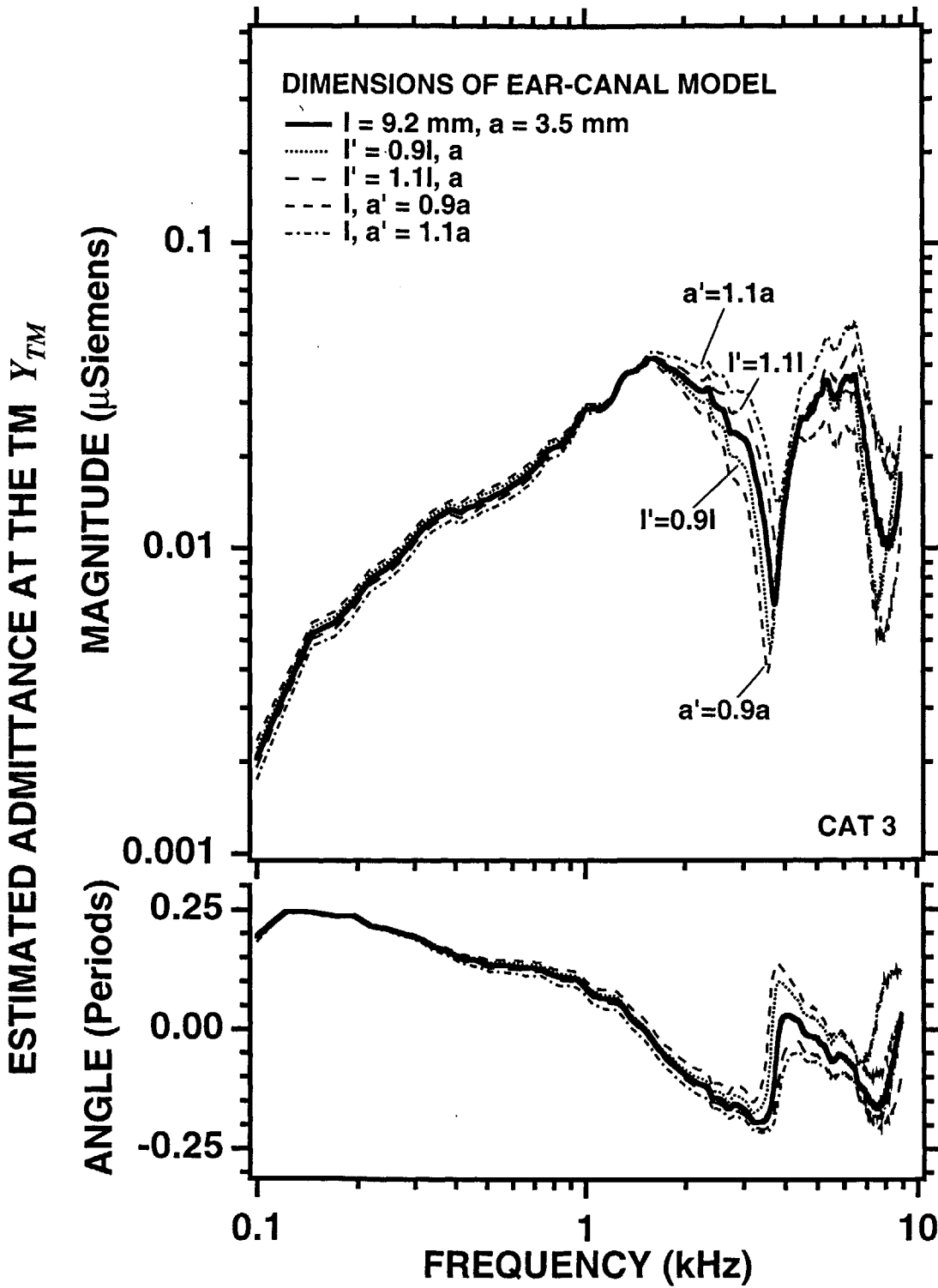
FIG. 2.17: Repeatability of the admittance-location transformation (from Y_{EC} to estimated Y_{TM}) for 2 intact ears: (A) Cat 3, and (B) Cat 8. The upper plots show Y_{EC} for 2 insertions of the acoustic system into each of 2 intact ear canals. Data from these particular ears were selected to show (A) 2 quantitatively similar Y_{EC} measurements and (B) 2 quantitatively different Y_{EC} measurements. The lower plots show the estimated Y_{TM} curves obtained by transforming the Y_{EC} curves in the upper plots to the TM via Eq. (2.6). For each ear, estimate 1 is based on insertion 1, and estimate 2 is based on insertion 2. Between insertions 1 and 2, measurements were made with static pressures in the canal, and the acoustic system was removed from and recoupled to the ear.

FIG. 2.17

MULTIPLE MEASUREMENTS IN 2 EARS

(A) CAT 3

(B) CAT 8 (RIGHT)
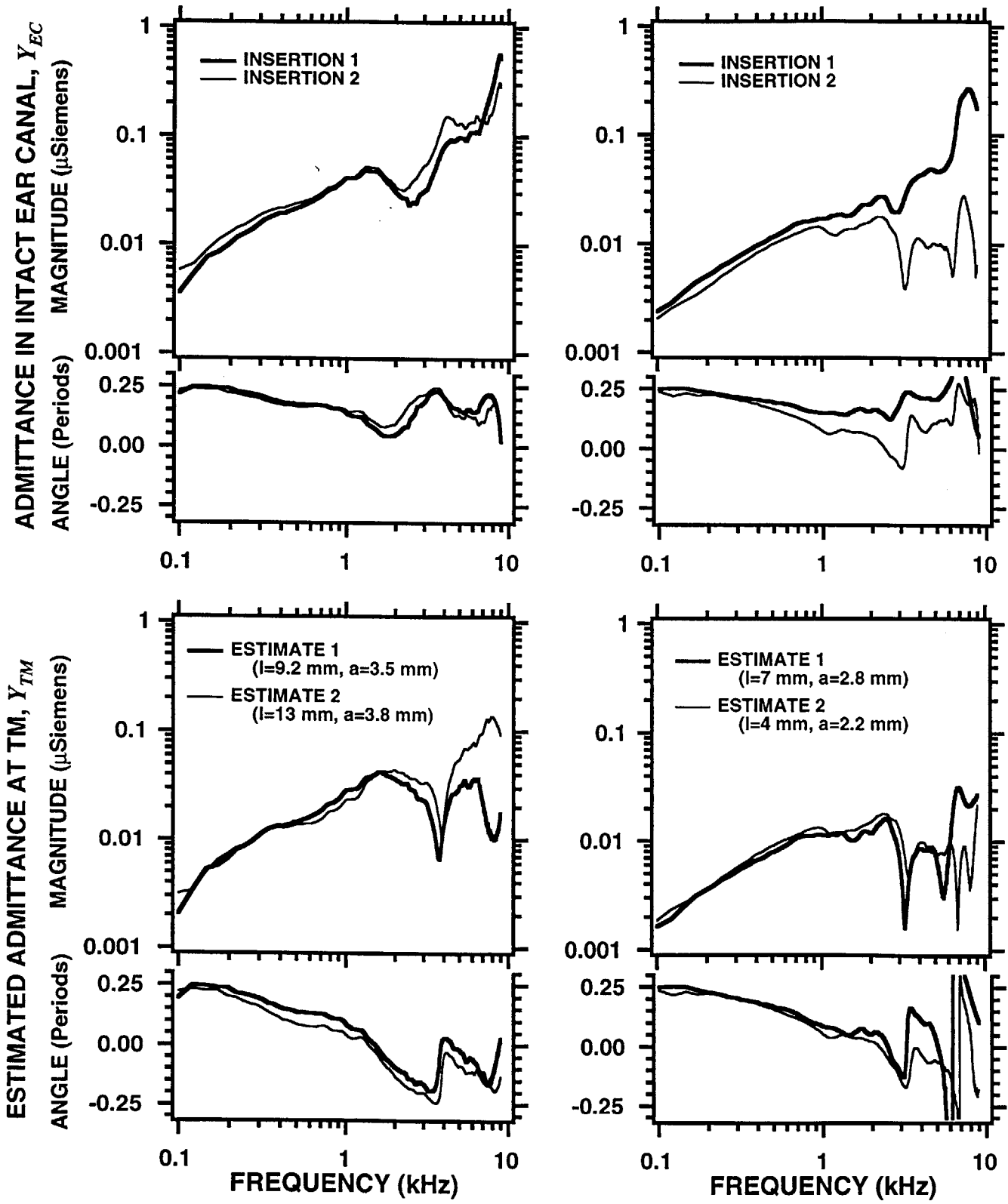
FIG. 2.18: Comparison of the estimated Y_{TM} to the measured Y_{TM} in 4 cat ears. The "estimated" curves are computed from measurements of Y_{EC} (from Fig. 2.12) transformed to the location of the TM via the uniform-tube model of Eq. (2.6). The ear-canal parameters were determined from the procedure described in the text and in the caption of Fig. 2.15. The "measured" curves were obtained with the microphone-tube tip near the TM, after resection of the external ear, as in Fig. 2.13.

FIG. 2.18

ESTIMATED AND MEASURED ADMITTANCES AT THE TM, Y_{TM}
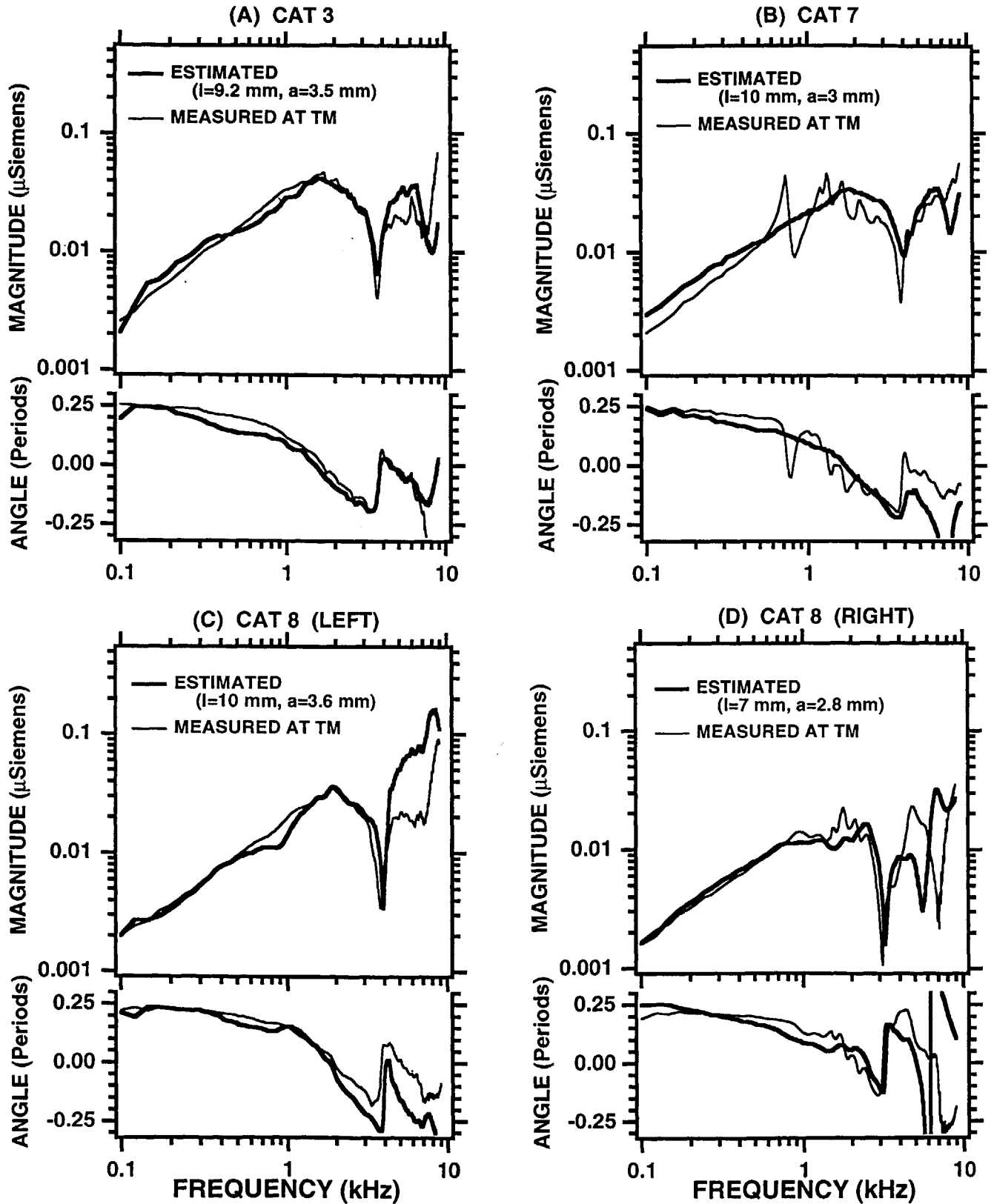
FIG. 2.19: Error ratios of the estimated Y_{TM} to the measured Y_{TM} for the 4 ears from Fig. 2.17. The dashed horizontal lines are 0 dB (magnitude) and 0 periods (angle).

FIG. 2.19

ERROR: (ESTIMATED Y_{TM}) / (MEASURED Y_{TM})

(A) CAT 3

(B) CAT 7

(C) CAT 8 (LEFT)

(D) CAT 8 (RIGHT)
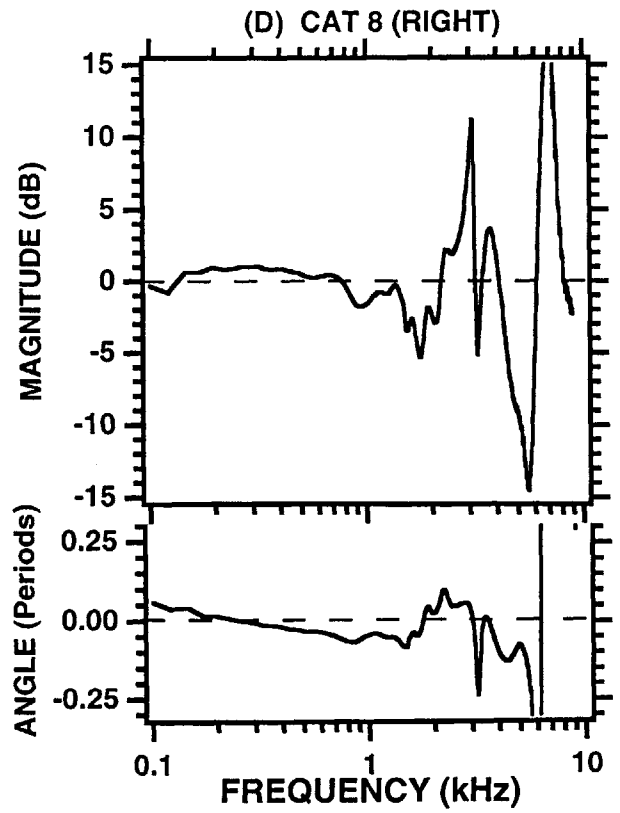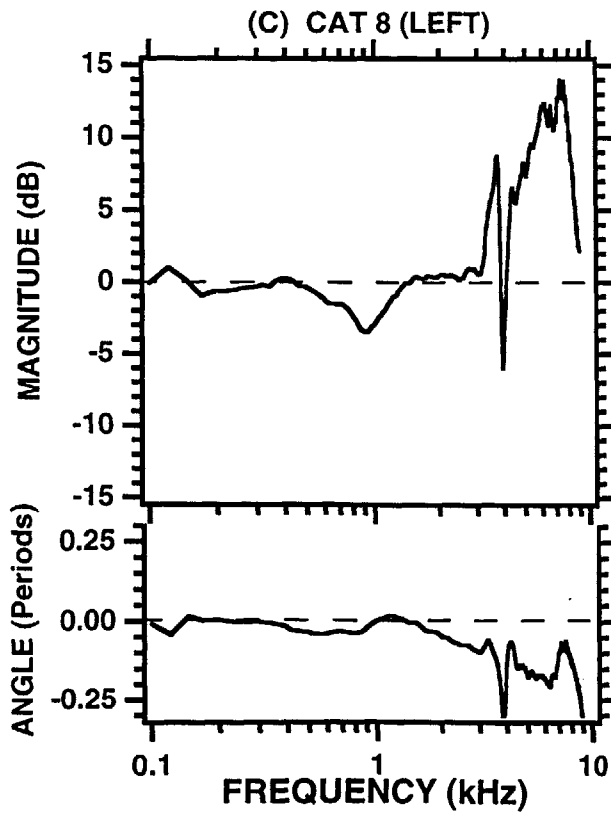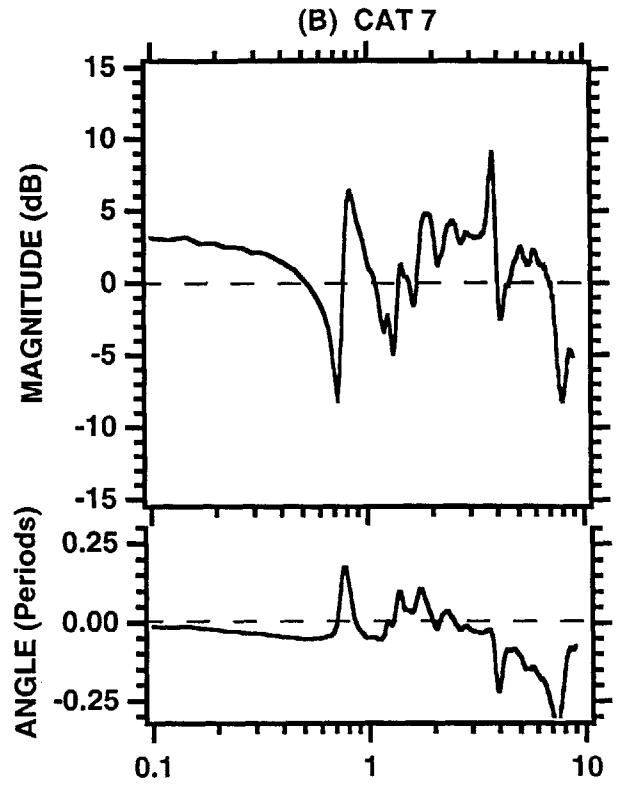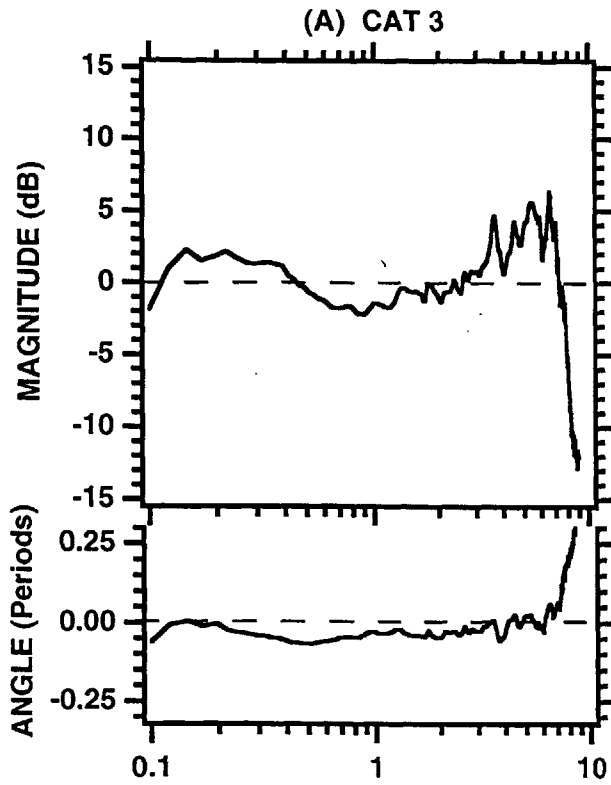
FIG. 2.20: Estimated and measured admittances Y_{TM} for an ear (Cat 5) in which the sealant around the eartip was incomplete. The lower panel shows the ratio of estimated admittance to measured admittance; the dashed horizontal lines are 0 dB (magnitude) and 0 periods (angle). For this insertion, the sealant (earmold material) injected behind the eartip guide did not completely fill the space in the canal and concha lateral to the guide.

FIG. 2.20

EFFECTS OF AN INCOMPLETE EAR-CANAL SEAL
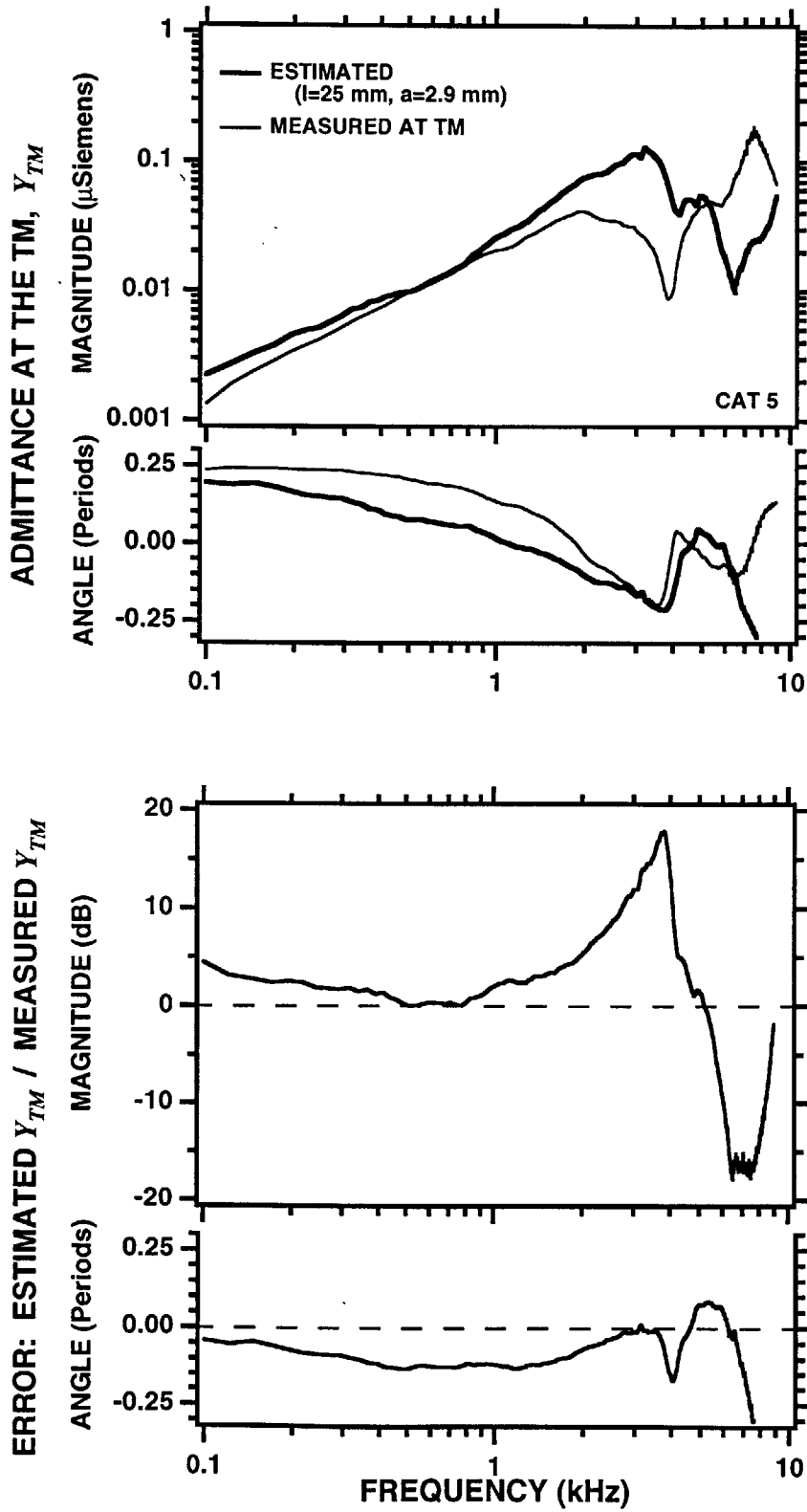
FIG. 2.21: Comparison of the power reflectance measured in the intact ear canal ($|R_{EC}|^2$) to the power reflectance measured near the TM ($|R_{TM}|^2$), for 4 ears. Power reflectance, the squared magnitude of the pressure reflection coefficient, was computed with Eq. (2.8) from the admittances (Y_{EC} and Y_{TM}) measured in the ears of Fig. 2.18 and the canal diameters estimated at the respective positions in the ears. For comparison, panel (A) shows power reflectances ("lateral" and "medial") computed from two admittances measured 10 mm apart in the ear simulator (Y_{EC} and Y_{MEDIAL} from Fig. 2.9, respectively).

FIG. 2.21

EAR-CANAL POWER REFLECTANCES $|R|^2$
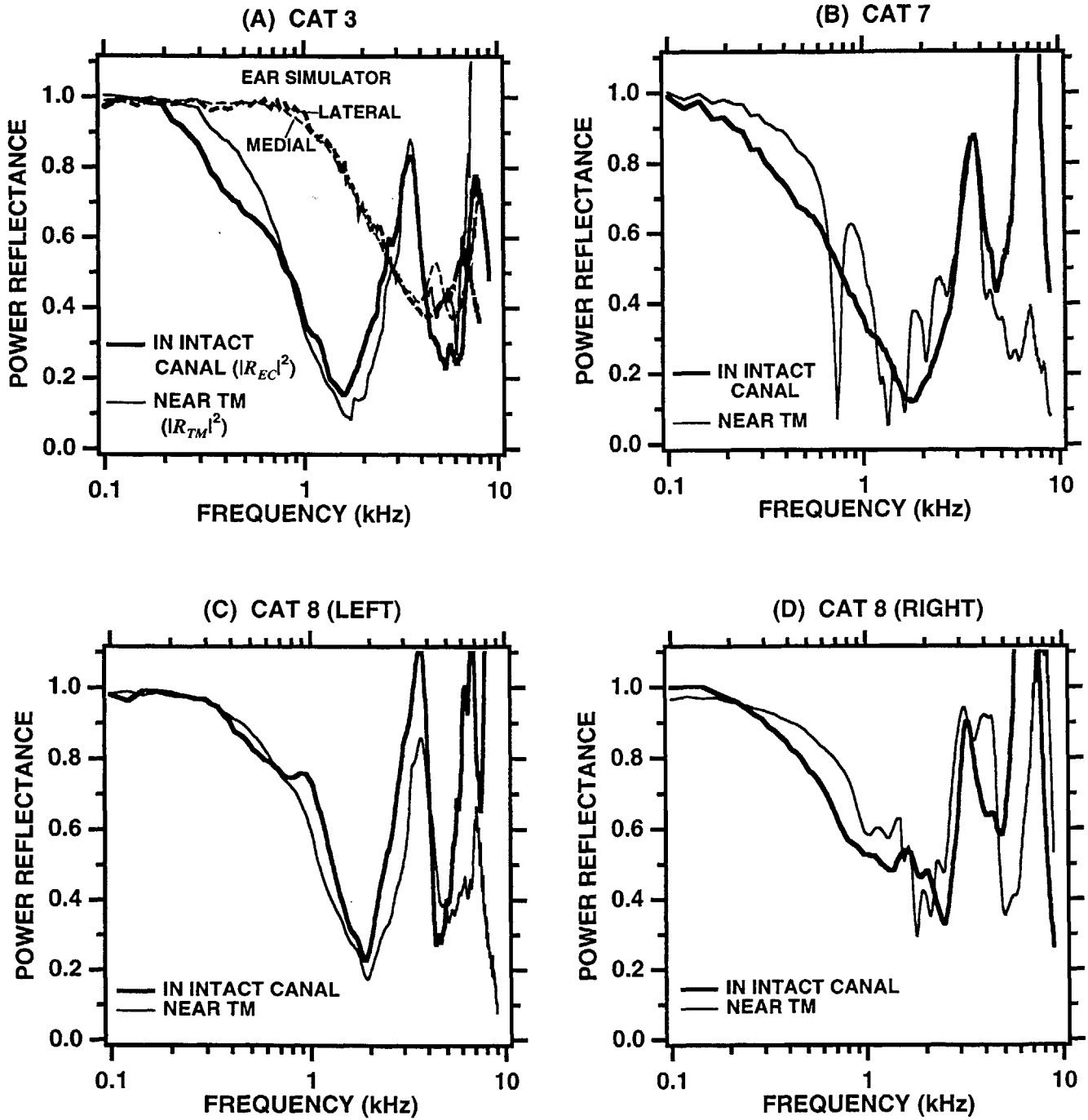
(A) CAT 3

EAR SIMULATOR
LATERAL
MEDIAL

POWER REFLECTANCE

IN INTACT
CANAL ($|R_{EC}|^2$)

NEAR TM
($|R_{TM}|^2$)

FREQUENCY (kHz)

(B) CAT 7

POWER REFLECTANCE

IN INTACT
CANAL

NEAR TM

FREQUENCY (kHz)

(C) CAT 8 (LEFT)

POWER REFLECTANCE

IN INTACT CANAL
NEAR TM

FREQUENCY (kHz)

(D) CAT 8 (RIGHT)

POWER REFLECTANCE

IN INTACT CANAL
NEAR TM

FREQUENCY (kHz)

123

CHAPTER 3

Relating middle-ear acoustic function to body size in the cat family: Measurements and models

ABSTRACT

We seek a quantitative description of the relationship between body size and the acoustic performance of the middle ear, which influences the dependence of the auditory threshold on sound frequency. The cat family was chosen for its qualitatively uniform middle-ear structure, its large range of species size, and the extensive structural and physiological data available from domestic-cat ears. We report measurements of the acoustic middle-ear input admittance Y_{TM} (as a function of frequency) and the inferred power reflectance in the intact ear canals of 17 anesthetized adults (21 ears) from 12 species of the family, including domestic cat. [Data from 13 other ears were rejected on the bases of (1) the ear's acoustic variations in response to static- pressure variations and (2) the configuration of the acoustic seal in the canal.] Body weight and head length are used as measures of each specimen's size.

The acoustic responses are qualitatively similar among the species; interpretation of Y_{TM} (f) is organized by a middle-ear lumped-network model. The net middle-ear acoustic compliance (equivalent air volume 0.4-1.7 cm^3) increases with body size. The frequencies of a prominent notch in admittance magnitude (2.3-4.0 kHz) and the first minimum in power reflectance (0.8-1.9 kHz) decrease with body size. The (inferred) acoustic compliance of the tympanic membrane and ossicular chain (generally 0.6-2.7 cm^3) is *not* correlated with body size.

The data are used to develop and test structure-based rules that describe the dependence of two features of middle-ear sound transmission on body size: (1) the low-frequency "cavity gain", the fraction of the ear-canal sound pressure that drives the ossicular chain, and (2) the frequency of the notch in admittance (and transmission) that results from an antiresonance of the middle-ear cavities. The predictive rules explain about half of the variance in the data and are consistent with hypotheses concerning possible selective pressures that influence hearing behavior. Body size thus provides a quantitative description of some acoustic features of auditory function in the cat family. These results suggest that the comparative approach to relating structure and function to survival can be applied to the cat family (and possibly other taxonomic groups) in an effort to construct hypotheses concerning the evolution of mammalian hearing function.

INTRODUCTION

The frequency range of hearing in terrestrial mammals varies widely, e.g., from roughly 3-70 kHz in mice (*Mus musculus*) to 0.03-7 kHz in Indian elephants (*Elephas maximus*) (Heffner and Masterton, 1980; Heffner and Heffner, 1980; Rosowski, 1992, p. 621; Calder, 1996, p. 240). Calder's interspecies review of highest audible frequencies (1996, p. 237) leads to his rather casual remark, "So mice squeak and elephants bellow!" Before connecting hearing function to adaptive behaviors such as intraspecific communication, we wish to describe the acoustic bases for these variations in auditory function. That is, we seek mechanistic arguments concerning the observation that larger animals generally hear sounds of lower frequencies than smaller animals, an observation that is based on extensive audiometric data (Heffner and Masterton, 1980; Fay, 1988). In fact, body size is a powerful variable in predicting many features of an animal's physiological, ecological, and behavioral life history (McMahon and Bonner, 1983; Peters, 1983; Schmidt-Nielsen, 1984; Calder, 1996); functions as seemingly diverse as metabolism, mode of locomotion, territorial size, and life span are all rather dependent on an animal's body size.

Correlational evidence indicates that the external and middle ears contribute significantly to the frequency dependence of the auditory threshold (Dallos, 1970; Rosowski et al., 1986; Rosowski, 1991, 1992). The mammalian middle ear -- in which three ossicles provide the linkage from the tympanic membrane (TM) to the inner ear -- is thought to have evolved in early mammals in part for increased sensitivity to high frequencies (Hopson, 1966; Masterton et al., 1969; Crompton and Parker, 1978; Kermack and Musset, 1983). To gain insight into the middle ear's role in determining the frequency range of hearing, one might quantify relationships between an animal's audible-frequency range and the size of various middle-ear structures. Indeed, correlations have been determined between auditory thresholds and TM area, stapes footplate area, and middle-ear cavity volume (Rosowski, 1992, pp. 622-623). As the size of these structures is closely related to an animal's body size (Rosowski, 1994, Fig. 6.15), the middle ear seems to be a

reasonable starting point for the development of mechanistic rules that relate auditory function to body size.

Comparative studies of middle-ear function are complicated by differences among species in the configurations of the TM (large pars flaccida versus small pars flaccida), ossicles (firmly attached to the tympanic bone versus suspended by ligaments), and cavity air spaces (one space versus multiple connected spaces, enclosed by bony walls versus no bony walls) (Fleischer, 1978; Rosowski, 1994). A logical first step is to restrict our study to animals that have middle-ear structural features in common. Indeed, rules relating acoustic responses to body size would seem to be most likely to have predictive value, if they are developed in a taxonomic group that can be organized primarily by size.

To try to isolate the effects of body size, we focus on the structurally-similar species of the cat family (*Felidae*). This taxonomic group was chosen for its species' qualitatively similar (and distinctive) middle-ear structure, large range of species size, manageable number of species (37), and for the wealth of structural and physiological data from one species, domestic cat (e.g., Møller, 1965; Guinan and Peake, 1967; Khanna and Tonndorf, 1972; Decraemer et al., 1990; Peake et al., 1992; Lynch et al., 1994). In particular, the acoustic effects of the felid middle-ear cavity structures have been characterized (Guinan and Peake, 1967; Peake et al., 1992; Lynch et al., 1994; Huang et al., 1997b); however, the significance of these structures to hearing (if any) is not known.[19] As a first step toward relating middle-ear function to structure and body size in this family, we compared acoustic and anatomical measurements made post-mortem in ears of lion (*Panthera leo*) and bobcat (*Lynx rufus*) to similar measurements in domestic cat (Huang et al., 1997a, b; see also Chapter 1, Fig. 1.4). The results are consistent with the hypothesis that middle-

---

[19] Domestic cats are unusual among terrestrial mammals in that their hearing is good for both low (0.2 kHz) and high (60 kHz) frequencies (Heffner and Masterton, 1980, p. 1597; Fay, 1988; Rosowski, 1992, p. 621). Explanation of the possible role of the middle ear in this performance enhances interest in the ears of the cat family.

ear structural similarity leads to qualitatively similar acoustic responses in the family, with quantitative differences due, at least in part, to middle-ear structural size.

In this chapter, we report measurements of acoustic middle-ear input admittance and inferred power reflectances in the intact ear canals of live, anesthetized exotic and domestic-cat adult specimens. The specimens provide a reasonably extensive sample of species (11 exotics plus domestic cat) and span a large size range (body weights 3-180 kg). From these measurements and the use of a lumped middle-ear network model (Peake and Guinan, 1967; Lynch, 1981; Peake et al., 1992; Huang et al., 1997b), we arrive at a measure of middle-ear sound transmission which depends on the size of the middle-ear cavities and thereby, by empirical structural rules (Peake and Rosowski, in prep.), on body size.

This chapter has three main goals: (1) to test the hypothesis that middle-ear structural similarity is associated with qualitatively similar acoustic performance in all species of the cat family; (2) to determine correlations between the ear's acoustic performance and body size; and (3) to develop and test structure-based rules that relate features of middle-ear sound transmission to body size for the family. The results demonstrate the effects of body size on some features of auditory function in a group of structurally similar (and distinctive) ears, and can be applied to the analysis of selective pressures involved in the evolution of hearing in the cat family and possibly other terrestrial mammals.

I. METHODS

A. Experimental specimens

Measurements on the intact ears of anesthetized exotic-cat species were made over the course of one year in cooperation with curators and veterinarians at three locations. Measurement sessions were conducted during two visits to the Center for Research on Endangered Wildlife at the Cincinnati Zoo (Cincinnati, OH), two visits to the Carnivore Preservation Trust (Pittsboro,

NC), and one visit to North County Veterinary Services (Oswego, NY). Our visits were arranged to coincide with other procedures requiring these animals to be anesthetized.

Exotic-cat species were anesthetized with injections of either (1) ketamine (21-28 mg/kg), (2) ketamine supplemented with valium (0.4-0.8 mg/kg), (3) Telazol (5-8 mg/kg), a mixture of tiletamine and zolazepam, or (4) Domator, a reversible agent consisting of metatomidine (0.024 mg/kg) and ketamine (2.4 mg/kg). During most measurement sessions, animals were also given isoflurane (2-3%) to respire via intubation or a snout mask. All measurements were made indoors with the animal on a table. The average duration of the acoustic-measurement procedure was 25-30 minutes per ear.

Data are reported from 17 intact ears of 14 adult specimens (10 males, 4 females) from 11 exotic-cat species (Table 3.1). The subjects had no known history of middle-ear disease or infection. Prior to acoustic measurements, the ear canal and (when possible) the tympanic membrane (TM) were viewed through an otoscope. In the larger animals, the greater length of the ear canal and depth of the concha made it impossible to attain the plane of focus and viewing angle necessary to see the TM; in these ears, only the most lateral 5-10 mm of the canal were visible. In all ears from which data are reported, the visible portion of the canal was relatively free of debris (i.e., wax, mites, blood) and the TM (if visible) was translucent. In a few specimens, both ears were initially examined by otoscope, and the canal that appeared cleaner was chosen for acoustic measurements. The criteria for accepting acoustic data are discussed below (Section I C).

This report also includes acoustic-admittance measurements from 4 ears of 3 adult domestic cats (1 male, 2 females), made near the tympanic membrane with most of the cartilaginous ear canal removed (Chapter 2, Section II B). These data were used to test the admittance-location transformation in the ear canal (Chapter 2, Fig. 2.18) which we used in the exotic-cat ears.

B. Acoustic methods

1. Approach

The goal of our acoustic-measurement procedure was to determine two related measures of middle-ear function: (1) the middle-ear input admittance, and (2) the power reflectance in the ear canal. Our basic approach was to measure the acoustic admittance in the intact ear canal with varying static air pressures in the canal. From these data, the dimensions of the ear canal between the measurement point and the TM were estimated. From these results (admittance and canal dimensions), the reflectance at the measurement point and the admittance transformed to the location of the TM were computed (Chapter 2, Section II).

2. Measurement of ear-canal admittance and reflectance

a. Basic method and accuracy

Broadband acoustic measurements were made with a portable system that was developed and tested in domestic-cat ears (Chapter 2). Briefly, the hardware consisted of an earphone and microphone assembly (modified Etymotic Research ER-10C), a laptop personal computer, and a digital-signal-processing board. To enable measurement of acoustic admittance, the sound source was characterized by a Norton equivalent circuit consisting of a volume-velocity source in parallel with a source admittance (e.g., Rabinowitz, 1981; Lynch et al., 1994); these source parameters were determined from sound-pressure measurements in two "calibration" loads of known admittance.

Comparisons of measured and theoretical admittances are shown in Fig. 3.1, for two loads into which the acoustic system was sealed with eartips used in felid ears.[20] The plots illustrate the accuracy of the admittance-measurement system in loads having inner diameters similar to those of

---

[20] The main difference between Fig. 1 and other similar figures (e.g., Chapter 2, Fig. 2) is that here the method of sealing the measurement system into the load is the same as that used for cat ears (see below).

felid ear canals. In the left panel, for frequencies between 0.06-8 kHz, the measured and theoretical admittances agree within 10% in magnitude and 0.03 periods in angle, except near the frequencies of the sharp extrema. In the right panel, in which the load's diameter and the source-admittance magnitude are larger, the same error limits describe the results for all frequencies up to 7 kHz. Above 8 kHz, there are large errors in both the source admittances (indicated by angles far outside the range ±0.25 periods) and the measured admittances. Our interpretation is that the accuracy of admittance measurements deteriorates at high frequencies because of errors in the source-calibration measurements.[21] For low frequencies, accuracy is limited by the signal-to-noise ratio: Measurements made in ears at different stimulus levels show that noise (biological and environmental) is significant below 0.1-0.2 kHz. Based on these observations, we restrict our report of admittance and reflectance measurements in ears to frequencies between 0.1-8 kHz.

b. Procedure in ears

The acoustic system was coupled to the intact ear canal via insertion of a custom-made eartip (Chapter 2, Sections II B 3-4). These eartips -- consisting of separate microphone and earphone tubes (length 30-45 mm) and a flexible silicone "guide" -- were designed to pass through the felid ear's deep concha and around the sharp bend at the canal-concha border. Larger species generally required longer tubes and guides. After insertion, responses to acoustic stimuli were used as indicators of the patency of the sound tubes and the approximate location of the eartip (e.g., in the canal versus in the concha).

To provide a static-pressure (and acoustic) seal between the eartip and the canal, earmold impression material was injected into the concha behind the eartip (Chapter 2, Fig. 2.11). Achievement of an effective seal often required several attempts, where "effectiveness" was

---

[21] Errors in our calibration measurements above 7 kHz may be the result of non-uniform waves generated at the interface between the narrow earphone tube and the load which become significant at the tip of the microphone tube (Chapter 2, Section III A 1; see also Keefe et al., 1992, p. 478). The relative size of these modes is expected to increase with increasing load diameter. Noise is not a problem for these frequencies (signal-to-noise ratio of 20-30 dB); however, electric crosstalk between the earphone and microphone is significant above 10 kHz (Chapter 2, Section II B 3).

generally indicated by (1) an increase in the acoustic response (compared to pre-injection), particularly for low frequencies ($f < 0.5$ kHz), and (2) the ability to introduce stable static-pressure levels in the canal via syringe. Acoustic responses were then measured with controlled static pressures in the canal (Chapter 2, Section II B 4 and Fig. 2.14).

After completion of the ear-canal measurements for each ear, the source was calibrated (with its eartip) in reference loads having diameter within 15% (and usually within 10%) of the canal diameter at the measurement point. The canal diameter was estimated from the measured admittance (Keefe et al., 1992; Chapter 2, Section II D 2 a).[22] With the source parameters determined, the admittance in the ear canal Y_{EC} was then calculated [e.g., Chapter 2, Eq. (2.1)].

Acoustic reflectance in the ear canal (R_{EC}), the ratio of the reflected (outward traveling) pressure wave to the incident (inward traveling) pressure wave, was computed as $R_{EC} = (Y_0 - Y_{EC})$ / $(Y_0 + Y_{EC})$, where Y_0 is the characteristic admittance based on the canal's diameter at the measurement point (e.g., Keefe et al., 1992, p. 470; Voss and Allen, 1994, p. 372). The power reflectance $|R_{EC}|^2$, the fraction of power reflected in the canal at the measurement point, has been shown in domestic-cat ears to be approximately equal to the fraction of power reflected at the TM, at least between 0.5-5 kHz (Chapter 2, Fig. 2.21). The quantity ($1 - |R_{EC}|^2$) is thus a measure of the acoustic power transmitted to the middle ear.

3. Transformation of admittance to the TM

To estimate the middle-ear input admittance Y_{TM}, a location transformation was applied to the measured admittance (Chapter 2). Briefly, the ear-canal space between the measurement point and the TM was approximated by a rigid uniform tube (analogous to an electric transmission line).

---

[22] To obtain another estimate of each canal's cross-sectional area, we injected earmold impression material into the concha (with a cotton dam in the canal to stop the flow of material) in the absence of the eartip. However, in the great majority of ears (17 out of 21), the impression material did not enter the canal because of the depth of the concha and the constriction of the canal-concha bend. In a few ears (4), impressions of the lateral portion of the canal *were* obtained. For these ears, the mean of 2 perpendicular diameters of the earmold at the approximate location of the microphone-tube tip agreed with the acoustically-estimated canal diameter to within 12%.

The dimensions of the tube were determined from (1) the canal's diameter at the measurement point (see above) and (2) ear-canal admittance measurements made with large negative static pressures in the canal which give a canal-volume estimate.

The effects of the admittance-location transformation are shown in Fig. 3.2, for both ears of a medium-sized specimen (a caracal). For frequencies below 0.8 kHz, the transformation results in (1) a roughly constant decrease in admittance magnitude $\Delta|Y|$ -- corresponding to the subtraction of the lumped-compliance admittance of the ear-canal volume (1.2 cm^3 for the left, 0.9 cm^3 for the right) -- and (2) a more negative angle. At 3.3 kHz, a sharp notch in magnitude and positive transition in angle appear in the transformed admittance, a feature which is consistent with a middle-ear cavity antiresonance observed in other felid species (Møller, 1965; Guinan and Peake, 1967; Peake et al., 1992; Huang et al., 1997a, b). The agreement between the estimated left and right middle-ear input admittances below 5 kHz shows that for this frequency range the method gives repeatable results. Above 5 kHz, the estimated admittances differ in the two ears, particularly in angle; for these frequencies, errors in both the measured admittance and the location transformation can be significant (Chapter 2, Section III A 2).

The effective ear-canal length (18-19 mm) and diameter (8-9 mm) used for the location transformations (Fig. 3.2) are both greater than those used for domestic cats (length 8-12 mm, diameter 5-7 mm). Larger dimensions are consistent with observations made via otoscope that the canal (and concha) is longer and wider in caracal (and in most other felid species) than in domestic cats.

Our methods, tested on domestic cats, have been shown to give reasonably accurate estimates of Y_{TM} for frequencies between 0.1-5 kHz, with larger errors above 5 kHz (Chapter 2, Section III A 2 and Table 2.1). Specifically, the estimate of the middle ear's compliance for low frequencies was found to be accurate within $\pm14\%$, and the estimate of the frequency of the middle-ear admittance notch was found to be accurate within $\pm5\%$. These error magnitudes will be assumed to apply to the measurements reported here.

C. Acoustic-data selection

1. Acceptance criteria

Measurements of acoustic admittance in the ear canal were considered acceptable if and only if two criteria were met: (1) the measurements were made with a "proper" acoustic seal of the measurement system in the ear canal; and (2) "normal" admittance responses were obtained with varying static-pressure levels in the canal. These criteria, developed from tests of our methods on domestic cats, are detailed below.

(1) Generally, the injected sealant was required to reach the lateral face of the eartip guide over at least half of its circumference, as judged by the configuration of the sealant upon removal of the acoustic system and sealant from the ear. [If the sealant does not fill the space lateral to the guide, this air space may be acoustically coupled to the load and can introduce large errors in the inferred Y_{TM} (Chapter 2, Section II E 2 and Fig. 2.20).] However, this criterion was relaxed for three ears (leopard, jaguar, and tiger) in which there were changes of less than 8% in $|Y_{EC}|$ (from 0.1-8 kHz) before and after injection of the sealant. Our interpretation is that for these eartip placements, the guide alone formed a good acoustic seal to the canal.

(2) For frequencies below 0.5 kHz, $|Y_{EC}|$ was required to exhibit the following responses to static-pressure variations in the canal: (a) monotonic decreases with increasing static-pressure magnitude, with a total decrease of at least 30% (3 dB) between 0 and -300 mm H_2O, and (b) a return to within 20% of the initial zero-pressure measurement, 30-40 seconds after the static pressure was returned to zero. These acoustic behaviors were interpreted as "normal" tension and relaxation responses of the TM to variations in static pressure (e.g., Chapter 2, Fig. 2.14).

2. Success rate

Based on the above criteria, acoustic-admittance data from exotic cats were accepted from 17 ears (Table 3.1) and rejected from 13 ears, including 2 ears from individuals in Table 3.1 (a

mountain lion and the serval) and 11 ears from other individuals (1 specimen of each of the following species: leopard, snow leopard, ocelot, caracal, serval, margay, pampas cat, and Pallas's cat). Of the 13 rejected ears, 8 failed to meet only the acoustic-seal criterion, 3 failed to meet only the static-pressure-response criterion, and 2 ears failed to meet either criterion. In summary, out of a total of 30 ears on which measurements were made, 17 ears yielded useful acoustic results, for an experimental success rate of 57%.

3. Operational difficulties

There are two apparent reasons for the rather low experimental yield. The first reason is the difficulty in placing and sealing the eartip in the intact ear canals of these animals. Most felids -- particularly the larger species (mountain lion, leopard, jaguar, tiger) and servals -- were found to have deep conchas that required long eartips, which made it difficult to inject the sealant to a deep enough point to reach the guide. Some of the smaller felid species (e.g., pampas cat and Pallas's cat) had very narrow conchas, which resulted in similar sealing problems. In general, the size of the acoustic assembly (see Chapter 2, Fig. 2.11) limited our ability to insert to the proper depth both the eartip and the syringe used to inject the sealant. A smaller acoustic assembly and/or longer sound tubes could be developed and tested in the future. Another possibility would be to use an inflatable cuff built around the eartip to form a seal (e.g., Rabinowitz, 1981); however, advancing such an assembly past the bend at the canal-concha border in cats might be difficult.

The second reason for the low yield is apparently the condition of some of the specimens' ears. Most (4 out of 5) cases of "abnormal" acoustic responses to static-pressure variations occurred in ears in which a substantial amount of wax was observed in the canal. In some ears, wax continually blocked the earphone tube and/or the microphone tube, requiring the eartip to be removed, cleaned, and reinserted. In other ears, wax observed deep in the canal might have impeded the normal motion of the TM or perhaps indicated an abnormal middle ear. Unless the veterinarian were to clean the canal during an earlier examination, little can be done to improve these conditions aside from removing excess wax in the concha with cotton swabs.

D. Structural methods

1. Approach

With the goal of relating features of the ear's acoustic response to body size, we established measures of both body size and middle-ear structural size for each specimen. Body size was determined from a combination of head-length and body-weight measurements and species means from a structural database (Peake and Rosowski, in prep.). Measures of some middle-ear dimensions for each specimen were necessary to develop and test structure-based predictive rules. As middle-ear structural measurements could not be made on our live specimens, we made use of species-mean data obtained on museum skulls and empirical rules.

2. Measures of size for each specimen

We have a database of structural measurements made on over 400 museum skulls of 35 species of the cat family, with roughly 10 specimens of each species (Peake and Rosowski, 1997; Peake and Rosowski, in prep.). This database uses skull length as a measure of body size, because it can be well defined and is widely used as an indication of body size (e.g., Pocock, 1951; Van Valkenburgh, 1990).[23] Specifically, the database uses the condylobasal skull length L_{CB}, the distance between the anterior face of the upper incisors and the posterior edge of the occipital condyles.

The length L_{CB} cannot be measured directly in live specimens, because of lack of access to the occipital condyles. For each specimen, an estimate of L_{CB} was determined from the mean of three independent estimates. The first estimate is based on a skull dimension that can be measured in live specimens -- the "greatest" skull length L_G, the distance (on the midline) between the upper

---

[23] The use of skull length (instead of body weight, for example) as the reference size measure for the live specimens is arbitrary. In fact, body weight is included in our estimate of each specimen's size (see below) and could have been chosen as the reference.

incisors and the lambdoidal ridge which usually could be felt through the skin. Head-length measurements were made with hand-held calipers (or, for the largest animals, a length of string pulled taut along the head and marked off). An empirical rule based on measurements of both L_{CB} and L_G on skulls from the database was then used to estimate L_{CB} from L_G:

$$L_{CB}(\text{mm}) = 1.099 \, [L_G(\text{mm})]^{0.9625}; \text{ N=413, R}^2\text{=0.92,} \tag{3.1}$$

where the units of each variable are in parentheses,[24] N is the number of cat-family specimens sampled, and R^2 is the coefficient of determination for the regression (representing the fraction of variance in the data explained by the fit). The second estimate of L_{CB} was based on the specimen's body mass, M. Each specimen was weighed on a scale, except for three of the largest animals (tiger, jaguar, and a mountain lion) whose weights were estimated by the veterinarian. The estimate of L_{CB} was then obtained from the empirical relations (Peake and Rosowski, in prep.)

$$L_{CB}(\text{mm}) = 57.85 \, [M(\text{kg})]^{0.307} \tag{3.2a}$$

for males, and

$$L_{CB}(\text{mm}) = 61.71 \, [M(\text{kg})]^{0.292} \tag{3.2b}$$

for females, which are based on a literature review (for weights) and analysis similar to that of Van Valkenburgh (1990). The third estimate of L_{CB} was a species-mean value from direct measurements on the skulls of each species in the museum database. Inclusion of the species mean should generally reduce the error in our estimates of L_{CB}, especially in the largest animals for which both L_G and M have significant error.

In summary, the value of L_{CB} attributed to each specimen is the mean of an estimate from Eq. (3.1) based on a measured head length, an estimate from Eq. (3.2) based on the measured body weight, and a species-mean L_{CB} from the museum-skull database. Among all the specimens,

---

[24] In this report, equations that involve empirical rules give the dimensions of each variable and imply that numerical coefficients have the proper dimensions for consistency.

the coefficient of variation or "relative spread" (the ratio of the standard deviation to the mean) of these three estimates is fairly small, ranging from 1-10% with an average of 6%. The coefficient of variation for L_{CB} in the museum skulls of these species ranges from 4-10% with an average of 8% (computed from Peake and Rosowski, in prep.). Conservatively, we estimate the total error in determining L_{CB} in live specimens to be ±10%.

To estimate each specimen's total middle-ear cavity volume (V_{CAV}), we used a species value from the skull database (in contrast to the three-way estimate of L_{CB}). First, we assumed the species-mean value of the product of auditory-bullar length, width, and depth ($L_B W_B D_B$). This mean value, based on measurements of three approximately orthogonal bullar dimensions in roughly 10 skulls (of both sexes) from each species, was then related to V_{CAV} by an empirical rule based on volumetric measurements made on skulls of five species spanning the size range of interest (Peake and Rosowski, 1997),

$$V_{CAV}(\text{cm}^3) = 0.489 \ [L_B W_B D_B(\text{cm}^3)]^{0.963}; \ N=16, \ R^2>0.99. \tag{3.3}$$

To estimate the error in V_{CAV} for each species, the mean $L_B W_B D_B$ plus and minus one standard deviation were substituted into Eq. (3.3) to give a range of cavity volumes. The error varies among species but is generally ±18-31% (see Table 3.1).

II. RESULTS

A. Structural measures

A main goal of this paper is to relate features of the ear's acoustic performance to body size in a structurally similar taxonomic group. In this section, we describe the body-size and inferred middle-ear-cavity size variations among our subjects. Table 3.1 gives the estimated skull length (L_{CB}) and body weight (M) for each specimen, organized in descending order of L_{CB}, our primary measure of body size. The specimens span a factor of 60 in body weight and a factor of 3.6 in skull length. In comparison to our cat-family museum-skull database (Peake and Rosowski, in

prep.), 12 of the 14 exotic-cat specimens have skull lengths that are greater than their species' mean in the skull database, with 7 specimens larger than one standard deviation above the mean (see asterisks in Table 3.1) and none smaller than one standard deviation below the mean. A possible reason for this apparent bias toward larger animals is that our subjects were captive and well fed, whereas the museum specimens were mostly from the wild.

For the purpose of organizing the acoustic results, we divide the species into the following (somewhat arbitrary) size groups: small (L_{CB}<110 mm, M<10 kg: domestic cat, sand cat, Indian desert cat, and jungle cat), medium (110<L_{CB}<140 mm, 10<M<20 kg: serval, caracal, ocelot, and Asian golden cat), and large (L_{CB}>140 mm, M>20 kg: mountain lion, leopard, jaguar, and tiger).

We estimate that our specimens' middle-ear cavity volumes (species means from the skull database V_{CAV}, listed as acoustic compliances C_{CAV} in Table 3.1)[25] span a factor of about 12. However, the relative spread in the museum-skull C_{CAV} values (from the database distributions) is quite large for some of the species, e.g., ±38% for mountain lion, and ±31% for jungle cat and tiger. We argue that a live specimen with L_{CB} greater than one standard deviation above its species mean is expected to have a cavity volume C_{CAV} in the upper half of the range listed in Table 3.1 (for specimens marked with asterisks). That is, taking the species-mean value of C_{CAV} for a specimen that is large for its species is likely to underestimate the cavity volume, because auditory-bullar dimensions are tightly correlated with skull length over the family (Peake and Rosowski, 1997, Fig. 1). This argument is used in determining error bounds in the computation of the acoustic compliance of the TM and ossicular chain in these specimens (Section III B 2); the error bounds are smaller with this assumption.

---

[25] The acoustic compliance (C) of a volume of air (V) is given by $C = V/(\rho_0 c^2)$, where ρ_0 is the density of air, c is the propagation velocity of sound in air, and $1/(\rho_0 c^2)$ is the adiabatic compressibility of air. In this paper, all acoustic compliances are expressed numerically in terms of equivalent volumes of air.

B. Acoustic measurements

1. Overview

In this section, measurements of middle-ear input admittance and ear-canal power reflectance are presented for each species (Figures 3.3-3.5). To aid in searching for size-dependent features of the measurements, the results are grouped by species size (see Section II A): small (Fig. 3.3), medium (Fig. 3.4), and large (Fig. 3.5). Each of the three figures shows middle-ear input admittances in the upper panel and ear-canal power reflectances (computed from the admittances shown) in the lower panel, on the same frequency scale. The admittances plotted were measured just prior to the introduction of static pressures into the canal, to minimize any residual effects of stressing the TM, which generally amounted to differences of 10-20% in magnitude. For species in which measurements in more than one ear were available, the measurement made with the smallest ear-canal coupling volume (between the measurement point and the TM) is plotted; in principle, given a choice between a measurement in the canal and a measurement at the canal-concha border, we select the former because the uniform-tube approximation of the coupling space (Section I B 3) should be more accurate for that case.

Broadly, we focus on comparisons of qualitatively similar features that occur in all (or nearly all) the frequency responses among the species. In general, comparisons are made for frequencies below 5 kHz, as errors in the estimates of the middle-ear input admittance increase greatly above this frequency (Chapter 2, Fig. 2.19). Our goal is to relate these acoustic-performance features to body size and, ultimately, to possible adaptive consequences for hearing function.

2. Middle-ear input admittance

The middle-ear input admittances (Y_{TM}) have qualitatively similar features among the species (Figs. 3.3-3.5, upper panels). For low frequencies ($f < 0.3$ kHz), Y_{TM} is roughly compliancelike, with a magnitude slope of nearly 1 on the log-log scale and an angle near 0.25

periods. Between 0.3-2 kHz, Y_{TM} becomes more resistancelike, in that the magnitude flattens with increasing frequency and the angle decreases gradually (and generally monotonically) through an angle of 0 periods. Between 2-5 kHz, there are sharper variations with frequency in both magnitude and angle, including a fairly well-defined magnitude notch in most species. For frequencies above 5 kHz, the curves continue to show large variations with frequency and tend to diverge. Notable exceptions to the above trends include (1) tiger's admittance angle of less than 0.15 periods below 0.2 kHz (Fig. 3.5) and (2) jungle cat's magnitude peak and sharper negative transition in angle near 1.5 kHz (Fig. 3.3). The former feature is probably the result of a small leak in the ear-canal seal, while the latter feature is consistent with a middle-ear resonance not observed in the other species.

In comparing the admittances across size groups, we find that $|Y_{TM}|$ is generally greater for frequencies between 0.3-1 kHz in the large species than in the small or medium-sized species, with the exception of sand cat and jungle cat (Fig. 3.3). This result implies that within this frequency range a given sound pressure at the TM generally produces a larger TM volume-velocity magnitude in the large species compared to smaller species. Also, the lowest frequency for which the angle of Y_{TM} is 0 is generally lower in the large species than in the other species, with the exception of Indian desert cat (Fig. 3.3) and Asian golden cat (Fig. 3.4).

To make quantitative comparisons among species, we first define two features of Y_{TM}. (1) For low frequencies, the acoustic response of the felid middle ear is compliance dominated (i.e., springlike) with a smaller resistive component, which is consistent with measurements made in a wide variety of animal species (for a review, see Rosowski, 1994, Fig. 6.16). The net middle-ear compliance C_{ME} is computed from the reactive part of Y_{TM} for low frequencies, by averaging the values of $\text{Im}\{Y_{TM}\}/(2\pi f)$ over 10 frequency points between 0.12-0.34 kHz, where $\text{Im}\{\}$ denotes the imaginary part. The results of this process are entered in Table 3.1.

(2) The middle-ear response of domestic cats has a sharp transmission (and input-admittance) minimum near 4 kHz that results from an antiresonance of the middle-ear cavities

141

(Møller, 1965; Guinan and Peake, 1967; Peake et al., 1992; Lynch et al., 1994). In lion and bobcat, this minimum or "notch" has been shown to occur at lower frequencies as a result of quantitative differences in the relevant structural features (Huang et al., 1997a, b). However, the significance (if any) of this feature to survival is not known. With the goal of testing hypotheses concerning possible acoustic benefits of this feature, we wish to relate the frequency of the notch (f_{Ynotch}) to body size and possibly other ecological variables (e.g., external-ear size, frequencies of intraspecific vocalizations). We define the notch in terms of Y_{TM} as (a) a local minimum in magnitude that is at least 56% (>5 dB) below the preceding (i.e., lower in frequency) local maximum in magnitude with (b) an angle increase of at least 0.2 periods passing through the frequency of the magnitude minimum. By this definition, all of the admittances in Figures 3.3-3.5 have a transmission notch except for those of sand cat and ocelot (see Table 3.1); however, admittances measured in two other leopard ears and two other mountain-lion ears also did *not* exhibit clear notches. Possible reasons for the absence of a clear notch include (1) errors in estimates of Y_{TM} resulting from a more lateral measurement point (e.g., at the canal-concha border) in larger ears, (2) f_{Ynotch} being above the range of our methods (> 5-8 kHz), and (3) middle-ear pathologies not screened by our static-pressure tests.

The dependence of these two acoustic-performance measures on body size is discussed below (Section II C and Section III B 3).

3. Ear-canal power reflectance

The power reflectance in the ear canal is a measure of the ineffectiveness of the ear in absorbing acoustic power incident on the middle ear. Reflectance can be a useful measure because its magnitude is less sensitive than admittance to the exact measurement position in the ear canal (Keefe et al., 1993; Voss and Allen, 1994; Chapter 2, Fig. 2.21). Recent studies suggest that measurements of reflectance may have clinical utility (Keefe et al., 1993; Keefe and Levi, 1996; Levi et al., 1998).

142

The power reflectances $|R_{EC}|^2$ (Figures 3.3-3.5, lower panels) have qualitative similarities that are determined by features of the admittances Y_{TM}. For the lowest frequencies (f<0.2 kHz), $|R_{EC}|^2$ generally approaches 1 -- which is consistent with previous measurements in humans and domestic cats (Keefe et al., 1993; Voss and Allen, 1994; Lynch et al., 1994) -- because Y_{TM} is almost purely imaginary and also because $|Y_{TM}|$ is much smaller than the characteristic admittance of the ear canal.[26] Between 0.2-1 kHz, $|R_{EC}|^2$ decreases and approaches a fairly broad minimum (generally less than 0.3) where Y_{TM} is resistive and most nearly matched to the (resistive) characteristic admittance of the canal; this trend is qualitatively similar to that of reflectances measured in humans. For frequencies above 2 kHz, the curves diverge quantitatively but tend to reach a peak at a frequency near the admittance-notch frequency f_{Ynotch}; this trend is different from that of reflectances measured in humans, whose middle-ear admittances do not exhibit a notch. Interestingly, the broad minimum in $|R_{EC}|^2$ in humans usually extends to 4 kHz (Keefe et al., 1993), which is approximately the "best" or most sensitive audiometric frequency for humans, and then increases for higher frequencies, whereas in domestic cats $|R_{EC}|^2$ dips and stays low from 6-10 kHz (Lynch et al., 1994, Fig. 23), a range which spans the best audiometric frequency for domestic cats of 8 kHz (Rosowski, 1992, Table 29.1).

In domestic cats, computations of reflectance based on admittances measured at the TM show good agreement between the frequency of a reflectance peak and f_{Ynotch} (Lynch et al., 1994, p. 2204; Chapter 2, Figures 2.18 and 2.21). In contrast, the reflectance-peak frequency differs noticeably from f_{Ynotch} in some of the data from larger species reported here (jaguar, leopard, and mountain lion in Fig. 3.5). The difference could arise from errors in the spatial transformation. That is, above 2 kHz, errors resulting from the admittance-location transformation (affecting the

---

[26] The exceptions are tiger and jaguar, in which $|R_{EC}|^2$ < 0.8 at 0.1 kHz. In both cases, the small reflectance values result from admittance angles being significantly less than 0.25 periods. In jaguar, the more resistive angle of Y_{TM} and the canal's relatively small characteristic admittance (small radius of 2.3 mm) result in smaller values of $|R_{EC}|^2$ below 1 kHz, as compared to the other species.

estimate of f_{Ynotch}) and/or nonuniformities in the canal's geometry (affecting the spatial dependence of R_{EC}) may be greater in these longer canals.

To make quantitative comparisons among species, we define the first reflectance minimum to be the lowest-frequency minimum (global or local) of $|R_{EC}|^2$ with value less than 0.4. The frequency of this minimum f_{Rmin} represents the frequency of greatest (at least locally) transmission of sound energy from the canal to the middle ear (Table 3.1). The error in f_{Rmin} is estimated to be $\pm 15\%$, based on the mean of differences among f_{Rmin} values measured in domestic cats at different locations in the ear canal (Chapter 2, Fig. 2.21). We choose this frequency measure as opposed to (for example) the value of $|R_{EC}|^2$ at this frequency, because in domestic cats the error in estimating the frequency is generally smaller. [Potentially large errors in $|R_{EC}|^2$ above 5 kHz (Chapter 2, Section III B) prohibit the use of a higher-frequency measure such as the frequency of the next dip (see above).]

C. Correlations of acoustic measures with body size

1. General approach

To quantify the relationships between middle-ear acoustic properties and body size, we plotted acoustic measures for each ear (defined above) versus the estimated skull length (L_{CB}) of each specimen (see Table 3.1). Linear regressions were performed on the log-log data with a least-squares algorithm to yield power-function fits to the data. Scatter plots with regression lines are shown in Figures 3.6 and 3.7 for four relatively well determined variables: (1) total middle-ear compliance C_{ME}, (2) middle-ear cavity compliance C_{CAV}, (3) the admittance-notch frequency f_{Ynotch}; and (4) the reflectance-minimum frequency f_{Rmin}.

2. Middle-ear compliances

The total acoustic compliance of the middle ear C_{ME} is positively correlated with L_{CB} with a slope (exponent) of approximately 0.9 (Fig. 3.6, upper). That is, within this group of animals, C_{ME} generally increases as body size increases. This compliance, measured acoustically,

144

presumably includes the contributions of (1) the compliance of the TM-ossicular system and (2) the compliance of the middle-ear cavity air volume. Significant outliers -- i.e., ears that show deviations from the regression line that are greater than the error bars -- include sand cat (Sa: L_{CB} = 85.6 mm, C_{ME} = 1.29 cm^3, a very compliant ear), ocelot (O: L_{CB} = 130.3 mm, C_{ME} = 0.53 cm^3, relatively stiff), and tiger (T: L_{CB} = 296 mm, C_{ME} = 1.11 cm^3, relatively stiff). The slope (exponent) of the power-law fit is significantly different from zero (p<0.01), and the fit explains more than half (55%) of the variance in the data.

In the lower panel (Fig. 3.6), the acoustic compliance of the middle-ear cavities C_{CAV} is plotted for the same specimens, where a species mean from the museum-skull (structural) database is assumed for each specimen [see Eq. (3.3)]. C_{CAV} is positively and tightly correlated with L_{CB} with a slope of approximately 1.8. The cavity compliance thus increases with body size with a slope that is significantly greater than that of the total middle-ear compliance C_{ME} (0.9). [A notable outlier is sand cat, whose unusually large middle-ear cavity (C_{CAV} = 1.92 cm^3) contributes to its large total compliance C_{ME}.] These results suggest that the flatter body-size trend in C_{ME} and the greater scatter in C_{ME} (Fig. 3.6, upper) are largely due to the compliance of *other* middle-ear structures (e.g., TM, ossicles, ligaments) having a weaker dependence on body size.

3. Frequencies of minima in admittance and reflectance

Next, we examine the dependence on body size of the frequencies of specific features in the middle-ear responses of the family. First, the frequency of the admittance notch f_{Ynotch} correlates negatively with L_{CB} with a slope of approximately -0.4 (Fig. 3.7, upper). That is, f_{Ynotch} generally decreases as body size increases, with the slope being significantly different from zero and the least-squares fit explaining 52% of the total variance. This trend, together with the application of a middle-ear network model (Section III A), will be used to develop a structure-dependent predictive rule relating f_{Ynotch} to body size for the family (Section III B 4). The trend can provide some insight into the possible functional significance of this sharp decrease in middle-ear sensitivity; a potential acoustic benefit is discussed in Section III C 2.

Our hypothesis has been that the admittance notch is present in the middle-ear response of all species of the cat family, because of the structural similarity of the middle-ear cavities among species (Huang et al., 1997a, b). The majority of exotic-cat data reported here (11 out of 17 ears) exhibit this feature. However, in 6 ears of 4 species (sand cat, ocelot, leopard, and mountain lion), no prominent notch was observed. A notch *was* observed in other ears of leopard and mountain lion (Fig. 3.5). It seems possible that the longer length of the canal (compared to domestic cat) and/or the greater uncertainty in the configuration of the acoustic seal could have resulted in errors in the estimated Y_{TM} that are similar in size to errors in Fig. 2.20 (Chapter 2). We conclude that more samples of these species are necessary to test our hypothesis, particularly for species in which data from only one ear were accepted.

The lower panel (Fig. 3.7) shows that the reflectance-minimum frequency f_{Rmin} correlates negatively with L_{CB} with a significant slope of approximately -0.6. That is, f_{Rmin} decreases with body size, with the fit explaining 38% of the total variance. This slope (-0.6±0.2) is not significantly different from the slope of f_{Ynotch} versus L_{CB} (-0.4±0.1). These results are consistent with the idea that in larger felids the frequency response of the middle ear is shifted to lower frequencies. Comparisons over the family between these frequency measures and lowest audible frequencies and best audible frequencies might, in principle, lead to rules that relate these measures to hearing capabilities. However, audiometric data on felids are available only for domestic cats and not for any exotic-cat species to our knowledge. The interpretation of reflectance-minimum frequencies is an area of ongoing clinical research (e.g., Keefe et al., 1993), as the health of the middle ear may affect these measures.

4. Summary

The results of this section all show that linear regressions based on body size represent a substantial fraction of the variance in these acoustic measures, for the cat family. In the following sections, these trends will be used to develop and test predictive rules that relate middle-ear sound

transmission properties to body size, based on middle-ear structural rules and an acoustic lumped-network model.

III. DISCUSSION

A. Felid middle-ear network model

1. Approach

We have a theoretical framework for representing frequency responses of the middle ear in the cat family. A six-element lumped network model (Fig. 3.8) has been shown to capture the main features of middle-ear acoustic admittance and sound-transmission measurements in three felid species -- domestic cat, bobcat, and lion (Peake and Guinan, 1967; Lynch, 1981; Peake et al., 1992; Huang et al., 1997a, b). Use of the model assumes that (1) the sound pressure in the tympanic cavity is proportional to the volume velocity of the TM, and (2) the TM-ossicular-chain system is driven by the sound-pressure difference across the TM, $(P_{TM} - P_{CAV})$. [27]

In this section, the network model is used to express a measure of middle-ear sound transmission in two frequency regions: (1) for low frequencies (roughly 0.1-0.3 kHz), and (2) at the frequency of the middle-ear cavity antiresonance (ranging from 2-4 kHz among species). The derived expressions will be used to develop and test structure-based rules that relate these performance features to the size of the animal (Section III B).

---

[27] This model belongs to a class of "series-network" models that represent the middle ear as a series connection of (1) the impedance (reciprocal of admittance) of the TM and ossicular chain, and (2) the impedance of the middle-ear cavities (Onchi, 1961; Zwislocki, 1962; Mundie, 1963; Møller, 1965). This type of model has been applied to a wide variety of mammalian ears.

2. Middle-ear sound transmission

a. Definition of cavity gain, G_{CAV}

We define the "cavity gain", a measure of sound transmission through the middle ear, to be the fraction of the ear-canal sound pressure that drives the ossicular chain (Fig. 3.8),

$$G_{CAV} = (P_{TM} - P_{CAV}) / P_{TM} \tag{3.4}$$

where $(P_{TM} - P_{CAV})$ is the sound-pressure difference across the TM (Rosowski, 1994, p. 228; Peake and Rosowski, 1997).[28] This expression can be rewritten in terms of admittances and in general involves all six of the model's elements. The cavity gain can be interpreted as the cavities' effect on the middle-ear gain (or transmission). The presence of a closed volume of air behind the TM reduces the response of the middle ear by impeding the motion of the TM; some of the sound pressure incident on the TM in the ear canal acts to compress the air in the cavity.

b. Midfrequency transmission notch

All felid species have the distinctive middle-ear cavity structure of two air spaces divided by a bony septum and acoustically coupled through a narrow hole or "foramen" (Fig. 3.8). This structure introduces a sharp feature in the input admittance that we refer to as the admittance notch or cavity notch, in the frequency range 2-4 kHz.

The network model predicts a local minimum in $|Y_{TM}|$ and in $|G_{CAV}|$ at the frequency of the parallel antiresonance between the acoustic mass of the foramen (M_F) and the acoustic compliances of the bullar cavity (C_{BC}) and tympanic cavity (C_{TC}). For high Q (quality factor), this frequency is approximately determined by the three reactive cavity elements and is given by

$$f_{Ynotch} = 1/(2\pi) \, [M_F \, C_{TC} \, C_{BC} \, / \, (C_{TC} + C_{BC})]^{-1/2} \,, \tag{3.5}$$

---

[28] This transfer function is called the "cavity gain" because it represents the middle-ear gain relative to the condition of an infinite-volume (or widely opened) cavity.

148

where each compliance is proportional to the volume of the indicated cavity. For the specimens in Table 3.1, the measured f_{Ynotch} ranges from 2.3-3.9 kHz. This cavity antiresonance has been shown to produce a transmission notch in the magnitude of G_{CAV} of 6-20 dB among domestic cats, bobcats, and a lion (Huang et al., 1997a)

c. Low-frequency approximation

In the low-frequency limit (e.g., to apply to 0.1 kHz), the model predicts that Y_{TM} is primarily determined by the compliances C_{TOC}, C_{TC}, and C_{BC}, with the net middle-ear compliance

$$C_{ME} = C_{TOC}\, C_{CAV}\, /\, (C_{TOC} + C_{CAV}) \tag{3.6}$$

where C_{TOC} represents the compliance of the TM and ossicular chain, and $C_{CAV} = (C_{TC} + C_{BC})$ is the total cavity compliance, which is proportional to the total middle-ear cavity volume. Because the compliances essentially determine the acoustic response of the middle-ear system, the cavity gain G_{CAV} is well approximated by

$$G_{CAV} = 1\, /\, (1 + C_{TOC}\, /\, C_{CAV}). \tag{3.7}$$

Thus, middle-ear sound transmission for low frequencies is controlled by the ratio of the TM-ossicular compliance C_{TOC} to the cavity compliance C_{CAV}. As the middle-ear cavity volume increases for a given C_{TOC}, the gain approaches 1.

B. Relating middle-ear transmission to body size: Predictive rules

1. Overview

In this section, the network relationships derived above are used to develop and test rules that relate two features of middle-ear sound transmission to body size. The first feature is the value of G_{CAV} for low frequencies, the computation of which requires inferring a value of the TM-ossicular compliance C_{TOC} for each specimen. The distribution of C_{TOC} as a function of body size is an interesting result by itself (Section III B 2). We then compare the computed values of

149

G_{CAV} to a structure-based rule for the family that follows the approach of Peake and Rosowski (1997), and the predictive power of the rule is evaluated. The second feature is the frequency of the admittance notch f_{Ynotch}. The trend of these data with body size (Fig. 3.7, upper) is used to develop a simple predictive rule that is consistent with available structural data from domestic cat.

2. Compliance of the TM and ossicular chain, C_{TOC}

From previous acoustic measurements on a few species (8 specimens of 4 species) with the middle-ear cavities opened, it was found that C_{TOC} varied from 0.4-1.5 cm^3 with a weak dependence on tympanic-ring size and body size (Peake and Rosowski, 1997). Our data can be used to test this idea further by inferring values of C_{TOC} for each of the live specimens, based on the network model. Rearrangement of Eq. (3.6) gives

$$C_{TOC} = C_{CAV} C_{ME} / (C_{CAV} - C_{ME}).$$ (3.8)

Substitution of values for the total middle-ear compliance C_{ME} and the cavity compliance C_{CAV} from Table 3.1 (or Fig. 3.6) into Eq. (3.8) gives an estimate of C_{TOC} for each ear, plotted in Fig. 3.9 versus L_{CB}. The large size of errors in the C_{TOC} data are the result of taking worst-case combinations of errors in C_{CAV} and C_{ME} for each specimen, i.e., pairing the largest C_{ME} with the smallest C_{CAV} and the smallest C_{ME} with the largest C_{CAV}. [Equation (3.8) is rather sensitive to small changes in the compliances on its right side, because the difference ($C_{CAV} - C_{ME}$) can be small relative to C_{CAV} or C_{ME}.]

From Fig. 3.9, we conclude that the values of C_{TOC} (generally 0.7-2.7 cm^3) show rather little dependence on L_{CB}. A flat regression line at the mean value $C_{TOC} = 1.3$ cm^3 represents the data almost as well as the least-squares fit. This weak correlation is consistent with the reduction in correlation observed between the total compliance C_{ME} and L_{CB} relative to the strong correlation between the cavity compliance C_{CAV} and L_{CB} (see Fig. 3.6). The result supports the idea that the compliance of the TM and ossicular chain is *not* controlled by body size in the cat family. An interpretation is that the structural properties thought to determine C_{TOC} -- the stiffnesses of the

150

TM and ossicular ligaments -- are not especially constrained by the size of surrounding bony structures of the ear.

3. Low-frequency cavity gain, G_{CAV}

In this section, the data are used to test the predictive power of a structure-based rule that relates the low-frequency cavity gain G_{CAV} to L_{CB} (Peake and Rosowski, 1997). First, we briefly review the development of the functional rule, which incorporates middle-ear structural rules for the family. An empirical relation between the product of auditory-bullar dimensions (see Section I C 2) and skull length,

$$L_B W_B D_B (\text{cm}^3) = 2.02 \times 10^{-4} [L_{CB}(\text{mm})]^{2.06}; \text{N}=362, \text{R}^2=0.92, \quad (3.9)$$

is combined with Eq. (3.3) to give an expression for the middle-ear cavity volume as a function of skull length for the family,[29]

$$V_{CAV}(\text{cm}^3) = 1.35 \times 10^{-4} [L_{CB}(\text{mm})]^{1.98}. \quad (3.10)$$

Next, the simplifying assumption is made that $C_{TOC} = 1.3$ cm^3 -- i.e., C_{TOC} is *independent* of L_{CB} -- where this average value is suggested by the results in Fig. 3.9. With C_{TOC} given in terms of a volume, substitution of V_{CAV} (for C_{CAV}) and C_{TOC} into Eq. (3.7) gives a structure-based predictive rule for the family,

$$G_{CAV} = (1 + 9630 [L_{CB}(\text{mm})]^{-1.98})^{-1}. \quad (3.11)$$

The compliance data from the live specimens can be used to test this rule. Values for C_{TOC} (Fig. 3.9) and C_{CAV} (Fig. 3.6) are substituted into Eq. (3.7) to give values of the low-frequency cavity gain G_{CAV} for each ear (Table 3.1). To estimate the error in G_{CAV}, worst-case

---

[29] Note that this approach is *not* the same as our method of estimating the cavity volume for a given specimen. In that case, the species-mean is used, rather than the family rule in Eq. (10). Also, the exponent 1.98 in Eq. (10) is somewhat larger than the exponent 1.835 (based on 12 species) in the middle panel of Fig. 6. We choose to incorporate Eq. (10) into our "family" functional rule because it is based on a greater number of species.

combinations of the errors in C_{TOC} and C_{CAV} for each specimen were substituted into Eq. (3.7) to define a range of values for the cavity gain.

In Fig. 3.10, the individual G_{CAV} values and error ranges are plotted versus L_{CB} and compared with the family rule [Eq. (3.11)]. The total number of independent test points (ears) is 29, including previous data (denoted by triangular markers) from live domestic cats (4) and post-mortem specimens (2 bobcats, 1 tiger, and 1 lion). The individual G_{CAV} values range from approximately 0.3-0.9 (a 10 dB range). In grouping the species into the size bins of Figures 3.3-3.5, we observe the following trends in the data: (1) For the large species, G_{CAV} is greater than 0.6; (2) for the medium-sized species, G_{CAV} is between 0.4 and 0.7; and (3) for the small species, G_{CAV} is between 0.3 and 0.6.

The data are generally consistent with the structure-based rule, which predicts that (for low frequencies) the largest species have G_{CAV} values that are 8-10 dB greater than in the smallest species. The rule explains a substantial portion (41%) of the variance in the data, computed as $\{1 - \text{mean}[(G_{CAV} - \text{rule})^2] / \text{var}(G_{CAV})\}$, where the second term's numerator is the mean-squared vertical deviation of the G_{CAV} data points from the rule of Eq. (3.11), and the denominator is the variance of the G_{CAV} data. This measure of the "goodness of fit" is not particularly sensitive to small changes in the assumed value of C_{TOC} (1.3 cm^3); assumptions of C_{TOC} = 1.0 and 1.5 cm^3 both lead to rules that explain 38% of the variance. The large errors in some of the data points of Figures 3.9 and 3.10 indicate the need for (1) more data samples and (2) improvements in the method that reduce the errors in the acoustic measurements (e.g., a more reproducible seal to the canal) and/or allow middle-ear structural measurements to be made on the specimens (e.g., CT scans of the ears made post-mortem).

4. Admittance-notch frequency, f_{Ynotch}

In this section, the data are used to develop and test a rule that relates the frequency of the cavity antiresonance (admittance or transmission notch) f_{Ynotch} to L_{CB}. First we develop a functional rule, driven by the fit of the data in Fig. 3.7 (upper), and also incorporating structural

152

family rules. The data suggest that the notch frequency varies as $L_{CB}^{-0.37\pm0.1}$. As f_{Ynotch}

depends on the individual compliances (or volumes) of the tympanic and bullar cavities [see Eq. (3.5)], we make use of empirical family rules that relate the respective cavity compliances to skull length. Previous volumetric measurements in 10 ears of 5 species (domestic cat, bobcat, clouded leopard, tiger, and lion) lead to the empirical relations

$$C_{TC}(\text{cm}^3) = 1.9 \times 10^{-4} \, [L_{CB}(\text{mm})]^{1.6}; \; n=10, \, R^2=0.96 \qquad (3.12a)$$

for the tympanic cavity, and

$$C_{BC}(\text{cm}^3) = 7.2 \times 10^{-5} \, [L_{CB}(\text{mm})]^{2.1}; \; n=10, \, R^2=0.90 \qquad (3.12b)$$

for the bullar cavity (Huang et al., 1997a). To simplify the rule, as the sample sizes are small, the cavity volumes are assumed to both vary with the mean of the exponents in Equations (3.12a) and (3.12b), i.e., as $L_{CB}^{1.85}$. Choosing the coefficients to match the domestic-cat volumetric data gives the simpler combination

$$C_{TC}(\text{cm}^3) = 5.4 \times 10^{-5} \, [L_{CB}(\text{mm})]^{1.85} \qquad (3.13a)$$

and

$$C_{BC}(\text{cm}^3) = 2.5 \times 10^{-4} \, [L_{CB}(\text{mm})]^{1.85}. \qquad (3.13b)$$

The notch frequency f_{Ynotch} also depends strongly on the acoustic mass of the foramen (M_F) that couples the tympanic and bullar cavities (Fig. 3.8). With the adoption of the f_{Ynotch} data's dependence of $L_{CB}^{-0.37}$ as a constraint, the substitution of Equations (3.13a) and (3.13b) into Eq. (3.5) implies that M_F should vary as approximately L_{CB}^{-1}.

To relate the foramen's acoustic mass to its dimensions, the foramen can be approximated by a tube of length l_F and radius a_F, flanged on both ends (Lynch, 1981; Huang et al., 1997b). For frequencies f (Hz) for which $a_F(\text{m}) > 0.01f^{-1/2}$ and $a_F < 10/f$, the acoustic mass of the foramen can then be approximated by

$$M_F = \rho_0 (l_F + 1.7 \, a_F) \, / \, (\pi a_F^2), \qquad (3.14)$$

where the term 1.7 a_F represents the end corrections (Beranek, 1986, pp. 137-138).

Few data are available on how the dimensions of the foramen might vary with skull size. Measurements in domestic cat, bobcat, and lion suggest that the shape of the foramen can vary greatly among species, and that the areas of the interfaces between the foramen and the tympanic and bullar cavities do increase with increasing skull size (Huang et al., 1997a). From examination of Eq. (3.14), we deduce that the foramen's length and radius can both be chosen to vary proportionally with L_{CB} to give the desired power-law dependence of M_F on L_{CB}. That is,

$$l_F(\text{mm}) = 4.63 \times 10^{-2} \, [L_{CB}(\text{mm})]^1 \qquad (3.15)$$

and

$$a_F(\text{mm}) = 1.62 \times 10^{-2} \, [L_{CB}(\text{mm})]^1 , \qquad (3.16)$$

where the coefficients are chosen such that the foramen dimensions are consistent with data from a domestic cat whose foramen structure was studied via histological sections (Huang et al., 1997b). Substitution of these two structural rules into Eq. (3.14) gives an expression for the foramen's acoustic mass as a function of skull length,

$$M_F(\text{kg/m}^4) = 1.06 \times 10^5 \, [L_{CB}(\text{mm})]^{-1}, \qquad (3.17)$$

and substitution of Equations (3.13a), (3.13b), and (3.17) into Eq. (3.5) then gives a rule --shaped by the acoustic data -- for relating the notch frequency to skull length for the family,

$$f_{Ynotch} \, (\text{kHz}) = 27.1 \, [L_{CB}(\text{mm})]^{-0.43}. \qquad (3.18)$$

To determine its predictive value, in Fig. 3.11 the rule is compared to the f_{Ynotch} data from Y_{TM} (Table 3.1) and previous data from live domestic cats (5) and post-mortem specimens (2 bobcats, 1 lion). The rule explains a substantial fraction (53%) of the total variance in the data. The slope -0.43 is not significantly different from that of a least-squares fit to the data in Fig. 3.11 (slope of -0.37±0.06, n=23). Although different structural assumptions -- e.g., use of Eq. (3.12)

154

instead of Eq. (3.13), or different foramen scaling rules -- would change the form of the functional rule, the advantage of this rule is that it is the simplest and represents the data reasonably well.

From the notch-frequency data, predictions can be made concerning the structure of the foramen in the cat family. From Equations (3.15) and (3.16), the linear dimensions of the foramen are generally expected to increase with the first power of the skull length of the species. This prediction can be tested, with detailed structural measurements on deceased specimens, to determine its accuracy over the size range of the family. From measurements in the ear of one deceased lion, the shape of the lion's foramen was observed to be unlike that of any other felid species examined to date (domestic cat, bobcat, tiger). In fact, the lion's foramen is inconsistent with the structural rules of Equations (3.15) and (3.16), in that its cross section resembles a wide, elongated slit rather than a circular hole (Huang et al., 1997b, p. 1538). This observation is qualitatively consistent with the lion's notch frequency ($f_{Ynotch} = 2.8$ kHz) being significantly higher than predicted by the functional rule (Fig. 3.11), as a wider foramen would have a smaller acoustic mass [Eq. (3.14)] and would therefore produce a cavity antiresonance at a higher frequency [see Eq. (3.5)].

C. Ethological significance of size dependence

1. General approach

A long-term goal of this work is to formulate and test hypotheses that unify structural and functional properties of the ear with ethological processes that depend on hearing. In this section, we consider the effects of the correlations of acoustic performance on size (described in Figures 3.10 and 3.11) on auditory function. Connections are suggested between family trends and selective pressures involved in the survival of felid species. Also, a potential acoustic benefit of the felid middle-ear cavity structure is proposed.

155

2. Middle-ear cavity volume and low-frequency hearing sensitivity

a. Family trend

The transfer function G_{CAV} represents the middle-ear gain or transmission relative to an effectively infinite-volume cavity. G_{CAV} is a measure of the middle-ear cavities' effect on sound transmission; it is a factor in determining the overall auditory threshold. For a constant C_{TOC}, the gain increases with the volume C_{CAV}, as predicted by the functional rule shown in Fig. 3.10 approaching 1 asymptotically. That is, an animal with larger middle-ear cavities would presumably have greater middle-ear sensitivity to low frequencies. The rule predicts that, for this process (G_{CAV}) in this group of animals, low-frequency transmission through the middle ear increases with body size, because of the scaling of cavity volume with body size. The acoustic-measurement-based data in Fig. 3.10 are generally consistent with the rule and thus provide some empirical support for the idea that, other factors being equal, larger animals detect low frequencies more sensitively than do smaller animals. In summary, with the assumption of a constant TM-ossicular compliance (Fig. 3.9), we conclude that the largest felid species have 8-10 dB of increased middle-ear transmission for low frequencies over the smallest felid species. We also note that large species (which have C_{CAV} substantially greater than C_{TOC}) would gain little adaptive benefit, at least for low-frequency hearing, from having even larger middle-ear cavities.

In exploring the ethological significance of low-frequency hearing in felids, one variable of interest is the territorial area of mammalian carnivores, which varies directly with body weight (reviewed by Calder, 1996, p. 291). For example, a lion would tend to have a much greater home range than a bobcat. It has been proposed that lions mark their territory in part by roaring, a vocalization that is rich in low-frequency energy, i.e., below 0.2 kHz (Schaller, 1972, pp. 103-110). Since the greatest threats to lions (other than humans) are intraspecific, survival might be improved by increased sensitivity to these low-frequency vocalizations, for both competition and cooperation (Schaller, 1972; Heinsohn and Packer, 1995; Packer and Pusey, 1997). In contrast, smaller felids such as bobcats (which do not roar) might be less interested in low frequencies.

Low-frequency hearing may also be beneficial for finding prey; larger felids generally have larger prey (Peters, 1983, pp. 108-117) which might be expected to produce sounds of lower frequencies, either through vocalizations or locomotion. In this way, a large felid such as a tiger or jaguar hunting in an environment with limited visibility (dense jungle and/or in the dark) would seem to benefit from its sensitivity to low-frequency sound. In summary, qualitative connections can be proposed between the low-frequency functional rule (for G_{CAV}) and possible consequences for survival.

b. Deviation from family trends: Sand cat

The idea of this section is to examine data from one felid species that does *not* follow the family trends of compliances versus body size. Examples of the apparent adaptive benefits of outliers in middle-ear-cavity size can be found in some rodents, e.g., kangaroo rat and gerbil, whose large auditory bullae may be related to their increased hearing sensitivity to low-frequency sounds (Lay, 1972; Webster and Webster, 1980; Webster and Plassmann, 1992). It has been postulated that this increased sensitivity is an adaptive benefit for the detection of specific predators (owls and snakes) in their desert habitats. Might sand cat, a small species with a similarly arid habitat, natural predators, and enlarged middle-ear cavities (Fig. 3.6, lower), share this benefit?

Our data indicate that sand cat has a small low-frequency cavity gain (G_{CAV}=0.33, Fig. 3.10) because of the large compliance of its TM-ossicular system.[30] This result does *not* imply that the middle ear of sand cat is insensitive to low frequencies, because sensitivity (i.e., motion of the TM for a given stimulus sound pressure) should vary with the net middle-ear compliance C_{ME}, which is large in sand cat (Fig. 3.6, upper). [In fact, a similar pair of middle-ear compliances occurs in chinchilla ($G_{CAV} < 0.2$, from Rosowski, 1994, Fig. 6.29), a rodent with good low-frequency hearing (reviewed in Rosowski, 1991, Fig. 1).] Although we cannot reach a firm conclusion as to sand cat's low-frequency hearing sensitivity, its enlarged cavities should improve

---

[30] This analysis is preliminary, in that we have data from only one ear of sand cat, with a rather large error in its estimated G_{CAV} value.

low-frequency transmission for its given C_{TOC}. On the bases of the available data, we conclude

that sand cat is an outlier in *two* acoustic properties of its middle ear and demonstrates that

allometric descriptions do not describe *all* of the variation in the family.

3. Middle-ear septum and midfrequency notch in sensitivity

a. General ideas

The midfrequency notch in admittance (Y_{TM}) and transmission (G_{CAV}) magnitude is

associated with a minimum in the cochlear response in domestic cats (Møller, 1965; Guinan and

Peake, 1967) and presumably a minimum in hearing sensitivity. As noted earlier, the potential

benefits (if any) of this feature to hearing are not known. The notch might (1) have acoustic-

functional significance, e.g., for filtering an acoustic signal such as an intraspecific vocalization, or

as a byproduct of another adaptive benefit to hearing, or (2) be unrelated to any benefit for hearing

(e.g., a consequence of structural constraints). In the latter case, the notch feature would be

somewhat analogous to a blind spot in the retina, with some differences. For example, one could

argue that binocular vision reduces the effect of a visual blind spot more than binaural hearing

would reduce the effect of the notch, for which approximately the same narrow frequency range is

affected in both ears.

b. Connection to auditory space perception: An hypothesis

Let us consider a specific hypothesis concerning the structural features that bring about the

transmission notch. The underlying antiresonance is controlled by the compliances of the tympanic

and bullar cavities and the mass of the foramen that connects them (Fig. 3.8). This distinctive

middle-ear structure -- two cavities divided by a nearly complete bony septum -- is in fact a

defining characteristic of the superfamily of "catlike" carnivores (*Feloidia*), which includes the cat

family, hyenas, mongooses, and civets (see Chapter 1, Section II C 1). We ask the broader

question, "What might be the adaptive benefits of the septum and foramen?", with the idea that the

answers might suggest hypotheses concerning the functional significance of the transmission notch.

To answer this question, we consider the hypothetical function of the felid middle ear in the *absence* of the septum, with other structural features unchanged. A prediction based on acoustic considerations indicates that in domestic cat the absence of the septum and foramen -- i.e., replacement of the distinct tympanic and bullar cavities with one large middle-ear cavity -- would eliminate the cavity-admittance notch near 4 kHz and introduce a new notch at roughly 10 kHz (Puria, 1991, pp. 131-133). This new notch may be interpreted as a half-wave resonance in a cavity of effective length 1.7 cm, which agrees roughly with the size of the large cavity. The exact shape of the cavity is not crucial; the key idea is that wave effects in the cavity would introduce resonances in the cavity admittance (and in middle-ear input admittance and transmission) in a frequency range around 10 kHz that is normally (with septum) smooth. This idea is consistent with preliminary measurements of Y_{TM} and cochlear potentials made in domestic-cat ears before and after removing the septum (Rosowski et al., in prep.). Thus, an acoustic consequence of having a bony septum is the elimination of sharp features in the middle-ear response that would occur near 10 kHz (in the septum's absence) with one large cavity.

In domestic cat, sharp spectral features between 8-15 kHz in the acoustic response of the external ear (pinna flange, concha, and canal) are thought to be cues for determining the position of a sound source, particularly elevation angle in the median plane for which interaural-difference cues are minimized (Musicant et al., 1990; Rice et al., 1992).[31] Specifically, the 8-15 kHz region of the external-ear transfer function contains a "first notch", the frequency of which is correlated with the elevation of a broadband noise source. A notch in the middle-ear response near 10 kHz could interfere with the detection and processing of this external-ear first-notch frequency. We hypothesize that the presence of the septum with a foramen allows a large total middle-ear volume

---

[31] In humans, the external-ear gain has similar directionally-dependent features which are thought to be important for sound localization (e.g., Shaw, 1974; Blauert, 1983).

that benefits low-frequency hearing (see previous section), without associated resonances from wave effects that would occur at frequencies important for the determination of sound-source elevation.

This hypothesis could be tested in a number of ways. For example, attempts could be made to correlate the presence of a bony septum in catlike carnivores with hunting behaviors that depend on localization of sound sources off of the horizontal plane (e.g., hunting of birds or arboreal animals). Also, physical measurements could be made of bullar structure and function in *non*-catlike carnivores (e.g., dogs and bears, who lack such a complete septum), to test whether high-frequency notches occur in the acoustic response of these middle ears.

c. Family trend

The family trend is that the middle-ear notch frequency decreases by approximately a factor of two with increasing body size (Fig. 3.11). If we assume that the first-notch frequency of the external-ear gain is inversely related to the largest dimension of the pinna flange, this frequency would also decrease by approximately a factor of two from domestic cat to tiger, based on greatest pinna-edge dimensions measured in the live specimens.[32] If the hypothesis is correct, a selective pressure would occur for the middle-ear notch frequency to decrease with increasing body size in order to stay below the frequency range of the external-ear first notch. Tests of this hypothesis might include post-mortem measurements of middle-ear input admittance and source-angle dependence of external-ear gain in catlike species with and without the septum, and correlations of the position of the septum and the size of the tympanic and bullar cavities with measures of the importance of sound localization for the survival of these species (e.g., in arboreal versus ground-dwelling felid species).

---

[32] Some greatest pinna-edge dimensions: domestic cats (50-55 mm) (also see Rosowski et al., 1988, p. 1699), ocelot (55 mm), leopards (77-84 mm), mountain lions (83-100 mm), jaguar (83 mm), serval (102 mm), and tiger (113 mm).

IV. SUMMARY

We have reported measurements of acoustic middle-ear input admittance (and reflectance) in anesthetized species of the cat family. Analysis of these measurements, organized conceptually by a lumped-network model of the middle ear, leads to a description of relations between middle-ear acoustic properties and body size. The net middle-ear compliance increases with body size, but the compliance of the TM-ossicular system is *not* correlated with size. The frequencies of a prominent notch in admittance (and transmission) magnitude and the first minimum in reflectance magnitude both decrease with body size. Structure-based rules relate two middle-ear sound transmission properties to middle-ear size and body size across the family: (1) The low-frequency cavity gain, the fraction of the ear-canal sound pressure that drives the TM-ossicular system, increases with body size via the interaction of the compliances of the TM-ossicular system and the middle-ear cavities; (2) the frequency of the transmission notch decreases with body size via the interaction of the individual cavity compliances and the acoustic mass of the foramen that connects the cavities. These trends are consistent with the idea that in larger felids the middle-ear frequency response is shifted to lower frequencies, with potential benefits for detecting environmental sounds that may be important for survival (intraspecies vocalizations and spectral cues for sound-source localization). In this way, body size provides a quantitative description of some features of auditory function in the cat family. These results suggest that our approach of relating middle-ear structure and function -- which should be integrated with descriptions of the external and inner ears -- is a reasonable starting point for describing mechanistic bases of the widely varying hearing capabilities of terrestrial mammals.

TABLE 3.1: Summary of structural and acoustic measurements made on 21 ears of 12 species of the cat family. Species abbreviations (used in figures) are given in parentheses after the species' common names. For each species, measurements are from one ear of one subject, except for 4 species in which data are from multiple ears. The "dittos" (") mean "same as the entry above" and signify a row of data taken from the same individual as the row above. Braces indicate two ears from the same individual. Entries followed by "(mean)" are the mean of values from the individual ears of the species in the table. (A) Skull length L_{CB} is the distance between the upper incisors and the posterior edge of the occipital condyles. Each L_{CB} value is the mean of (1) a head-length measurement, (2) a regression from the individual's body weight, and (3) a species mean from a museum-skull database (Peake and Rosowski, in prep.). Values of L_{CB} marked with an asterisk (*) are greater than one standard deviation above the database species mean. Body weights were measured on a scale except for those entries designated "(est.)", which were estimated by the veterinarian. Each middle-ear cavity volume C_{CAV} is a species mean plus or minus an error from the skull database, based on measured means and standard deviations of auditory-bullar dimensions and an empirical relation between total cavity volume and bullar dimensions (Peake and Rosowski, in prep.). (B) Total middle-ear acoustic compliance values C_{ME} are computed as the average of $\text{Im}\{Y_{TM}\}$ / $(2\pi f)$ over 10 frequency points f from 0.1-0.3 kHz, where $\text{Im}\{Y_{TM}\}$ denotes the imaginary part of the middle-ear input admittance. The average error in C_{ME} is $\pm14\%$, based on acoustic measurements in domestic cats (Chapter 2, Section III C and Table 2.2). The TM-ossicular compliance C_{TOC} is computed from a low-frequency approximation of the middle-ear network model (Fig. 3.8), given in Eq. (3.8). The error in C_{TOC} varies among species and is the result of worst-case combinations of errors in C_{CAV} and C_{ME} (see Fig. 3.9). The reflectance-minimum frequency f_{Rmin} is the frequency of the lowest-frequency minimum in the ear-canal power reflectance with a value less than 0.4. It represents the frequency of best sound-energy transmission between the ear canal and the middle ear. (C) The admittance-notch frequency f_{Ynotch} is the frequency of the local minimum in middle-ear input admittance whose magnitude is at least 5 dB below that of the preceding (lower frequency) local maximum, and whose angle increases through this frequency by at least 0.2 periods. By this definition, one ear each of ocelot and sand cat and two ears each of leopard and mountain lion do not exhibit a clear admittance notch (indicated by dashed-line entries). The low-frequency cavity gain G_{CAV} is the fraction of the ear-canal sound pressure that drives the ossicular chain, and is determined from the network model (Fig. 3.8) as in Eq. (3.7); it is a measure of middle-ear sound transmission for low frequencies, with 1 representing best transmission. The error in G_{CAV} varies among species (see Fig. 3.10) and is based on worst-case combinations of errors in C_{TOC} and C_{CAV}. The G_{CAV} and f_{Ynotch} data are used to test structure-based rules relating these acoustic-performance measures to body size (Figures 3.10 and 3.11).

TABLE 3.1
(A)

Species	Sex	Estimated skull length L_{CB} (mm)	Body weight M (kg)	Middle-ear cavity compliance C_{CAV} (cm^3 of air)
Tiger (T) (*Panthera tigris*)	F	296.0	180 (est.)	11.01 ± 3.37
Jaguar (Ja) (*Panthera onca*)	M	248.6 *	150 (est.)	6.21 ± 1.68
Leopard (Le) (*Panthera pardus*)		199.6 (mean)	70.5 (mean)	4.30 ± 0.96
Ear 1	F	184.1	45.5	
Ear 2	M	215.1 *	95.5	
Ear 3	"	"	"	
Mountain lion (M) (*Puma concolor*)		176.2 (mean)	39.4 (mean)	4.42 ± 1.68
Ear 1	M	186.3 *	55 (est.)	
Ear 2	F	172.4	34.1	
Ear 3	F	170.0	33.6	
Ear 4	"	"	"	
Asian golden cat (A) (*Catopuma temminckii*)	M	134.7 *	16.0	1.73 ± 0.32
Ocelot (O) (*Leopardus pardalis*)	M	130.3	12.8	1.84 ± 0.38
Caracal (C) (*Caracal caracal*)	M	127.3 *	13.9	1.70 ± 0.32
Ear 1	"	"	"	
Ear 2	"	"	"	
Serval (Se) (*Leptailurus serval*)	M	122.4 *	16.6	1.89 ± 0.35
Jungle cat (Ju) (*Felis chaus*)	M	109.8 *	8.6	1.28 ± 0.40
Indian desert cat (I) (*Felis silvestris ornata*)	M	90.2	3.5	1.08 ± 0.19
Sand cat (Sa) (*Felis margarita*)	M	85.6	3.1	1.92 ± 0.13
Domestic cat (D) (*Felis silvestris catus*)		85.6 (mean)	3.2 (mean)	0.89 ± 0.16
Ear 1	M	82.3	3.1	
Ear 2	F	86.8	3.2	
Ear 3	F	87.6 *	3.3	
Ear 4	"	"	"	

TABLE 3.1
(B)

Species	TM-ossicular compliance C_{TOC} (cm^3 of air)	Total middle-ear compliance C_{ME} (cm^3 of air)	Reflectance-minimum frequency f_{Rmin} (kHz)
Tiger (T) (*Panthera tigris*)	1.23	1.11	1.00
Jaguar (Ja) (*Panthera onca*)	1.77	1.38	0.83
Leopard (Le) (*Panthera pardus*)	2.15 (mean)	1.41 (mean)	0.77 (mean)
Ear 1	1.29	0.99	0.59
Ear 2	2.70	1.66	0.95
Ear 3	2.47	1.57	0.76
Mountain lion (M) (*Puma concolor*)	1.68 (mean)	1.20 (mean)	1.07 (mean)
Ear 1	2.23	1.48	0.90
Ear 2	1.24	0.97	1.17
Ear 3	2.11	1.43	1.05
Ear 4	1.14	0.91	1.17
Asian golden cat (A) (*Catopuma temminckii*)	1.92	0.94	1.54
Ocelot (O) (*Leopardus pardalis*)	0.74	0.53	1.64
Caracal (C) (*Caracal caracal*)	2.13 (mean)	0.95 (mean)	1.47 (mean)
Ear 1	2.21	0.96	1.66
Ear 2	2.05	0.93	1.27
Serval (Se) (*Leptailurus serval*)	1.26	0.73	1.46
Jungle cat (Ju) (*Felis chaus*)	2.06	0.79	1.42
Indian desert cat (I) (*Felis silvestris ornata*)	0.74	0.44	0.93
Sand cat (Sa) (*Felis margarita*)	3.93	1.29	0.85
Domestic cat (D) (*Felis silvestris catus*)	1.14 (mean)	0.47 (mean)	1.92 (mean)
Ear 1	1.03	0.48	1.73
Ear 2	2.22	0.64	1.59
Ear 3	0.75	0.41	1.88
Ear 4	0.57	0.35	2.49

TABLE 3.1
(C)

Species	Admittance-notch frequency f_{Ynotch} (kHz)	Low-frequency cavity gain G_{CAV}
Tiger (T) (*Panthera tigris*)	2.59	0.90
Jaguar (Ja) (*Panthera onca*)	2.08	0.78
Leopard (Le) (*Panthera pardus*)	3.12	0.67 (mean)
Ear 1	---	0.77
{Ear 2	3.12	0.61
Ear 3	---	0.64
Mountain lion (M) (*Puma concolor*)	2.45 (mean)	0.73 (mean)
Ear 1	---	0.66
Ear 2	---	0.78
{Ear 3	2.51	0.68
Ear 4	2.39	0.79
Asian golden cat (A) (*Catopuma temminckii*)	2.32	0.49
Ocelot (O) (*Leopardus pardalis*)	---	0.72
Caracal (C) (*Caracal caracal*)	3.29 (mean)	0.44 (mean)
{Ear 1	3.27	0.43
Ear 2	3.30	0.45
Serval (Se) (*Leptailurus serval*)	3.86	0.58
Jungle cat (Ju) (*Felis chaus*)	2.81	0.38
Indian desert cat (I) (*Felis silvestris ornata*)	3.52	0.59
Sand cat (Sa) (*Felis margarita*)	---	0.33
Domestic cat (D) (*Felis silvestris catus*)	3.82 (mean)	0.48 (mean)
Ear 1	3.81	0.47
Ear 2	3.71	0.30
{Ear 3	3.93	0.55
Ear 4	---	0.61

FIG. 3.1: Tests of the admittance-measurement system. LEFT PANEL: The test load is a closed, cylindrical, plexiglass tube of inner diameter 6.2 mm and length 30 mm. The dotted curve is the source admittance, determined from measurements in two calibration loads of known admittance having inner diameter 6.2 mm. RIGHT PANEL: The test load is a closed, cylindrical, tygon (flexible plastic) tube of inner diameter 7.9 mm and length 36 mm. The dotted curve is the source admittance, determined from measurements in two calibration loads of known admittance having inner diameter 7.9 mm. Measurements were made with an earphone and microphone acoustic assembly (Etymotic Research ER-10C) and custom eartips designed for use with cats. The eartip was sealed into each load with earmold impression material. The axes are the same in the left and right plots. Admittance-magnitude units: 1 μSiemen = 1/(mks MΩ) = 10^{-6} m^3/(Pa s). Angles are plotted in periods (1 period = 2π radians).

FIG. 3.1

Test Load Length = 30 mm
Inner Diameter = 6.2 mm

Test Load Length = 36 mm
Inner Diameter = 7.9 mm

MEASURED
THEORETICAL

SOURCE
ADMITTANCE

ACOUSTIC ADMITTANCE OF TEST LOADS

MAGNITUDE (μSiemens)

ANGLE (Periods)

FREQUENCY (kHz)
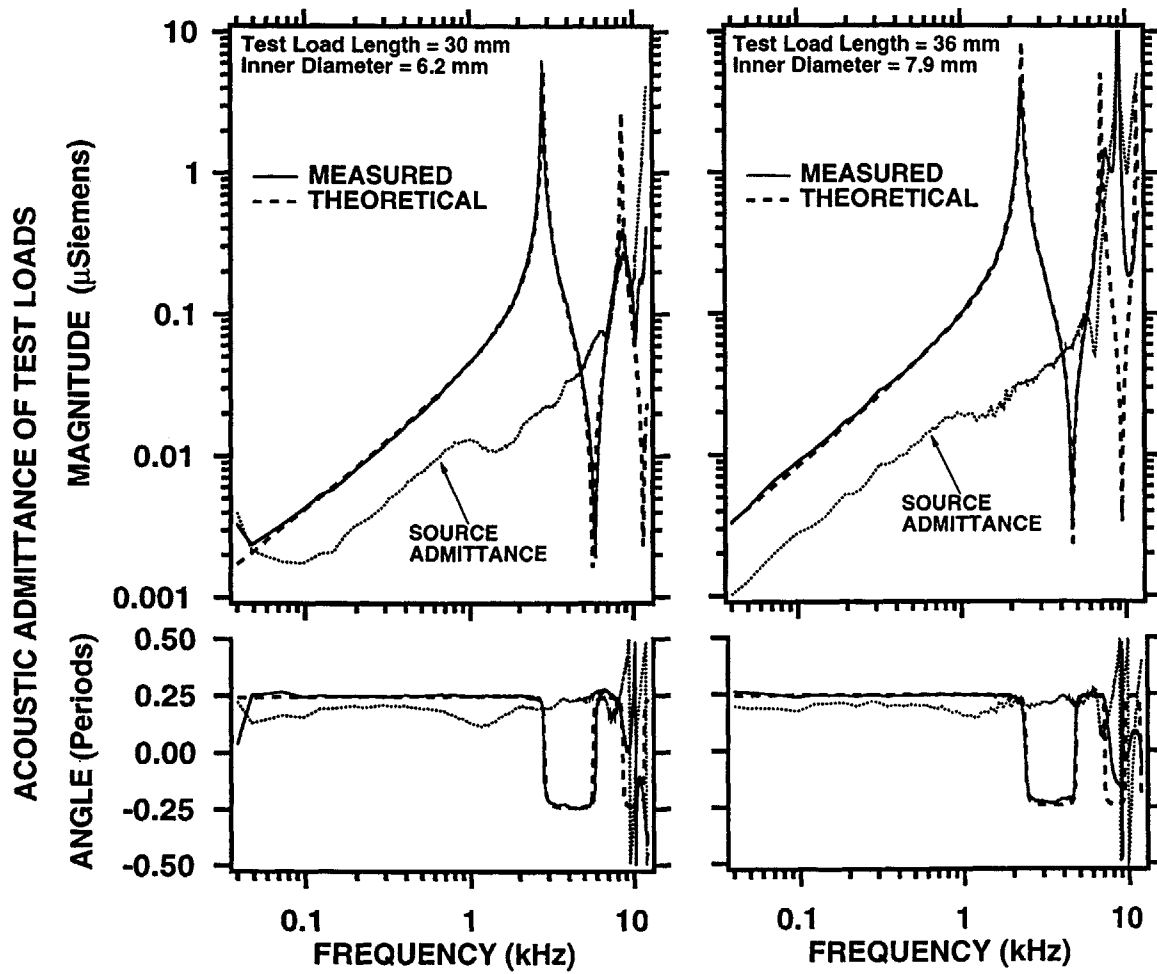
FIG. 3.2: Demonstration of the admittance-location transformation used to estimate the admittance at the tympanic membrane (TM). The specimen is a caracal (*Caracal caracal*), a medium-sized species: (A) left ear, (B) right ear. The axes are the same in the left and right plots. The thin curves are the admittances at the measurement point in the ear canal. The thick curves are the estimated admittances at the TM, obtained by approximating the ear-canal space between the measurement point and the TM by a rigid, uniform tube of length l and radius a. The procedure for choosing the tube's dimensions is reviewed in Section I B (see also Chapter 2, Section II D).

FIG. 3.2

ADMITTANCE-LOCATION TRANSFORMATION IN EAR CANALS
OF A CARACAL (*Caracal caracal*)

(A) LEFT EAR

(B) RIGHT EAR

169
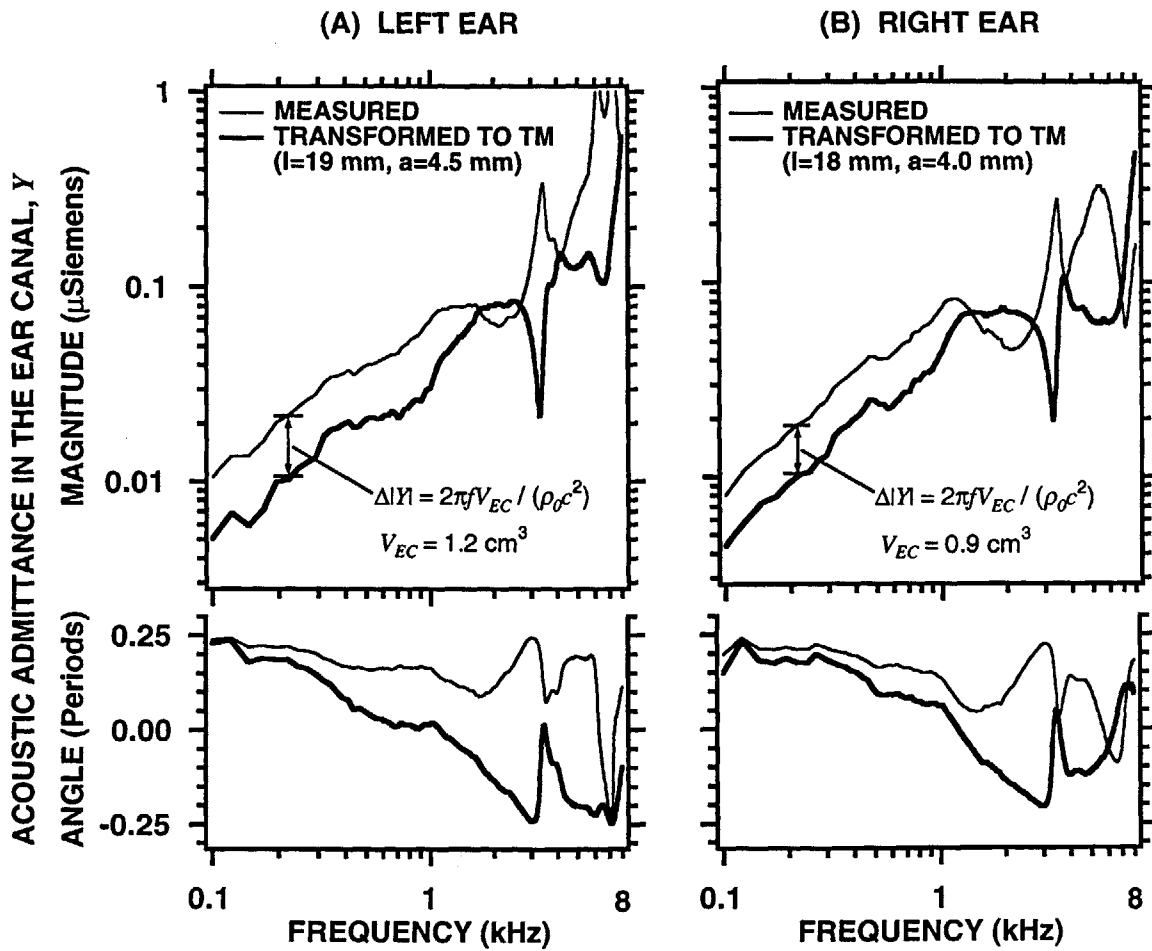
FIG. 3.3: Comparison of middle-ear input admittances (Y_{TM}) and ear-canal power reflectances ($|R_{EC}|^2$) from one ear of each of 4 SMALL species. UPPER PANEL: Admittances measured in the ear canal were transformed to the TM: Domestic cat (l=10 mm, a=3.6 mm), sand cat (l=9 mm, a=4.4 mm), Indian desert cat (l=14 mm, a=3.5 mm), and jungle cat (l=8.4 mm, a=3.8 mm). The horizontal lines in the angle plot are at 0 and 0.25 periods. LOWER PANEL: Reflectances were computed from the ear-canal admittances associated with the upper panel, with the estimate of the ear-canal radius (a) at the measurement point. Admittance angles outside the range ±0.25 periods and power-reflectance values greater than 1.0 must be in error but are plotted to show their qualitative shape. The frequency scales in the upper and lower panels are the same.

FIG. 3.3

SPECIES SIZE: SMALL
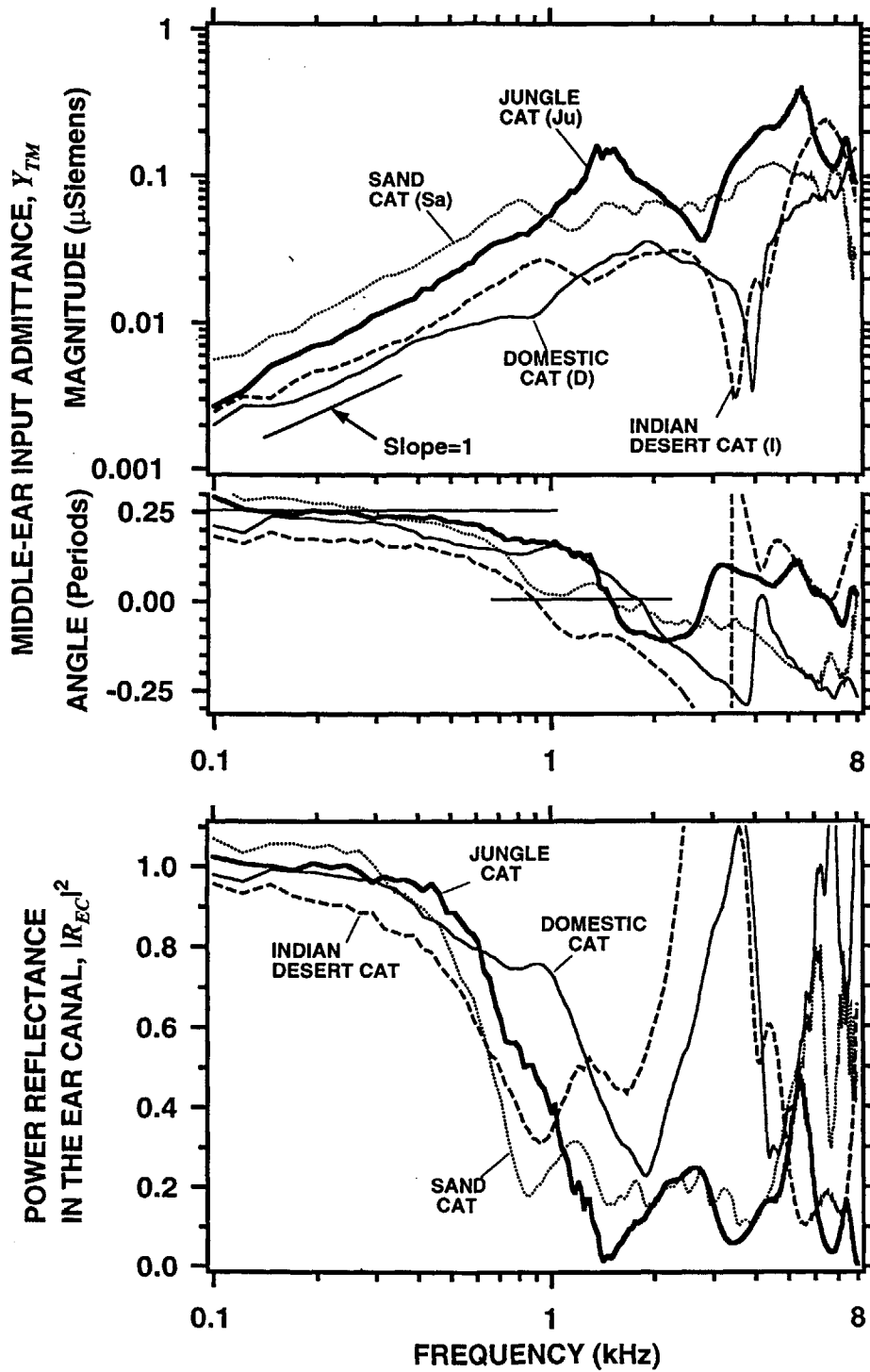
FIG. 3.4: Same as Fig. 3.3, for 4 MEDIUM-sized species. Admittance-location transformation

parameters: Ocelot (l=22 mm, a=3.0 mm), caracal (l=18 mm, a=4.0 mm), serval (l=15 mm,

a=2.7 mm), and Asian golden cat (l=27 mm, a=3.6 mm).

FIG. 3.4

SPECIES SIZE: MEDIUM

Y-axis (top panel): MIDDLE-EAR INPUT ADMITTANCE, Y_{TM} MAGNITUDE (μSiemens)

Top panel labels: Slope=1, CARACAL (C), ASIAN GOLDEN CAT (A), SERVAL (Se), OCELOT (O)

Top panel Y-axis values: 1, 0.1, 0.01, 0.001

Y-axis (middle panel): MIDDLE-EAR INPUT ADMITTANCE, Y_{TM} ANGLE (Periods)

Middle panel Y-axis values: 0.25, 0.00, -0.25

Middle panel X-axis values: 0.1, 1, 8

Y-axis (bottom panel): POWER REFLECTANCE IN THE EAR CANAL, $|R_{EC}|^2$

Bottom panel labels: CARACAL, OCELOT, ASIAN GOLDEN CAT, SERVAL

Bottom panel Y-axis values: 1.0, 0.8, 0.6, 0.4, 0.2, 0.0

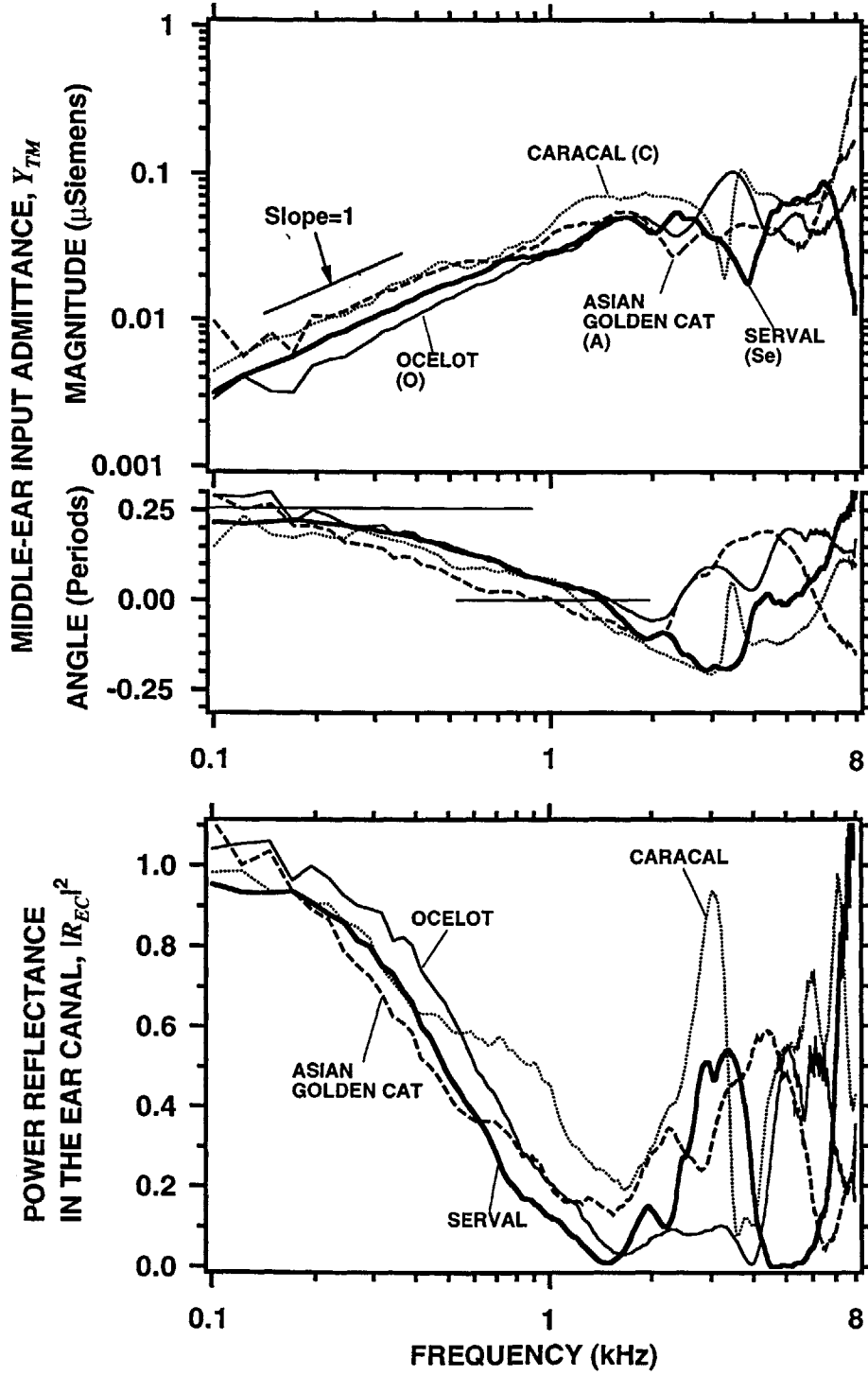Bottom panel X-axis values: 0.1, 1, 8

FREQUENCY (kHz)

173

FIG. 3.5: Same as Fig. 3.3, for 4 LARGE species. Admittance-location transformation parameters: Mountain lion (l=23 mm, a=4.6 mm), leopard (l=28 mm, a=3.4 mm), jaguar (l=24 mm, a=2.3 mm), and tiger (l=23 mm, a=3.6 mm).

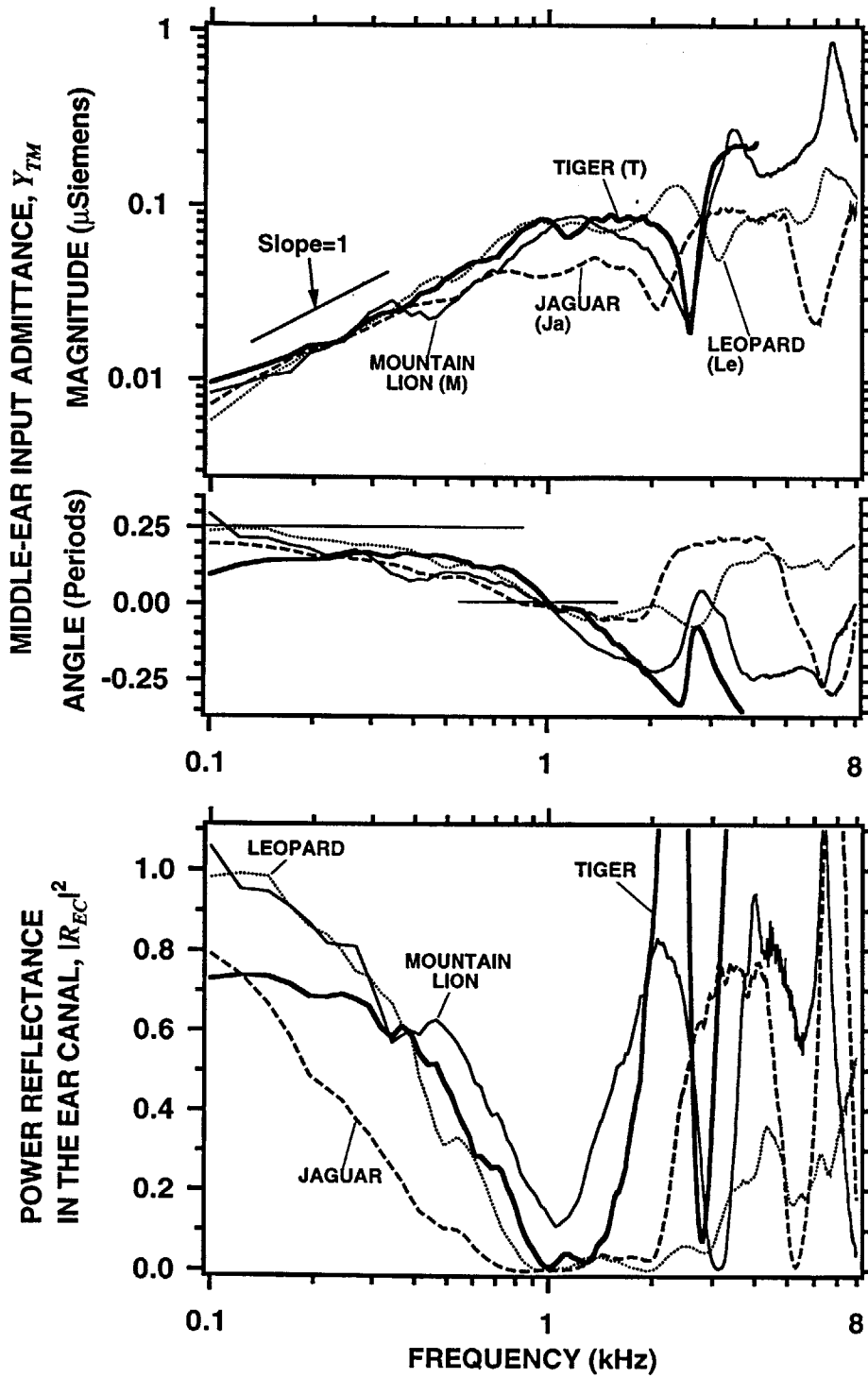**SPECIES SIZE: LARGE**   **FIG. 3.5**

FIG. 3.6: Dependence of middle-ear acoustic compliances on skull length L_{CB} for 21 ears of 17 individuals. Data points are labeled with species abbreviations from Table 3.1. UPPER PANEL: Total middle-ear compliance, C_{ME}, measured acoustically from low-frequency (0.1-0.3 kHz) values of the middle-ear input admittance of live specimens (Figs. 3.3-3.5). Each point represents one ear. Error bars are shown for one point (Sa) and apply to all points. Vertical error bars for all points are ±14%, representing the mean error in tests on domestic cats. LOWER PANEL: Compliance of the middle-ear cavities, C_{CAV}, from structural measurements (and an empirical description) of the cavity volume in skulls of each species (Peake and Rosowski, in prep.). Each point represents one *individual* whose C_{CAV} is taken to be the mean for its species (independent of L_{CB}). The vertical error bars result from substituting ±1 standard deviation in the product of bullar dimensions (skull database) into Eq. (3.3). BOTH PANELS: For each specimen L_{CB} is the measure of body size, computed as the mean of (1) an estimate from head length, (2) an estimate from body weight, and (3) the species mean from the skull database. The horizontal axis scale is the same in both plots, with size increasing to the right. The horizontal error for all data points in Figures 3.6, 3.7, 3.9, 3.10, and 3.11 are ±10% (see Section I D 2). The power-law equations were obtained from least-squares fits to the log-log data; the variables have the same dimensions as on the axes. Standard errors of the slopes (exponents) were calculated from Myers (1990, p. 8). "p" is the probability that the slope is 0 (Rohlf and Sokal, 969, p. 225). Acoustic compliances are expressed in terms of equivalent volumes of air.

FIG. 3.6

Top panel (y-axis: TOTAL COMPLIANCE OF MIDDLE EAR, C_{ME} (cm³ of air)):

LEAST-SQUARES FIT
$C_{ME} = 10.5 \times 10^{-3} L_{CB}^{0.895 \pm 0.185}$
n = 21, R^2 = 0.55, p < 0.01

Bottom panel (y-axis: COMPLIANCE OF MIDDLE-EAR CAVITIES, C_{CAV} (cm³ of air)):

LEAST-SQUARES FIT
$C_{CAV} = 27.7 \times 10^{-5} L_{CB}^{1.835 \pm 0.148}$
N = 17, R^2 = 0.91, p < 0.01
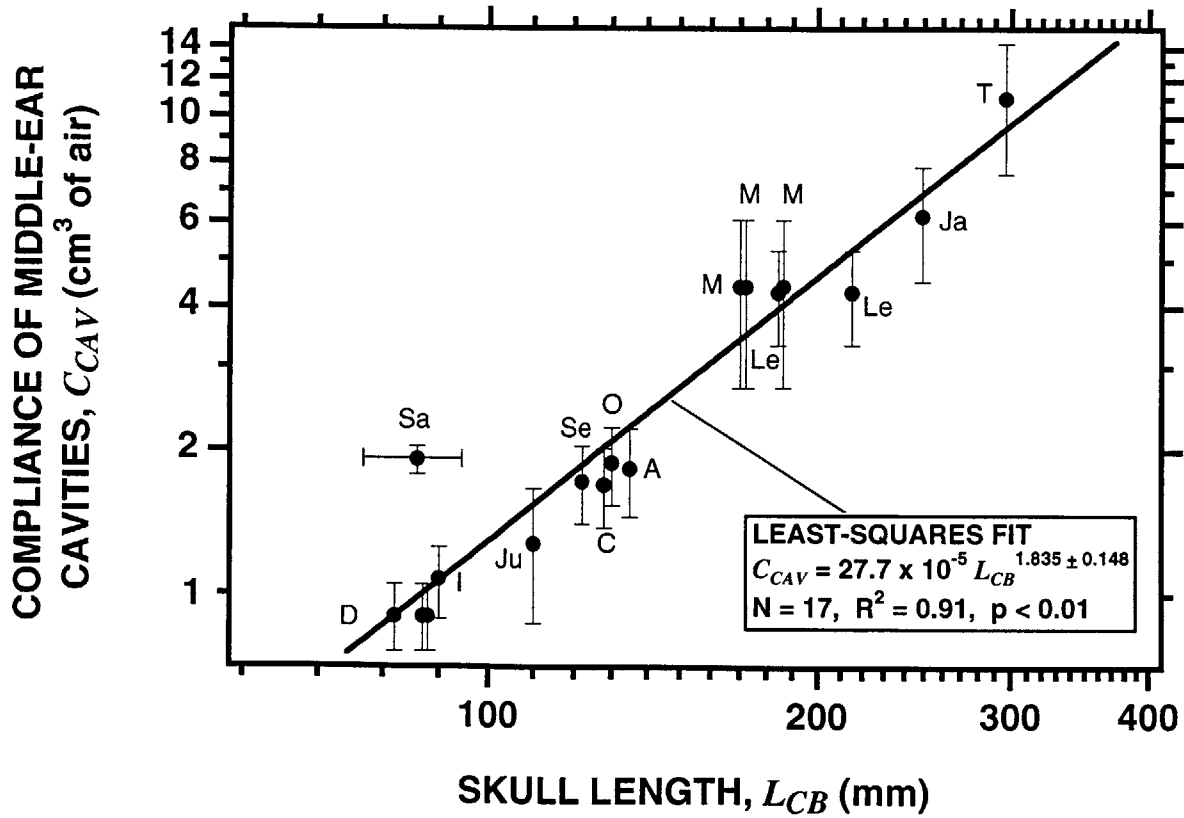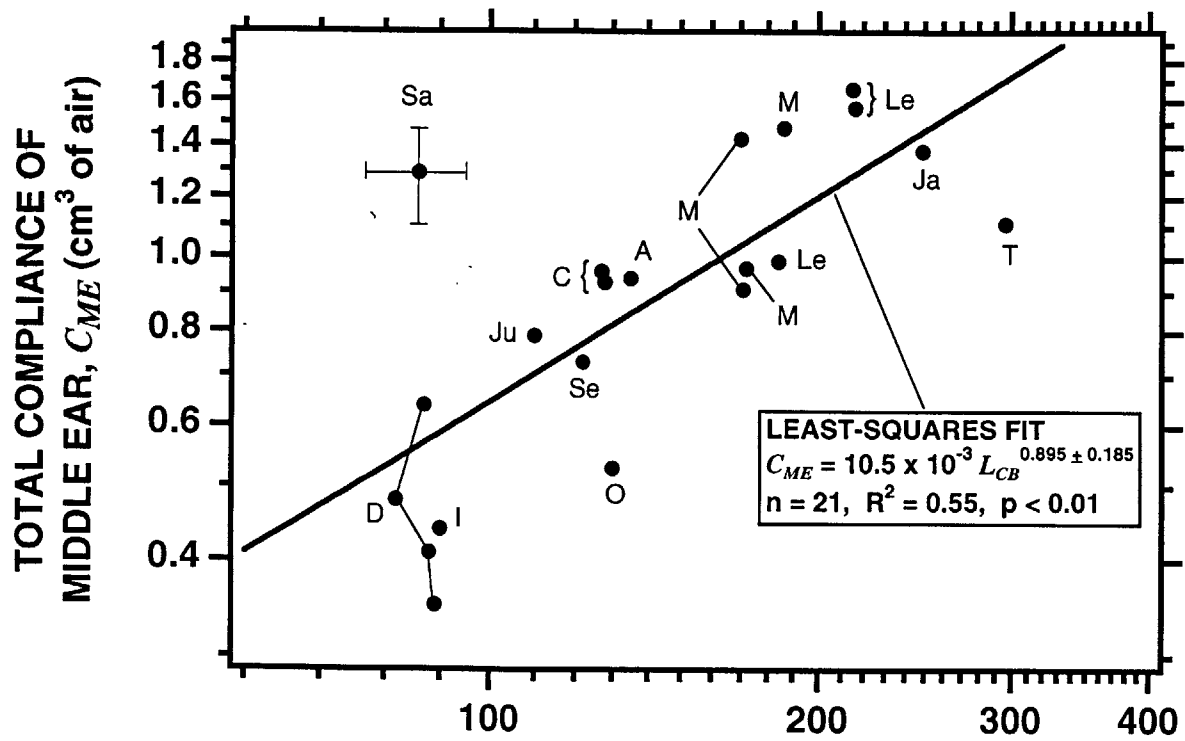
SKULL LENGTH, L_{CB} (mm)

177

FIG. 3.7: Dependence of "minimum" frequencies on skull length L_{CB}. The power-law fits to the data were obtained as in Fig. 3.6. UPPER PANEL: Frequency of the sharp minimum in middle-ear input admittance magnitude f_{Ynotch} for 15 ears. Each point represents one ear. Measurements in six ears did not exhibit a clear notch (see Table 3.1 caption). The error bars, shown on one point (Se), apply to all points. The vertical error bars are $\pm 5\%$, representing the mean error in estimating this frequency in domestic cats. LOWER PANEL: Frequency of the power-reflectance minimum f_{Rmin}, defined as the lowest-frequency minimum with a value less than 0.4, and regression. Each point represents one ear. The vertical error bars are $\pm 15\%$, representing the average error in the measurement in domestic cats.

FIG. 3.7

Top panel:

ADMITTANCE-NOTCH FREQUENCY f_{Ynotch} (kHz)

LEAST-SQUARES FIT
$f_{Ynotch} = 18.1 \, L_{CB}^{-0.365 \pm 0.097}$
n = 15, R^2 = 0.52, p < 0.01

Bottom panel:

REFLECTANCE-MINIMUM FREQUENCY f_{Rmin} (kHz)

LEAST-SQUARES FIT
$f_{Rmin} = 19.1 \, L_{CB}^{-0.561 \pm 0.165}$
n = 21, R^2 = 0.38, p < 0.01
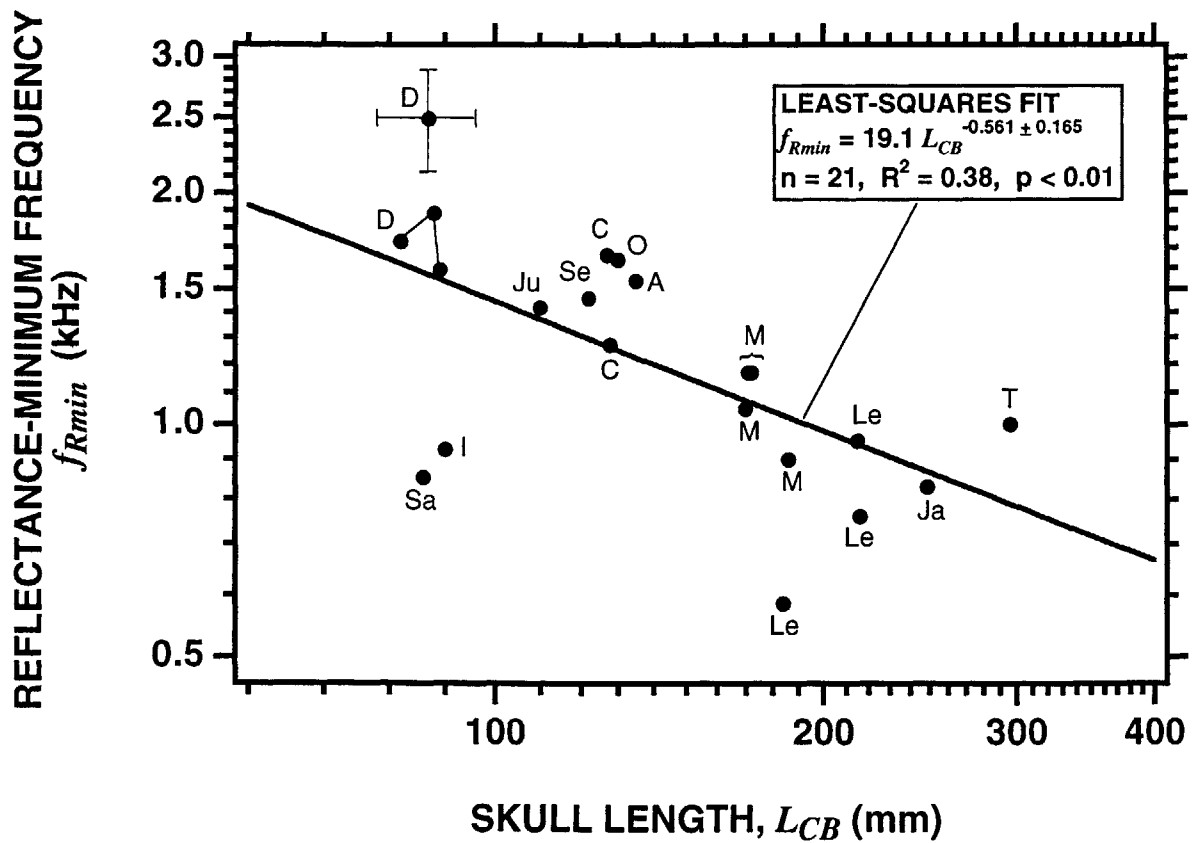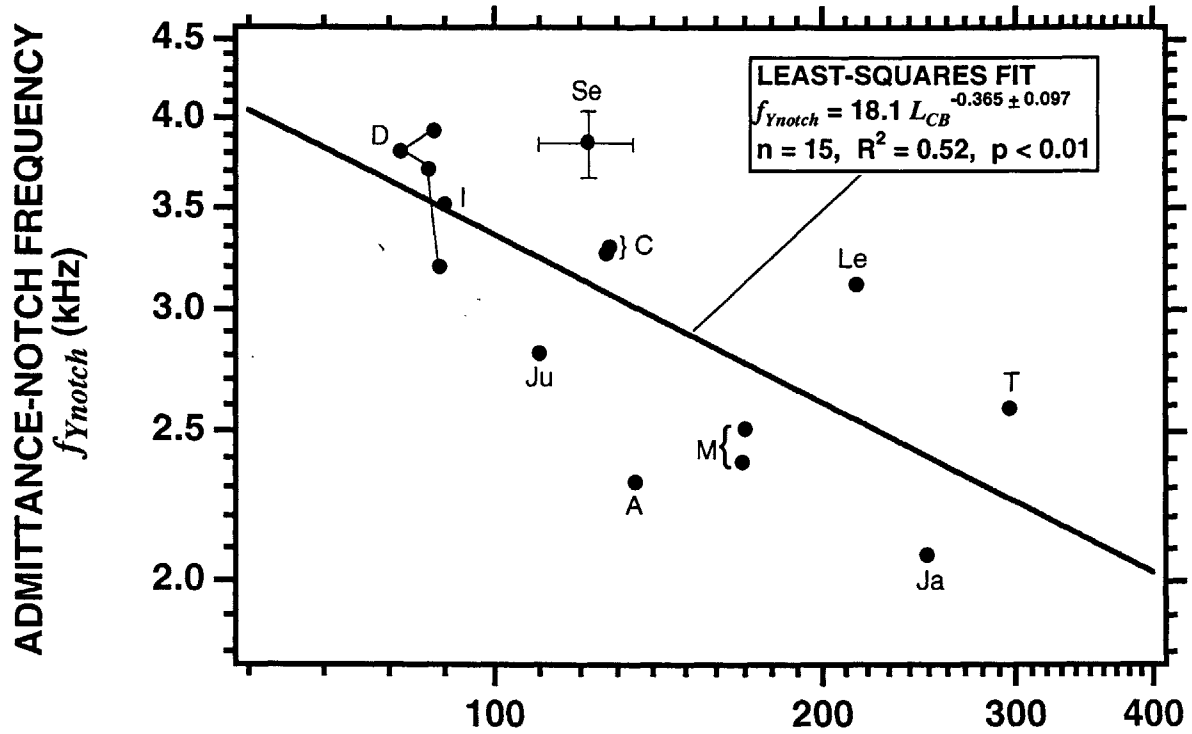
SKULL LENGTH, L_{CB} (mm)

FIG. 3.8: Lumped-network model for a felid middle ear. The superposed schematized middle-ear section shows the structural basis for the model. The middle-ear cavity is divided by a bony septum into two distinct air spaces -- the tympanic cavity and the bullar cavity -- which are coupled through a narrow foramen. Acoustic variables (acoustic admittance, sound pressure) are analogous to electric variables (electrical admittance, voltage). Y_{TM} is the middle-ear input admittance, P_{TM} is the sound pressure in the ear canal just lateral to the tympanic membrane (TM), and P_{CAV} is the sound pressure in the tympanic cavity. Lumped acoustic elements: C_{TOC} - compliance of the TM and ossicular chain, R_{TOC} - resistance of the cochlea, C_{TC} - compliance of the tympanic cavity, C_{BC} - compliance of the bullar cavity, M_F - mass of the foramen, R_F - resistance of the foramen.
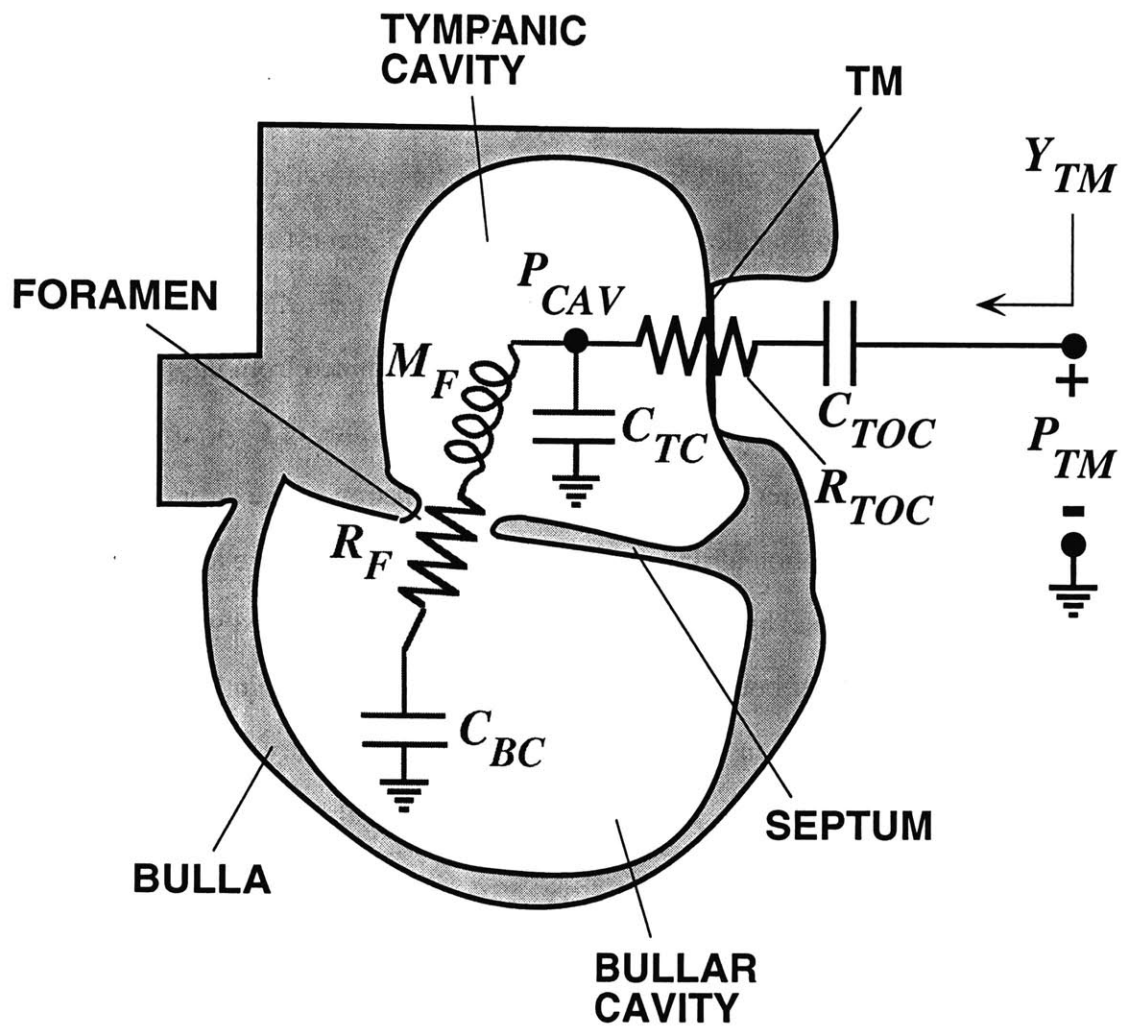
FIG. 3.8

FIG. 3.9: Inferred acoustic compliance of the TM and ossicular chain, C_{TOC}, versus skull

length L_{CB}. The compliance C_{TOC} was computed from the network model (Fig. 3.8) in the low-

frequency approximation and estimates of C_{ME} and C_{CAV} (Fig. 3.6) as $C_{TOC} = C_{CAV} C_{ME}$ /

$(C_{CAV} - C_{ME})$. Each marker represents one ear, labeled by a species abbreviation from Table 3.1.

Circles are ears from this study, and triangles are previous data from 5 domestic cats (unlabeled,

for clarity of the plot), 1 deceased bobcat (B), 1 deceased tiger (T), and 1 deceased lion (Li) (see

Peake and Rosowski, 1997); previous-data values of C_{TOC} were determined from input

admittances measured with the middle-ear cavities opened. The mean value of C_{TOC} over all ears

is 1.3 cm^3. The vertical error bars result from the worst-case combination of the errors in C_{ME}

and C_{CAV} in Fig. 3.6, with the exception of those specimens whose skull length exceeds their

species mean (from the skull database) by more than 1 standard deviation (marked with an asterisk

in Table 3.1), in which case the lower bound on C_{CAV} is taken to be the data point's value. In the

cases of two ears from the same specimen, one of the markers is shifted slightly in the horizontal

direction such that the vertical error bars are distinct. (This convention also holds for Fig. 3.10.)

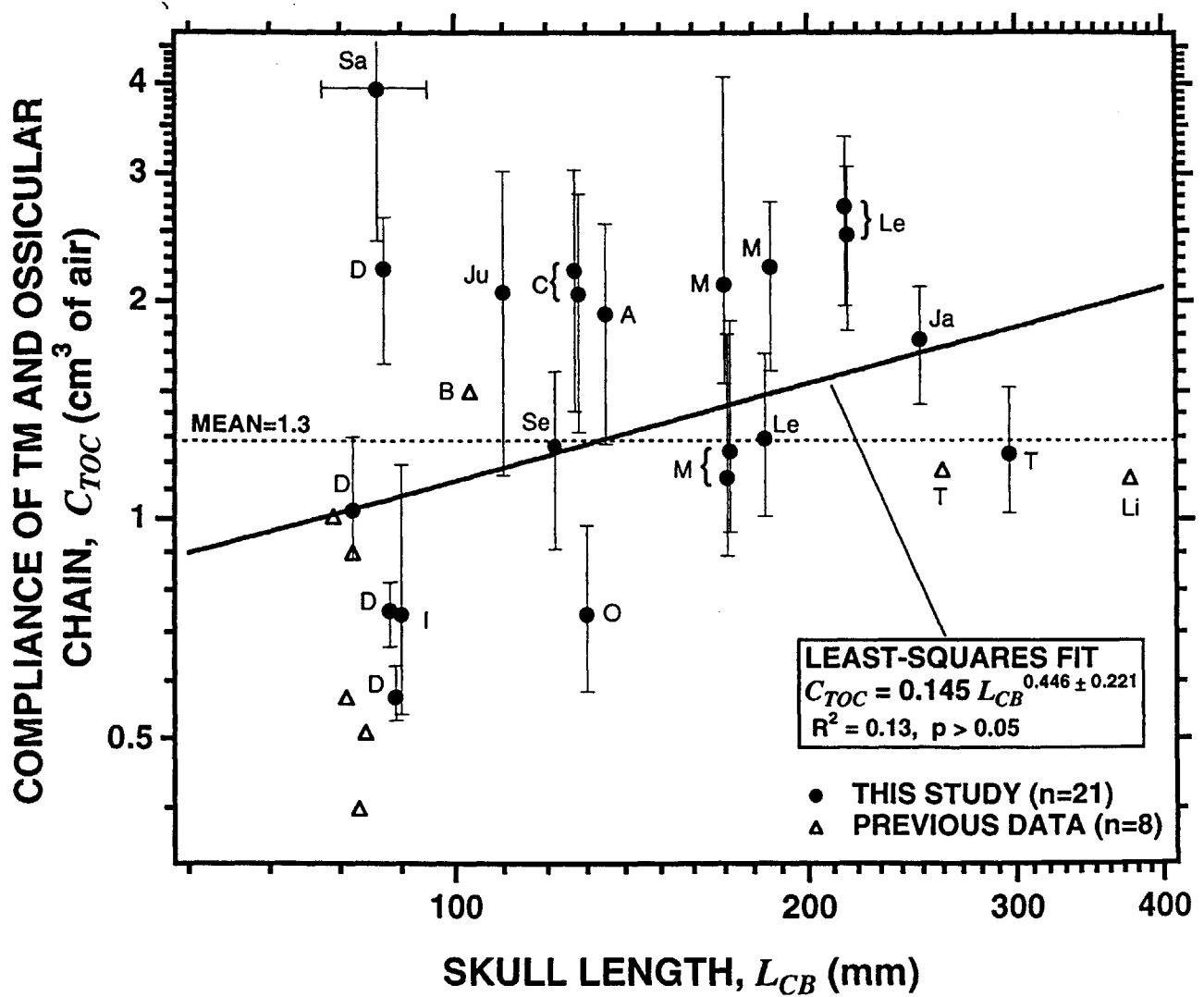**FIG. 3.9**

LEAST-SQUARES FIT
$C_{TOC} = 0.145\,L_{CB}^{0.446\,\pm\,0.221}$
$R^2 = 0.13,\ p > 0.05$

- ● THIS STUDY (n=21)
- △ PREVIOUS DATA (n=8)

COMPLIANCE OF TM AND OSSICULAR CHAIN, C_{TOC} (cm³ of air)

SKULL LENGTH, L_{CB} (mm)

MEAN=1.3

FIG. 3.10: Tests of a structure-based predictive rule relating the low-frequency cavity gain G_{CAV} to skull length L_{CB}. The cavity gain is a measure of middle-ear sound transmission -- the fraction of the ear-canal sound pressure that drives the ossicular chain. From the network model (Fig. 3.8) in the low-frequency approximation, $G_{CAV} = 1 / (1 + C_{TOC} / C_{CAV})$. The structure-based prediction assumes that $C_{TOC} = 1.3$ cm^3 (rather than 1.0 cm^3 used in Peake and Rosowski, 1997) is independent of L_{CB} and that C_{CAV} follows a family scaling rule. Each marker represents one ear. Circles are ears from this study, and triangles are previous data from 4 domestic cats (unlabeled), 2 deceased bobcats (B), 1 deceased tiger (T), and 1 deceased lion (Li) (see Peake and Rosowski, 1997). The vertical error bars result from the worst-case combination of the errors in C_{TOC} (Fig. 3.9) and C_{CAV} (Fig. 3.6). The predictive rule explains 41% of the total variance, computed as $\{1 - \text{mean}[(G_{CAV} - \text{rule})^2] / \text{var}(G_{CAV})\}$ where the numerator represents the mean-squared vertical deviation of the data from the rule and var() denotes the variance of the data.
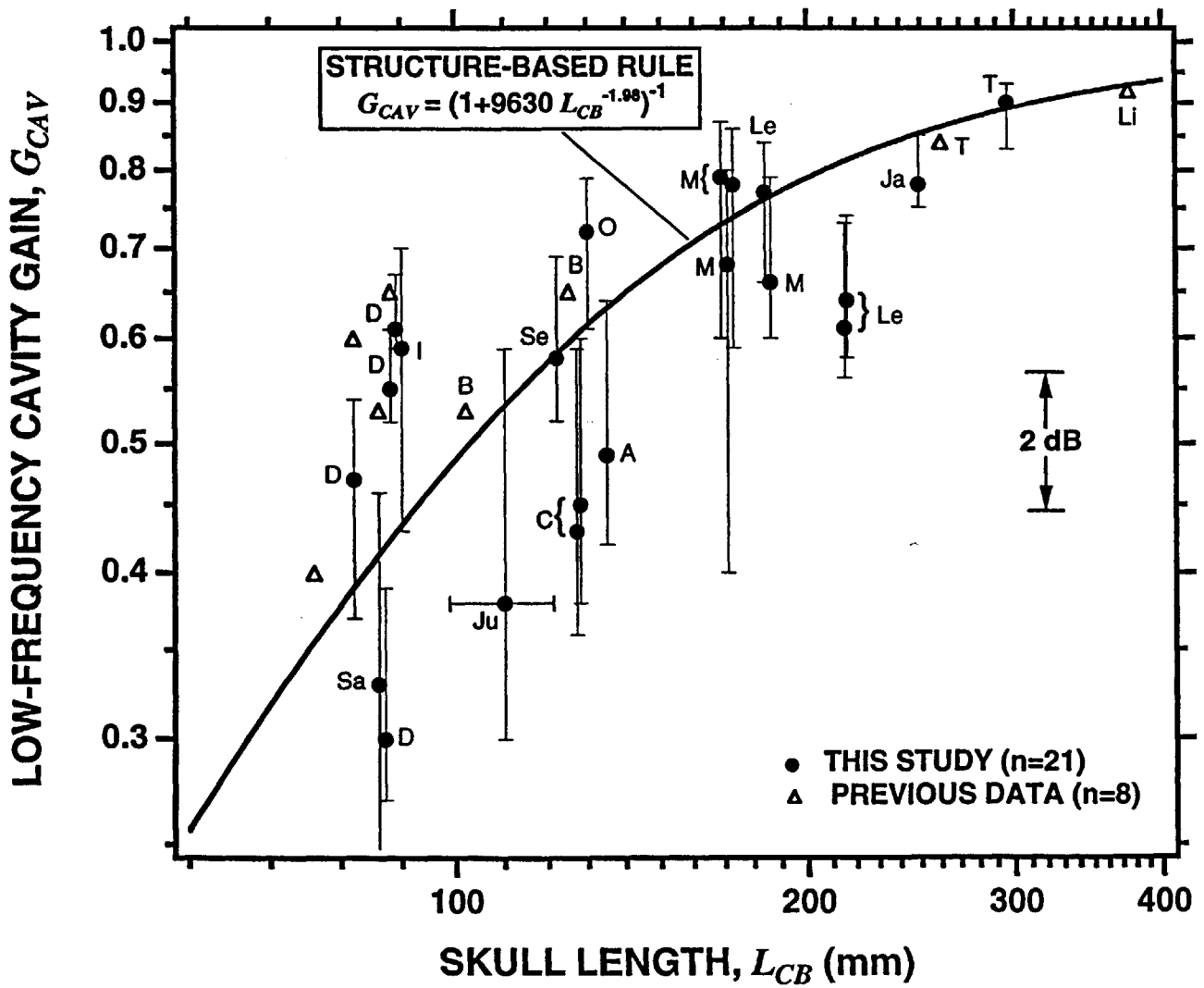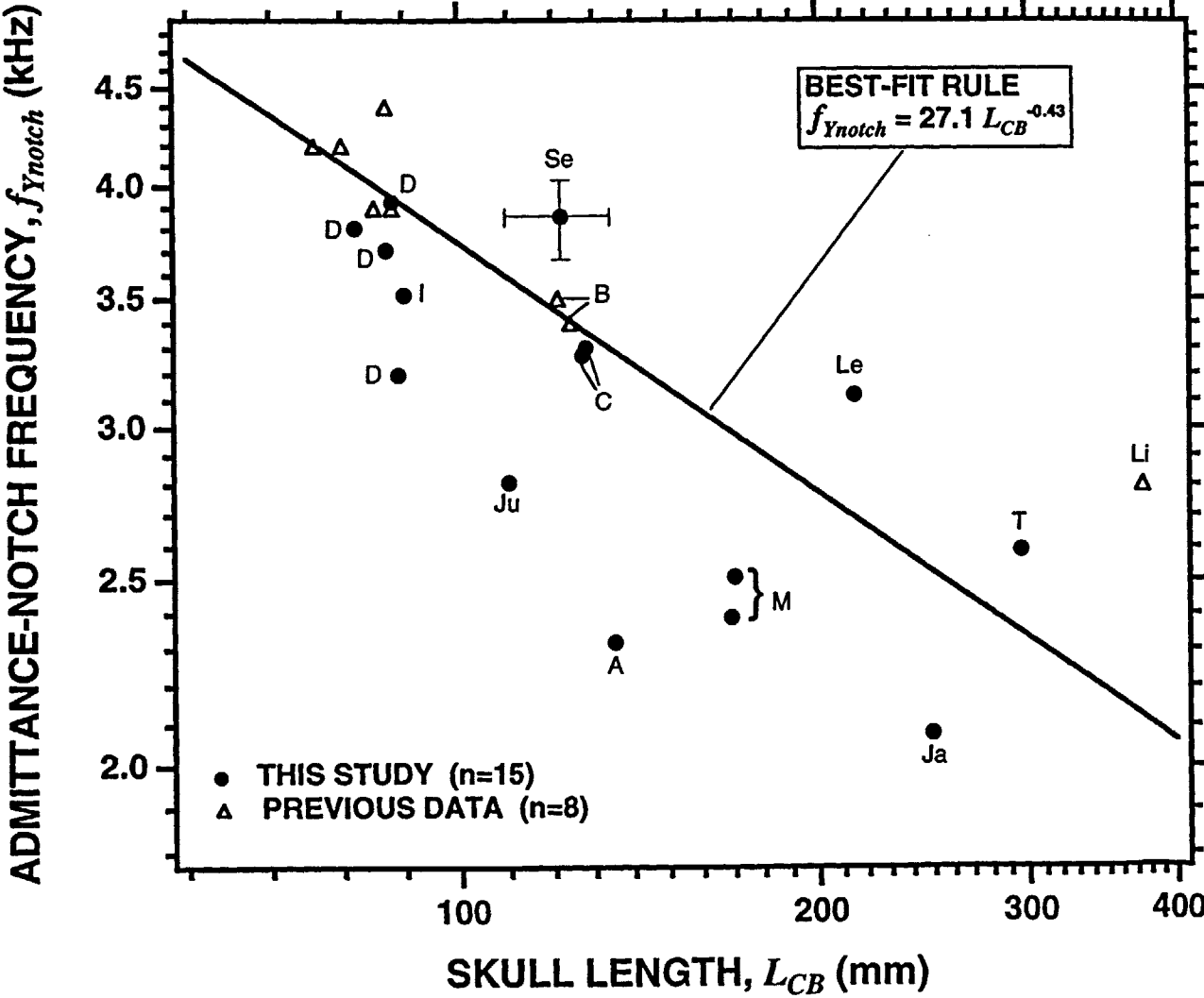
FIG. 3.10

FIG. 3.11: Comparison of admittance-notch-frequency (f_{Ynotch}) data to a best-fit predictive rule relating f_{Ynotch} to skull length L_{CB}. The notch results in a sharp decrease in middle-ear sound transmission over a narrow frequency band. Each marker represents one ear. Circles are ears from this study (same as in Fig. 3.7, upper), and triangles are previous data from 5 domestic cats (unlabeled), 2 deceased bobcats (B), and 1 deceased lion (Li). From the network model (Fig. 3.8), $f_{Ynotch} = 1/(2\pi) [M_F C_{TC} C_{BC}/(C_{TC}+C_{BC})]^{-1/2}$. The rule, which is constrained to have essentially the same slope (exponent) as that of the fit in Fig. 3.7 (upper), assumes that C_{TC} and C_{BC} follow an average family scaling rule [Eq. (3.13)], and that the effective dimensions (length and radius) of the foramen scale with the first power of L_{CB} so that the foramen's acoustic mass M_F scales as L_{CB}^{-1}. The vertical error bars are $\pm5\%$, representing the average error in the notch-frequency estimate in domestic cats. The predictive rule explains 53% of the total variance, computed as $\{1 - \text{mean}[(f_{Ynotch} - \text{rule})^2] / \text{var}(f_{Ynotch})]\}$, as in Fig. 3.10.

FIG. 3.11

BEST-FIT RULE
$f_{Ynotch} = 27.1\, L_{CB}^{-0.43}$

● THIS STUDY (n=15)
△ PREVIOUS DATA (n=8)

ADMITTANCE-NOTCH FREQUENCY, f_{Ynotch} (kHz)

SKULL LENGTH, L_{CB} (mm)

REFERENCES

Allen, J. B. (**1986**). "Measurement of eardrum acoustic impedance," in *Peripheral Auditory Mechanisms,* edited by J. L. Hall, J. B. Allen, A. Hubbard, S. T. Neely and A. Tubis (Springer-Verlag, New York), pp. 44-51.

Beranek, L. L. (**1986**). *Acoustics* (American Institute of Physics, New York), pp.137-138.

Blauert, J. (**1983**). *Spatial Hearing* (Massachusetts Institute of Technology, Cambridge, MA).

Brass, D. and Locke, A. (**1997**). "The effect of the evanescent wave upon acoustic measurements in the human ear canal," J. Acoust. Soc. Am. **101**, 2164-2175.

Burns, E. M., Keefe, D. H., and Ling, R. (**1998**). "Energy reflectance in the ear canal can exceed unity near spontaneous otoacoustic emission frequencies," J. Acoust. Soc. Am. **103**, 462-474.

Calder, W. A., III (**1996**). *Size, Function, and Life History* (Dover Publications Inc., Mineola, NY).

Chan, J. C. K., and Geisler, C. D. (**1990**). "Estimation of eardrum acoustic pressure and of ear canal length from remote points in the canal," J. Acoust. Soc. Am. **87**, 1237-1247.

Chan, J. C. K., Musicant, A. D., and Hind, J. E. (**1993**). "An insert earphone system for delivery of spectrally shaped signals for physiological studies," J. Acoust. Soc. Am. **93**, 1496-1501.

Crompton, A. W., and Parker, P. (**1978**). "Evolution of the mammalian masticatory apparatus," Am. Sci. **66**, 192-201.

Dallos, P. (**1970**). "Low frequency auditory characteristics: species dependence," J. Acoust. Soc. Am. **48**, 489-499.

Dallos, P. (**1973**). *The Auditory Periphery* (Academic Press, New York).

Decraemer, W. F., Khanna, S. M., Funnell, W. R. J. (**1990**). "Heterodyne interferometer measurements of the frequency responses of the manubrium tip in cat," Hearing Res. **47**, 205-218.

Dooling, R. J. (**1992**). "Hearing in birds," in *The Evolutionary Biology of Hearing,* edited by D. B. Webster, R. R. Fay, and A. N. Popper (Springer-Verlag, New York), pp. 545-559.

Echteler, S. M., Fay, R. R., and Popper, A. N. (**1994**). "Structure of the mammalian cochlea," in *Springer Handbook of Auditory Research, Volume 4: Comparative Hearing: Mammals,* edited by R. R. Fay and A. N. Popper (Springer-Verlag, New York), pp. 134-171.

Egolf, D. P. (**1977**). "Mathematical modeling of a probe-tube microphone," J. Acoust. Soc. Am. **61**, 200-205.

Fay, R. R. (1988). *Hearing in Vertebrates: A Psychophysics Databook* (Hill-Fay Associates, Winnetka, IL).

Fay, R. R. (**1994**). "Comparative auditory research," in *Springer Handbook of Auditory Research, Volume 4: Comparative Hearing: Mammals*, edited by R. R. Fay and A. N. Popper (Springer-Verlag, New York), pp. 1-17.

Flanders, P. B. (**1932**). "A method of measuring acoustic impedance," Bell System Tech. J. **11**, 402-410.

Fleischer, G. (**1978**). "Evolutionary principles of the mammalian middle ear," Adv. Anat. Embryol. Cell Biol. **55**, 3-69.

Funnell, W. R. J., Khanna, S. M., and Decraemer, W. F. (**1992**). "On the degree of rigidity of the manubrium in a finite-element model of the cat eardrum," J. Acoust. Soc. Am. **91**, 2082-2090.

Funnell, W. R. J., and Laszlo, C. A. (**1974**). "Dependence of middle-ear parameters on body weight in the guinea pig," J. Acoust. Soc. Am. **56**, 1551-1553.

Grinnell, A. D. (**1995**). "Hearing in bats: An overview," in *Hearing by Bats*, edited by A. N. Popper and R. R. Fay (Springer-Verlag, New York), pp. 1-36.

Guinan, J.J. Jr. and Peake, W. T. (**1967**). "Middle-ear characteristics of anesthetized cats," J. Acoust. Soc. Am. **41**, 1237-1261.

Hemilä, S., Nummela, S., and Reuter, T. (**1995**). "What middle ear parameters tell about impedance matching and high frequency hearing," Hear. Res. **85**, 31-44.

Heffner, H. E., and Masterton, R. B. (**1980**). "Hearing in glires: Domestic rabbit, cotton rat, feral house mouse, and kangaroo rat," J. Acoust. Soc. Am. **68**, 1584-1599.

Heffner, R. S., and Heffner, H. E. (**1980**). "Hearing in the elephant (Elephas maximus)," Science **208**, 518-520.

Heffner, R. S., and Heffner, H. E. (**1992**). "Evolution of sound localization in mammals," in *The Evolutionary Biology of Hearing*, edited by D. B. Webster, R. R. Fay, and A. N. Popper (Springer-Verlag, New York), pp. 691-715.

Heinsohn, R., and Packer, C. (**1995**). "Complex cooperative strategies in group-territorial African lions," Science **269**, 1260-1262.

Hemilä, S., Nummela, S., and Reuter, T. (**1995**). "What middle ear parameters tell about impedance matching and high frequency hearing," Hearing Res. **85**, 31-44.

Hopson, J. A. (**1966**). "The origin of the mammalian middle ear," Am. Zool. **6**, 437-450.

Huang, G. T., Rosowski, J. J., Cranston, B. R., and Peake, W. T. (**1997a**). "Middle-ear cavity structure and function in bobcat, Lynx rufus," Abstracts of the 20th Midwinter Meeting of the Association for Research in Otolaryngology, p. 140.

Huang, G. T., Rosowski, J. J., Flandermeyer, D. T., Lynch, T.J. III., and Peake, W. T. (**1997b**). "The middle ear of a lion: Comparison of structure and function to domestic cat," J. Acoust. Soc. Am. **101**, 1532-1549.

Huang, G. T., Rosowski, J. J., Puria, S., and Peake, W. T. (**1998**). "Noninvasive technique for estimating the acoustic impedance at the tympanic membrane in ear canals of different size," Abstracts of the 21st Midwinter Meeting of the Association for Research in Otolaryngology, p. 111.

Hudde, H. (**1983**). "Measurement of the eardrum impedance of human ears," J. Acoust. Soc. Am. **73**, 242-247.

Ingard, K. U. (**1948**). "On the radiation of sound into a circular tube, with an application to resonators," J. Acoust. Soc. Am. **20**, 665-682.

Jerger, J. F., editor (**1975**). *Handbook of Clinical Impedance Audiometry* (American Electromedics, New York).

Jerison, H. J. (**1973**). *Evolution of Brain and Intelligence* (Academic Press, New York).

Keefe, D. (**1984**). "Acoustical wave propagation in cylindrical ducts: Transmission line parameter approximations for isothermal and nonisothermal boundary conditions," J. Acoust. Soc. Am. **75**, 58-62.

Keefe, D. H. (**1997**). "Otoreflectance of the cochlea and middle ear," J. Acoust. Soc. Am. **102**, 2849-2859.

Keefe, D. H., Bulen, J. C., Arehart, K. H., and Burns, E. M. (**1993**). "Ear-canal impedance and reflection coefficient in human infants and adults," J. Acoust. Soc. Am. **94**, 2617-2638.

Keefe, D. H. and Levi, E. (**1996**). "Maturation of the middle and external ears: Acoustic power-based responses and reflectance tympanometry," Ear and Hearing **17**, 361-373.

Keefe, D. H., Ling, R., and Bulen, J. C. (**1992**). "Method to measure acoustic impedance and reflection coefficient," J. Acoust. Soc. Am. **91**, 470-485.

Kermack, K. A., and Musset, F. (**1983**). "The ear in mammal-like reptiles and early mammals," Acta Palaeontol. Polon. **28**, 148-158.

Khanna, S. M., and Tonndorf, J. (**1972**). "Tympanic membrane vibrations in cat studied by time-averaged holography," J. Acoust. Soc. Am. **52**, 1904-1920.

Khanna, S. M., and Tonndorf, J. (**1978**). "Physical and physiological principles controlling auditory sensitivity in primates," in *Neurobiology of Primates*, edited by R. Noback (Plenum Press, New York), pp. 23-52.

Kohllöffel, L. U. E. (**1984**). "Notes on the comparative mechanics of hearing. III. On Shrapnell's membrane," Hearing Res. **13**, 83-88.

Lawton, B. W., and Stinson, M. R. (**1986**). "Standing wave patterns in the human ear canal used for the estimation of acoustic energy reflectance at the eardrum," J. Acoust. Soc. Am. **79**, 1003-1009.

Lay, D. L. (**1972**). "The anatomy, physiology, functional significance and evolution of specialized hearing organs of gerbilline rodents," J. Morphol. **138**, 41-120.

Levi, E. C., Werner, L. A., and Keefe, D. H. (**1998**). "Toward using ear-canal impedance and reflectance measurements to screen middle-ear function in infants and young adults," in Abstracts of the 21st Midwinter Research Meeting of the Association for Research in Otolaryngology, p. 27.

Lynch, T. J., III (**1981**). "Signal processing by the cat middle ear: Admittance and transmission, measurements and models," Ph.D. thesis, Massachusetts Institute of Technology.

Lynch, T. J., III, Nedzelnitsky, V., and Peake, W. T. (**1982**). "Input impedance of the cochlea in cat," J. Acoust. Soc. Am. **72**, 108-130.

Lynch, T. J., III, Peake, W. T., and Rosowski, J. J. (**1994**). "Measurements of the acoustic input-impedance of cat ears: 10 Hz to 20 kHz," J. Acoust. Soc. Am. **96**, 2184-2209.

Manley, G. A. (**1990**). *Peripheral Hearing Mechanisms in Reptiles and Birds* (Springer-Verlag, New York).

Manley, G. A., and Gleich, O. (**1992**). "Evolution and specialization of function in the avian auditory periphery," in *The Evolutionary Biology of Hearing*, edited by D. B. Webster, R. R. Fay, and A. N. Popper (Springer-Verlag, New York), pp. 561-580.

Margolis, R. H., and Keefe, D. H. (**1997**). "Reflectance tympanometry," in Abstracts of the 20th Midwinter Research Meeting of the Association for Research in Otolaryngology, p. 49.

Margolis, R. H., Osguthorpe, J. D., and Popelka, G. R. (**1978**). "The effects of experimentally-produced middle ear lesions on tympanometry in cats," Acta Otolaryngol. **86**, 428-436.

Margolis, R. H., and Shanks, J. (**1985**). "Tympanometry," in *Handbook of Clinical Audiology*, edited by J. Katz (Williams & Wilkens, Baltimore, MD), 438-475.

Masterton, B., Heffner, H., and Ravizza, R. (**1969**). "The evolution of human hearing," J. Acoust. Soc. Am. **45**, 966-985.

McMahon, T. A., and Bonner, J. T. (**1983**). *On Size and Life* (Scientific American Books, New York).

192

Miles, J. A. (**1946**). "The analysis of plane discontinuities in cylindrical tubes. Part I.," J. Acoust. Soc. Am. **17**, 259-271.

Miller, M. R. (**1992**). "The evolutionary implications of the structural variations in the auditory papilla of lizards," in *The Evolutionary Biology of Hearing*, edited by D. B. Webster, R. R. Fay, and A. N. Popper (Springer-Verlag, New York), pp. 463-487.

Møller, A. R. (**1960**). "Improved technique for detailed measurements of middle ear impedance," J. Acoust. Soc. Am. **32**, 250-257.

Møller, A. R. (**1965**). "An experimental study of the acoustic impedance of the middle ear and its transmission properties," Acta Otolaryngol. **60**, 129-149.

Morse, P. M., and Ingard, K. U. (**1968**). *Theoretical Acoustics* (McGraw-Hill, New York), pp. 343-346.

Mundie, J. R. (**1963**). "The impedance of the ear -- a variable quantity," in U. S. Army Medical Research Lab. Report 576, edited by J. L. Fletcher, pp. 65-85.

Musicant, A.D., Chan, J.C.K., and Hind, J.E. (**1990**). "Direction-dependent spectral properties of cat external ear: New data and cross-species comparisons," J. Acoust. Soc. Am. **87**, 757-781.

Myers, R. H. (**1990**). *Classical and Modern Regression with Applications* (Duxbury Press, Wadsworth, Belmont, CA).

Nummela, S. (**1995**). "Scaling of the mammalian middle ear," Hearing Res. **85**, 18-30.

Onchi, Y. (**1961**). "Mechanism of the middle ear," J. Acoust. Soc. Am. **33**, 794-805.

Packer, C., and Pusey, A. E. (**1997**). "Divided we fall: Cooperation among lions," Scientific American **276**, 52-59.

Peake, W. T., and Guinan, J. J., Jr. (**1967**). "Circuit model for the cat's middle ear," MIT Quarterly Prog. Report of the Research Laboratory of Electronics **84**, 320-326.

Peake, W. T., and Rosowski, J. J. (**1997**). "Middle-ear structural and functional dependence on animal size," in *Proceedings of the International Symposium on Diversity in Auditory Mechanics*, edited by E. R. Lewis, G. R. Long, R. F. Lyon, P. M. Narins, C. R. Steele, and E. Hecht-Poinar, pp. 3-10.

Peake, W. T., and Rosowski, J. J. (**in preparation**). "Structural variation in the ears and skulls of the cat family."

Peake, W. T., Rosowski, J. J., and Lynch, T. J., III (**1992**). "Middle-ear transmission: Acoustic vs. ossicular coupling in cat and human," Hear. Res. **57**, 245-268.

Peters, R. H. (**1983**). *The Ecological Implications of Body Size* (Cambridge University Press, New York).

Pocock, R. I. (**1951**). "Catalogue of the genus felis," British Museum.

Puria, S. (**1991**). "A theory of cochlear input impedance and middle ear parameter estimation," Ph.D. thesis, City University of New York.

Rabbitt, R. D. (**1988**). "High-frequency plane waves in the ear canal: Application of a simple asymptotic theory," J. Acoust. Soc. Am. **84**, 2070-2080.

Rabbitt, R. D. and Friedrich, M. T. (**1991**). "Ear canal cross-sectional pressure distributions: Mathematical analysis and computation," J. Acoust. Soc. Am. **89**, 2379-2390.

Rabinowitz, W. (**1981**). "Measurement of the acoustic input immittance of the human ear," J. Acoust. Soc. Am. **70**, 1025-1035.

Rice, J.J., May, B.J., Spirou, G.A., and Young, E.D. (**1992**). "Pinna-based spectral cues for sound localization in cat," Hear. Res. **58**, 132-152.

Rohlf, F. J., and Sokal, R. R. (**1969**). *Statistical Tables* (W. H. Freeman and Co., San Francisco), p. 225.

Rosowski, J. J. (**1991**). "The effects of external- and middle-ear filtering on auditory threshold and noise-induced hearing loss," J. Acoust. Soc. Am. **90**, 124-135.

Rosowski, J. J. (**1992**). "Hearing in transitional mammals: Predictions from the middle-ear anatomy and hearing capabilities of extant mammals," in *The Evolutionary Biology of Hearing*, edited by D. B. Webster, R. R. Fay, and A. N. Popper (Springer-Verlag, New York), pp. 615-631.

Rosowski, J. J. (**1994**). "Outer and middle ears," in *Springer Handbook of Auditory Research, Volume 4: Comparative Hearing: Mammals*, edited by R. R. Fay and A. N. Popper (Springer-Verlag, New York), pp. 172-247.

Rosowski, J. J., Carney, L. H., Lynch, T. J., III, and Peake, W. T. (**1986**). "The effectiveness of the external and middle ears in coupling acoustic power into the cochlea," in *Peripheral Auditory Mechanisms*, edited by J. B. Allen, J. L. Hall, A. Hubbard, S. T. Neely and A. Tubis (Springer-Verlag, New York), pp. 3-12.

Rosowski, J. J., Carney, L. H., and Peake, W. T. (**1988**). "The radiation impedance of the external ear of cat: Measurements and applications," J. Acoust. Soc. Am. **84**, 1695-1708.

Rosowski, J. J., Huang, G. T., Atencio, C. A., and Peake, W. T. (**in preparation**). "Acoustic effects of multiple middle-ear air spaces," abstract submitted to Proceedings of the International Symposium on Diversity in Auditory Mechanics, Sendai, Japan, 1999.

Schaller, G. B. (**1972**). *The Serengeti Lion: A Study of Predator-Prey Relations* (University of Chicago Press, Chicago).

Schmidt-Nielsen, K. (**1984**). *Scaling: Why Is Animal Size So Important?* (Cambridge University Press, Cambridge, England).

Shanks, J. E. and Lilly, D. J. (**1981**). "An evaluation of tympanometric estimates of ear canal volume," J. Speech Hear. Res. **24**, 557-566.

Shaw, E. A. G. (**1974**). "The external ear," in *Handbook of Sensory Physiology: Volume V/1: Auditory System*, edited by W. D. Keidel and W. D. Neff (Springer-Verlag, New York), pp. 455-490.

Siebert, W. M. (**1970**). "Simple model of the impedance matching properties of the external ear," MIT Quarterly Prog. Report of the Research Laboratory of Electronics **96**, 236-242.

Stevens, K. N., Berkovitz, R., Kidd, G., Jr., and Green, D. M. (**1987**). "Calibration of ear canals for audiometry at high frequencies," J. Acoust. Soc. Am. **81**, 470-484.

Stinson, M. R. (**1985**). "The spatial distribution of sound pressure within scaled replicas of the human ear canal," J. Acoust. Soc. Am. **78**, 1596-1602.

Stinson, M. R. (**1990**). "Revision of estimates of acoustic energy reflectance at the human eardrum," J. Acoust. Soc. Am. **88**, 1773-1778.

Stinson, M. R., and Khanna, S. M. (**1989**). "Sound propagation in the ear canal and coupling to the eardrum, with measurements on model systems," J. Acoust. Soc. Am. **85**, 2481-2491.

Stinson, M. R., and Khanna, S. M. (**1994**). "Spatial distribution of sound pressure and energy flow in the ear canals of cats," J. Acoust. Soc. Am. **96**, 170-180.

Stinson, M. R., Shaw, E. A. G., and Lawton, B. W. (**1982**). "Estimation of acoustical energy reflectance at the eardrum from measurements of pressure distribution in the human ear canal," J. Acoust. Soc. Am. **72**, 766-773.

Van Valkenburgh, B. (**1990**). "Skeletal and dental predictors of body mass in carnivores," in *Body Size in Mammalian Paleobiology*, edited by J. Damuth and B. J. MacFadden (Cambridge University Press, Cambridge, England), pp. 181-205.

Voss, S. E., and Allen, J. B. (**1994**). "Measurement of acoustic impedance and reflectance in the human ear canal," J. Acoust. Soc. Am. **95**, 372-384.

Wada, H., Kobayashi, T., Suetake, M., and Tachizaki, H. (**1989**). "Dynamic behavior of the middle ear based on sweep frequency tympanometry," Audiology **28**, 127-134.

Webster, D. B., and Plassmann, W. (**1992**). "Parallel evolution of low-frequency sensitivity in old world and new world desert rodents," in *The Evolutionary Biology of Hearing*, edited by D. B. Webster, R. R. Fay, and A. N. Popper (Springer-Verlag, New York), pp. 633-636.

Webster, D. B., and Webster, M. (**1980**). "Morphological adaptations of the ear in the rodent family Heteromyidae," Am. Zool. **20**, 247-254.

195

White, R. E. C., Studebaker, G. A., Levitt, H., and Mook, D. (**1980**). "The application of modeling techniques to the study of hearing aid acoustic systems," in *Acoustical Factors Affecting Hearing Aid Performance*, edited by G. E. Studebaker and I. Hochberg (University Park Press, Baltimore, MD), pp. 267-296.

Wilber, L. A., and Feldman, A. S. (**1976**). "The middle ear measurement battery," in *Acoustic Impedance and Admittance: The Measurement of Middle Ear Function*, edited by A. S. Feldman and L. A. Wilber (Williams and Wilkins, Baltimore, MD), pp. 345-377.

Wozencraft, W. C. (**1989**). "The phylogeny of the recent Carnivora," in *Carnivore Behavior, Ecology, and Evolution*, edited by J. L. Gittleman (Cornell University Press, Ithaca, NY), pp. 495-535.

Wozencraft, W. C. (**1993**). "Order Carnivora," in *Mammal Species of the World, A Taxonomic and Geographic Reference*, 2nd ed., edited by D. E. Wilson and D. M. Reeder (Smithsonian Inst. Press, Washington, DC), pp. 279-348.

Zuercher, J. C., Carlson, E. V., and Killion, M. C. (**1988**). "Small acoustic tubes: New approximations including isothermal and viscous effects," J. Acoust. Soc. Am. **83**, 1653-1660.

Zwislocki, J. (**1962**). "Analysis of the middle-ear function. Part I: Input impedance," J. Acoust. Soc. Am. **34**, 1514-1523.

Zwislocki, J. J. (**1970**). "An acoustic coupler for earphone calibration," Laboratory of Sensory Communication Special Report LSC-S-7, Syracuse University.